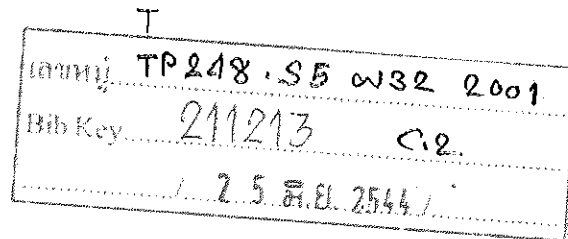# Synthesis and Characterization of a USY Zeolite

Wachira   Ritthichai

Master of Engineering Thesis in Chemical Engineering
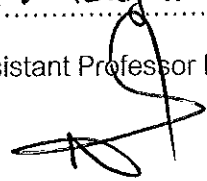
Prince of Songkla University
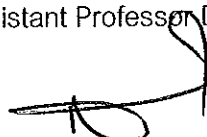
2001

Thesis Title   Synthesis and Characterization of a USY Zeolite

Author   Mr. Wachira Ritthichai

**Major Program**   Chemical Engineering

Advisory Committee

...................................(Chairman)

(Assistant Professor Dr. Chakrit Tongurai)

...................................(Committee)

(Dr. Sutham Sukmanee)

Examining Committee

...................................(Chairman)

(Assistant Professor Dr. Chakrit Tongurai)

...................................(Committee)

(Dr. Sutham Sukmanee)

...................................(Committee)

(Dr. Charun Bunyakan)

...................................(Committee)

(Associate Professor Dr. Lek Sikong)

The Graduate School, Prince of Songkla University, has approved this thesis as partial fulfillment of the requirement for the Master of Engineering degree in Chemical Engineering.

....

(Associate Professor Dr. Piti Trisdikoon)

Dean, Graduate School

(2)
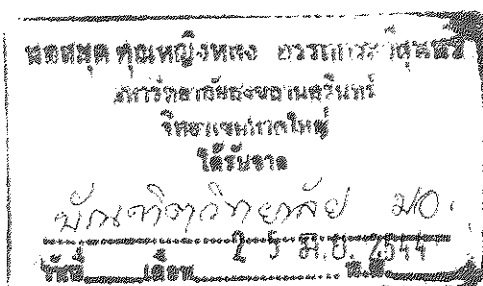
ชื่อวิทยานิพนธ์   การสังเคราะห์และศึกษาลักษณะเฉพาะของซีโอไลต์อัลตราสเตเบิลวาย
ผู้เขียน   นาย วชิระ ฤทธิชัย
สาขาวิชา   วิศวกรรมเคมี
ปีการศึกษา   2543

บทคัดย่อ

ซีโอไลต์อัลตราสเตเบิลวาย สังเคราะห์ได้จาก โซเดียมวายซีโอไลต์ (ความเป็นผลึก 89.23 %, โซเดียมออกไซด์ 12 %), แอมโมเนียมคลอไรด์ และน้ำปราศจากไอออน จากการศึกษาหาสภาวะที่เหมาะสมในการสังเคราะห์ซีโอไลต์แอมโมเนียมวาย พบว่าสภาวะที่เหมาะสมคือ การแลกเปลี่ยนไอออนที่อุณหภูมิ 90 °C, เวลา 1 ชั่วโมง และอัตราส่วนโดยน้ำหนักของวัตถุดิบ ซีโอไลต์: แอมโมเนียมคลอไรด์: น้ำ เท่ากับ 1:1:20 ซีโอไลต์แอมโมเนียมวายที่ได้มีความเป็นผลึก 85.16 % และมีโซเดียมออกไซด์ในโครงสร้างต่ำกว่า 1% สภาวะที่เหมาะสมในการบ่มไอน้ำคือ 600 °C, 2 ชั่วโมง และอัตราส่วนระหว่างน้ำต่อซีโอไลต์เท่ากับ 3:1 ซีโอไลต์อัลตราสเตเบิลวายที่เตรียมได้มีความเป็นผลึก 65.5%, เสถียรภาพของผลึกสูงกว่า 1,000°C, ขนาดของหน่วยเซลล์ 24.37 Å และพื้นที่ผิว 462 m^2/g

ตัวเร่งปฏิกิริยาซีโอไลต์อัลตราสเตเบิลวายได้ถูกเตรียมโดยผสมซีโอไลต์อัลตราสเตเบิลวาย กับ pheudoboemite และ kaolin clay ในอัตราส่วน 3:2:5 และนำมาลดความว่องไวภายใต้สภาวะไอน้ำ 100 %ที่ อุณหภูมิ 800 °C, 4 ชั่วโมง แล้วนำมาทดสอบประสิทธิภาพการแตกตัวเชิงเร่งปฏิกิริยากับแก๊สออยล์ด้วยเครื่องจุลกัมมันตภาพ (MAT) พบว่าตัวเร่งปฏิกิริยาซีโอไลต์อัลตราสเตเบิลวายมีการแตกตัวเชิงเร่งปฏิกิริยา 54.68 % ผลได้แก๊สโซลีน 35%มีสภาพการเลือกแก๊สโซลีน 64.01 % ผลได้โค้ก 3.30 %และมีสภาพการเลือกโค้ก 6.04%

Thesis Title   Synthesis and Characterization of a USY Zeolite

Author   Mr. Wachira Ritthichai

Major Program   Chemical Engineering

Academic Year   2000

ABSTRACT

USY zeolite (ultrastable Y zeolite) was synthesized by using NaY zeolite (Crystallinity 89.23%, and 12% Na_2O by weight), NH_4Cl, and de-ionized water. Various synthesis conditions were a studied. The suitable conditions for the synthesis of NH_4Y zeolite are an ion exchange temperature of 90 $^{\circ}C$ for 1 hour and a raw material weight ratio for NaY zeolite: NH_4Cl: H_2O of 1: 1: 20. The resulting USY zeolite had a crystallinity of 85.16 % and an Na_2O of 1 % by weight. The ideal conditions for the hydrothermal treatment (steam calcination) are a temperature of 600 $^{\circ}C$, for 2 hour and a water to zeolite ratio of 3:1. The resulting USY zeolite had a crystallinity of 65.5 %, a crystallinity stable region in excess of 1,000 $^{\circ}C$, a unit cell size 24.37 Å, and a surface area of 462 m^2/g.

The catalyst for the synthesis of USY zeolite was prepared by mixing USY zeolite ,pheudoboemite and kaolin clay at a 3:2:5 ratio. The catalyst was deactivated under 100 % steam at 800 $^{\circ}C$, for 4 hours . The catalyst performance was tested by cracking it in gas oil using the MAT Unit. The activity of the USY zeolite catalyst was 54.68 %, the gasoline yield was 35 %, the gasoline selectivity was 64.01 %, the coke yield was 3.30 by weight %, and the coke selectivity was 6.04 by weight %.

ACKNOWLEDGEMENT

Contents

Contents

Contents

List of Tables

List of Tables

List of Tables

List of Figures

List of Figures

List of Figures

List of Figures

List of Figures

CHAPTER 1

INTRODUCTION

1.1 Introduction

Since their successful introduction some thirty years ago, zeolite catalysts have been the subjects of considerable academic and industrial research efforts. Zeolites, or crystalline aluminosilicates, differ from more conventional crystalline materials in that the anhydrous crystal has a large, regular pore structure, making the internal surface available for adsorption or catalysis (Breck,1974). Compared to other types of catalysts, zeolites are extremely active, especially in hydrocarbon conversion reactions and their regular pore dimensions make them selective as to which molecules are adsorbed or converted. The major industrial process that utilizes zeolites is the catalytic cracking of petroleum and the replacement of amorphous silica-alumina materials by faujasite (type Y) zeolites in the 1960's has saved the petroleum industry billions of dollar (Plank,1964).

The direct synthesis of zeolite Y was restricted to product silica–alumina ratio of less than 6.0. Because of the increased change for low crystallinity or impurity formation when operating under conditions designed to yield silica–alumina values higher than 5.6, commercial production usually is limited to silica–alumina ratios below 5.6. However, in the early use of zeolite Y in FCC catalysis the hydrothermal stability of zeolite Y was discovered to be highly dependent on zeolite silica–alumina ratios. This conclusion led to methods of secondary synthesis designed to increase the silica–alumina ratio of as synthesized sodium Y zeolite. The recovery by Maher and McDaniel of ultrastable Y (USY) zeolite, the first of the aluminum deficient Y zeolites, led to its inclusion in FCC catalysts as early as 1964 in XZ–15 produced by Davison (McDaniel,1966). However, the use of USY aluminum deficient zeolite in FCC catalyst quickly disappeared because of its substantially lower activity compared to fully or partially rare earth exchanged Y zeolite (REY and REHY). The increased olefinicity and gasoline octane obtained by using USY did not become important until regulations

mandating the decreased use of lead in gasoline came on the scence in the mid–1970's.

The octacat series of catalysts containing USY in concentrations greater than 25 wt % appeared on the market in 1976, but the relaxation of the regulations restricting lead in gasoline temporarily decreased interest in zeolite octane catalysts. With the mandated elimination of leaded gasoline in the 1980's, octane–enhancing FCC catalysts again became extremely important to the oil industry. Catalysts containing USY zeolite again appeared on the market along with new technology for producing dealuminated (high silica–alumina ratio) Y zeolites.

Techniques have been developed for the chemical dealumination of the zeolite. Such dealumination would minimize the presence of nonframework (NFA) generated by the hydrothermal techniques used to produce USY zeolite. Union carbide patented and commercialized dealumination of zeolite by ammonium fluorosilicate (AFS) for use in FCC catalysts (Breck,1985). Commercial techniques involving the hydrothermal treatment of the zeolite to form a conventional USY zeolite containing NFA formed during dealumination which were then modified by chemical washing to eliminate the NFA. Because of the superior stability, octane-producing characteristics, and coke selectivity of these various aluminum deficient zeolites, quickly controlled the major portion of the United States and European catalyst markets.

The purpose of this work is to prepare the ultrastable Y (USY) zeolite by using basic preparation techniques from Research Institute of Petroleum Processing (RIPP) Sinopec, Beijing, China. Understanding from some literature reviews and patents has developed the further applications methods of experiments.

1.2 Objectives
1. To study the preparation of an ultrastable Y (USY) zeolite.
2. To determine the performance and characterization of prepared ultrastable Y (USY) zeolite.

1.3 Literature reviews

Kerr and coworkers (Kerr et al.,1965) stated that a method of preparing highly siliceous crystalline zeolite–type materials and materials resulting therefrom and, more particularly, to a novel technique for increasing the silica to alumina ratio of zeolites and to the zeolites or zeolite–type material resulting therefrom.

Kerr and coworkers (Kerr et al.,1966) claimed that a process for producing a hydrothermally stable catalyst composition of high hydrocarbon conversion activity. which comprises calcining an ammonium–Y crystalline aluminosilicate in the presence of rapidly flowing steam. Then base–exchanging the resultant steam product with an ammonium salt, treating the resultant exchanged product with a chelating agent capable of combining with aluminum at a pH between about 7 and 9, and recovering the final product.

Maher and coworkers (Maher et al.,1966) wrote that the process for preparing ultrastable Y (USY) zeolite consists of selecting a suitable zeolitic material and base exchanging the zeolite with an ammonium salt, amine salt or other salt. Examples of suitable compounds of this type include ammonium chloride, ammonium sulfate etc. The exchange temperatures in the range of 25 to $150^\circ C$ give satisfactory results, in this experiment it carried out rapidly at $100^\circ C$. The exchange is generally completed in a period of about 0.1 to 24 hours, conveniently for a period of 1 to 3 hours. The zeolite is filtered washed and dried. The composite is then calcined or steamed mildly at a temperature in the range of 200 to $1500^\circ F$ for a period of 0.1 to 12 hours. The exchanged zeolite is continually ion exchanged and calcined several times for decreased the amounts of Na_2O below than 1% and unit cell size in the range of 24.20-24.45 Å

Maher and coworkers (Maher et al.,1968) claimed that method of cation exchanging zeolites comprising a conventional ion exchange step, whereby the more easily exchangeable cations are ion exchanged. Followed by a calcination step at 400 to $1500^\circ F$., whereby the difficulty to exchange cations are redistributed. The redistributed cations are then ion exchanged by an additional conventional ion

exchange step. One or more calcinations and additional ion exchange steps may be used.

McDaniel and coworkers (McDaniel et al., 1968) proposed a new form of the zeolite faujasite described that is thermally stable at temperatures is excess of 1000 ^{o}C. This is in contrast with other reported hydrogen or decationated faujasite which are less stable than the cation forms. The preparation and ion exchange properties of this zeolite are shown to be different from the corresponding hydrogen or decationated forms. The preparation of these materials consists of two major steps. (1) The essentially complete removal of sodium ions from the zeolite in such a way as to leave the structure in a metastable condition with respect to thermal stability (2) The conversion of this material to an extremely stable form by heat treatment at temperatures of about 800°C or above. Several procedures have been found which will accomplish the ultrastable structure.

McDaniel and coworkers (McDaniel et al.,1969) contented a process for preparing a stabilized faujasite zeolite having an alkali metal content, expressed as the oxide, of less than 1%, comprises ion exchanging a suitable crystalline faujasite zeolite starting material with a solution containing hydrogen ions or cations which can be converted to hydrogen ions (e.g. ammonium ions, amine ions and like), to decreased the alkali metal content to from greater than 10 % by weight to 4% by weight. The product of this exchange is then calcined at or above a minimum temperature which is a function of the alkali metal content as $T=1238+60A$ where T is the calcination temperature, ^{o}F and A is the alkali metal weight % content expressed as the chemical equivalent weight of the oxide of sodium. This composition is then further exchanged to substantially remove the balance of the alkali metals present to leave a product having an alkali metal content, expressed as the oxide, of less than 1% by weight.

Eberly and coworkers (Eberly et al.,1969) stated that crystalline aluminosilicate zeolites having silica to alumina mole ratios substantially higher than prior art zeolites are prepared by a process wherein a conventional crystalline aluminosilicate zeolite is contacted with water at an elevated temperature and then treated to remove alumina from the crystal lattice. The water treatment can be accomplished by contacting the

crystalline aluminosilicate zeolite with a gas containing at least 2% water at a temperature between 800 and 1500°F. Higher concentrations of water preferably at least 5 % and most preferably 25%, and in accordance with the disclosure, pure steam may be used. In the preferred embodiment, the water treatment is accomplished in two steps; viz. by first treating the crystalline zeolite with a gas combining at least 2% water, followed by treatment with pure steam. The alumina so produced is in an amorphous form and remains within the gross structure of the zeolite. This amorphous alumina may be removed from the zeolite materials by appropriate treatment with a dilute mineral acid or an organic acid chelating agent.

Garwood and coworkers (Garwood et al.,1976) mentioned a method of removing alumina from a crystalline aluminosilicate composition having a silica to alumina mole ratio of above 3 to about 12, which comprises heating aluminosilicate composition to a temperature of greater than 50 °C to about 100°C in the presence of a cationic form of chromium, preferably Cr^{3+}, in an aqueous solution of about 0.1 Normal of a chromium salt of a mineral acid. Whereby the pH is less than 3.5, and such that the atomic ratio of chromium to aluminum is greater than 0.5 for a time sufficient to remove the alumina.

Ward (Ward,1977) declared that highly active, hydrothermally stable and ammonia-stable Y zeolite compositions are disclosed such compositions are useful as adsorbents, hydrocarbon conversion catalysts, and as acidic supports for catalytic metals. The stabilized Y zeolite composition is prepared from a sodium Y zeolite by a novel sequence of: (1) partial exchange of ammonium ions for sodium ions, (2) steam calcination under controlled conditions of time, temperature and steam partial pressure, and (3) further ion exchange of ammonium ions for sodium ions to reduce the final Na_2O content to below about one weight-percent.

Alafandi and coworkers (Alafandi et al.,1980) wrote that a method of producing an exchanged zeolite of the faujasite type which comprises mixing a sodium zeolite of the faujasite type with a solution of a salt of a member of the group consisting of ammonium and the metals of the groups 1b, 2a, 2b, 3a, 6b, and 7b, of the periodic system, and two or more thereof, the quantity of the zeolite, and the concentration of the

cations, being in quantity sufficient to establish a ratio of the equivalents of cation in the solution at super atmospheric pressure, per equivalent of Na cation in the zeolite in the mixture in excess of about 1, heating the solution to a temperature in the range of about 300°F and up but less than about 500°F for a period of time to reduce the sodium content of the zeolite, expressed as Na_2O, to less than about 0.1 equivalents per gram atom of Al in the exchanged zeolite, and washing the zeolite substantially free of anions of the salt in solution.

Scherzer (Scherzer, 1984) declared that the cracking of hydrocarbons with a mixture of acid dealuminated, rare earth metal exchanged Y zeolite having a silica to alumina molar ratio of more than 6 to 300, and non–dealuminated rare earth metal exchanged Y zeolite and matrix. The method for preparing these catalysts is sodium Y zeolite of silica to alumina ratio of 5 and containing about 13.5 Na_2O treated with 10% solution of ammonium sulfate using 10 ml. solution per gram of the zeolite on a volatile free basis. The exchange is carried on for an hour at room temperature while stirring. The slurry is filtered and washed until sulfate free. The washed filter cake is arranged in a deep bed and heated at 540 °C for two hours. The calcined zeolite is again exchanged twice as before, except that the temperature of exchange was 90°C and the zeolite to $(NH_4)_2SO_4$ to water weight ratio was 1:2:10. The washed filter cake is arranged in a deep bed, as before, and calcination at a temperature of 815°C for three hours. This calcined zeolite further treated with 1 to 5 Normal hydrochloric acid (HCl). Some of acid dealuminated zeolites are exchanged with rare earth metal, then prepared the catalyst and test the activity.

Fejes and coworkers (Fejes et al.,1985) reported that suitably selected volatile compounds (such as non metal, even metalloid and metal halides) exhibit excellent dealumination abilities at elevated temperatures. The same compounds, when they react at lower temperatures, are capable of introducing metallic components into exchange positions of the zeolitic framework in which might be of advantage in the case of salts liable to hydrolysis in aqueous media.

Scherzer and coworkers (Scherzer et al.,1985) declared that faujasite – type zeolites of high catalytic activity, low coke–forming proper and stable crystalline structure are prepared by using a combination of hydrothermal treatment and ion exchange resin removal of aluminum from the crystalline structure of the zeolites. The hydrothermal treatment is carried out by arranging the zeolite in a fixed bed configuration to a depth of at least 3 inches and maintaining it at self steaming condition at a temperature ranging from about 500 to 900°C for a period of 1 to 5 hours. The process allows for a substantial increase of the silica to alumina ratio in the zeolite without detrimentally affecting the strength of the structure. The process comprises the step of preparing aqueous slurry of the hydrothermally treated zeolite. By contacting the slurry with a strong acid cation exchanged resin of the sulfonated polystyrene type in the hydrogen form in a resin to zeolite weight ratio ranging from 3:1 to 5:1 at a temperature of 100°C for a time ranging from 1 to 4 hours, and recovering zeolite of increased silica to alumina ratio, reduced sodium content and high structural strength.

Skeels and coworkers (Skeels et al., 1986) claimed that aluminum from AlO_4– tetrahedral as–synthesized zeolites is extracted and substituted with silicon to form zeolite compositions having higher silica to alumina molar ratios and exhibiting distinctive chemical and physical properties. The preparative procedure involves contact of the starting zeolite with an aqueous solution of a fluorosilicate salt using controlled proportions and temperature and pH conditions that avoid aluminum extraction without silicon substitution.

Zukal and Patzelová (Zukal and Patzelová,1986) stated that six NH_4Na Y zeolite samples were treated hydrothermally under deep bed conditions, a small quartz reactor was used; the bed of the NH_4Na Y zeolite was 1.5 cm. in diameter and 5.5 cm. in height. The temperatures of 823 and 1043 K (550 and 770 °C) were reached by linear increase at a rate of 1.5 K min^{-1} at the pressure of water vapor, of 2.1 kPa. After this treatment, all samples were extracted twice with 0.1 N HCl to remove extra – lattice aluminum together with Na^+ cations. To obtain information on changes in the porous structure caused by the hydrothermal treatment, adsorption and desorption isotherms of benzene vapors,

were measured on the dealuminated and decationized samples. It was found that secondary mesopores are formed in the zeolite crystals at a degree of dealumination not exceeding 30%. If the degree of dealumination approaches 50%, formation of secondary micropores occurs, in addition to mesopores. The observed changes of the micropore volume suggest that the zeolitic lattice be destroyed on the mesopore surface.

Lynch and coworkers (Lynch et al.,1987) reported that the secondary pore system of dealuminated HY zeolites has been studied quantitatively at each step of the preparation procedure by electron microscopy and N_2 adsorption. The respective roles of self-steaming and acid leaching in the creation of the secondary pore system have been determined. The structure of the secondary pore system can be viewed approximately as being formed by cavities of spherical shape connected by small restrictions. Although large channels have been observed to break the surface of the crystals, by far the greater part of the external surface is embedded in an amorphous layer, which does not seem to be crossed by observable channels.

LaPierre and coworkers (LaPierre et al., 1989) reported that faujasite zeolites, especially zeolite Y, may be made stable to acid by a simple steam process. The process may be used with zeolites of the faujasite family, which have silica to alumina ratios from 3 to 25, for example, zeolite Y or zeolite ZSM-20. The process comprises calcining the zeolite under conditions that control the rate at which the chemically bound water tends to come off at temperatures above 400 $^{\circ}$C and accordingly, the calcination conditions are controlled at these temperatures. Elimination of the chemically bound water is controlled by calcining the zeolite in a steam, containing atmosphere with a controlled rate of heating in the temperature range in which the water is removed, generally from 500 to 650 $^{\circ}$C. In this range, the heating rate is maintained at a value below 2.5°C min^{-1}. Once this temperature range has been passed, heating may take place at a faster rate, if desired. The product of the stabilization treatment is a zeolite which is suitable to acid and which may, therefore, be subjected to an acid dealumination. The dealuminated zeolites produced by the acid extraction have higher

silica to alumina ratio than the starting materials; structural silica to alumina ratios of over 100:1 are readily attainable.

Paul and Jack (Paul and Jack, 1989) mention that dealuminated zeolites prepared both hydrothermally and using silicon tetrachloride were investigated to determine the effect of sodium addition on their catalytic activities. These materials were found to have drastically reduced activities upon sodium addition with each sodium atom effectively neutralizing the catalytic activity previously thought to be due to five framework BrØnsted acid sites. These results are interpreted to mean that isolated framework Al atoms are a necessary but insufficient condition for strong acidity, and only about one-fifth of the framework Al atoms are associated with this strong acidity. Extraframework Al is believed to impart, through inductive effects, strong acidity to these framework BrØnsted acid sites. An infrared study of the hydroxyl region revealed bands at 3675 and 3595–3610 cm^{-1} (± 2 cm^{-1}) that are attributed to protons associated with two different types of extraframework aluminum oxide or oxyhydroxide. A band at 3965 cm^{-1} is attributed to Na^{+} interacting with water that is hydrogen-bonded to a framework oxygen atom. A narrow band at 3602 cm^{-1} is attributed to a highly acidic BrØnsted sites in the zeolite lattice.

Linsten and coworkers (Linsten et al.,1991) mentioned that Y zeolite comprising aluminum ions supplied and fixed by ion exchange is produced by subjecting NaY zeolite to a series of treatment steps comprising e.q. ammonium ion exchange and calcination. In order to supply and fix the aluminum ions, aluminum ion exchange is carried out. Followed by further calcination in a saturated or substantially saturated steam atmosphere at 400 to 900°C. If the zeolite unit cell size is to be reduced to 24.15 to 24.35 Å, simultaneously as the aluminum ions are fixed, the last mentioned calcination is carried out in a saturated or essentially saturated (steam) water vapor atmosphere at 500 to 900°C. It is further disclosed that the steam used in the calcination step can be supplied either from an external source or solely by vaporization of water present in the zeolite.

Yoshida and coworkers (Yoshida et al.,1991) wrote that USY zeolite samples, which were prepared from sodium Y zeolite whose silica to alumina atomic ratios were in the range of 2.5 to 3.0, were treated hydrothermally under deep - bed conditions and with steam. The nonframework and framework aluminum was extracted with hydrochloric acid solutions. The hydrothermal stability under 100% steam of USY-Ex was examined in relation with the unit cell dimensions, chemical analyses, MASNMR, T.G., and I.R. observations. The hydrothermal stability of USY-Ex was affected mainly by the amounts of framework and nonframework aluminum, and the retention of crystallinity, but not by the amounts of residual alkali metal oxides and the amount of four-OH nest. Some of Si (3Al) and Si (2Al) units converted to nonframework Si (4Al), Si (3Al) and Si (2 Al) units and left the vacancies larger than four OH nests in zeolite framework. It was confirmed that the population of Si (2 Al) in parent sodium Y affects the retention of crystallinity of USY-Ex.

Shien–Jen Yang and Yu–Wen Chen (Shien–Jen Yang and Yu–Wen Chen,1995) claimed that the interaction of vanadium and nickel in USY zeolite has been investigated by X–Ray diffraction, nitrogen sorption, FTIR, temperature–programmed reduction and n-hexane cracking reaction. There is an interaction existing, either direct or indirect through nonframework aluminum, between vanadium and nickel. This leads to the inhibition effect for vanadium and nickel to affect the catalytic and physicochemical properties of USY zeolite. Nickel can inhibit the destruction of USY zeolite caused by vanadium. Vanadium can suppress the coke formation due to the presence of nickel.

Tao Long–Xiang and coworkers (Tao Long–Xiang et al.,1995) proposed that the nickel–deposited ultrastable Y (USY) zeolite samples were simulated by a method of impregnation with nickel naphthenate benzene solution followed by drying and calcination. Characterization of the Ni–impregnated USY zeolites was carried out by F.M.R. The reducibility, distribution, and dispersion of nickel deposited on USY zeolites were investigated after calcination in air, hydrogen reduction, and isooctane cracking reaction, respectively.

Calsavara and coworkers (Calsavara et al.,1996) asserted those two ultrastable Y zeolites with different degrees of dealumination were treated with NaOH solution at various temperatures and contact times. Filtrate analysis showed the transference of the solubilized nonframework aluminum species to the solid phase, at a rate that increase with both increasing temperature and dealumination degree. The reinsertion of this aluminum in the lattice was verified by the reduction in the structural silica to alumina ratios determined by ^{29}Si NMR and FTIR. The mesoporosity reduction points to a reinsertion in the structural defects. An estimate of the activation energy for the reinsertion process was obtained from the data fitting to a basic zeolite crystallization model.

Leiras Gomes and coworkers (Leiras Gomes et al.,1997) contented that ultrastable Y (USY) zeolites have been treated with sulfuric and/or phosphoric acids. Aiming at the determination of the interaction of both acids with either framework (FAL) or extraframwork (EFAL) aluminas, as well as the effect of such modifications on catalytic properties in ethylbenzene disproportionation. Zeolites have been characterized by means of several physico-chemical techniques (XRD, XRF, FTIR, ^{29}Si, ^{27}Al and ^{31}P-MASNMR, nitrogen adsorption and AA). Results revealed that the treatment with H_2SO_4 removed EFAL located in supercavities without attacking the zeolitic framework. Treatment with H_3PO_4 incorporates P in two quite distinct ways: as a monometric phosphate associated to framework aluminum atoms (for low EFAL concentrations) and as a polymeric phosphate originated from the reaction of EFAL with H_3PO_4 (for high EFAL concentrations). Regarding catalytic properties, initial activities are higher for H_2SO_4 leached samples when compared to those which have just been calcined. Nevertheless, initial activities of samples treated with H_3PO_4 depend strongly on the P_2O_5 content incorporated into the zeolite. With respect to isomers (otho-, meta- and para- diethylbenzene) generally formed in this disproportionation reaction, no considerable para–selectivity had been observed.

Da–Song Liu and coworkers (Da–Song Liu et al.,1997) claimed that H_4EDTA and $(NH_4)_2SiF_6$–liquid phase dealuminated Y zeolites (EDY and FDY) and hydrothermally

dealuminated Y zeolite (USY, was obtained by hydrothermal treatment of (80%NH$^+_4$) NaY zeolite at 550°C for 18 hours under 0.1 MPa of pressure, were treated with an aqueous solution of KOH at 40 to 100°C, stirring for 4 hours. The products were washed with water and dried in air at 100°C. These products were characterized by using XRD, NMR, FTIR, SEM, and fast atom bombardment mass spectroscopy 9FABMS techniques. A decrease of silica to alumina ratio was observed in the basic solution–treated samples. The results clearly show that dissolution of the surface of EDY and removal of silicon atom from the framework lattice of FDY occurs during basic solution treatment. Realumination of ultrastable Y (USY) zeolite take place through reinsertion of aluminum into the framework vacancies formed during hydrothermal treatment of NH$_4$NaY or formed during a basic solution treatment of USY.

Pawelec and coworkers (Pawelec et al.,1997) contented that either an ion exchange or an impregnation procedure has prepared Ni / USY catalysts. The modification of support and the effect of sulfidation on the Ni distribution were examined by various techniques (water adsorption, FTIR spectroscopy of chemisorbed NO, XPS, 129Xe NMR and Xe adsorption). In all catalysts the sulfidation of Ni is incomplete and the method of Ni introduction influenced the Ni distribution in Ni / USY zeolites. In unsulfided samples ion exchange technique led to Ni located essentially in hexagonal prisms, whereas in the other samples prepared by impregnation procedure the Ni concentrates were located at or near the outer zeolite surface. Some nickel redistribution has been observed during catalyst sulfidation.

Kuehne and coworkers (Kuehne et al.,1998) wrote that the acidic properties and 2–methylpentane cracking turn over frequencies (TOFs) were compared for HY and two dealuminated HY zeolites with similar levels of framework Al: HDY that was dealuminated by ammonium hexafluorosilicate, and a (H,NH$_4$)-USY zeolite that was dealuminated by steam. Microcalorimetry of NH$_3$ adsorption, and the types of acid sites determined the acid strength distributions by FTIR spectroscopy. All zeolites possessed BrØnsted acid sites with very few Lewis acid sites. The differential heat of adsorption of NH$_3$ on these zeolites was nearly constant: about 120 kJ/mol for HY and HDY and

approximately 7kJ /mol higher for the (H, NH$_4$)-USY zeolite. The cracking TOF for HDY was five times larger than HY, while the TOF of (H, NH$_4$)-USY zeolite was 80 times higher. These results suggest that the cracking activity may be affected by other factors in addition to acid strength.

Guoxing Niu and coworkers (Guoxing Niu et al.,1999) insisted that siliceous Y zeolite (silica to alumina ratio>150), prepared by treating NaY zeolite with SiCl$_4$ for 4 hours at 500°C, then treating it in 100 % steam at 800°C for 4 hours. Nonframework aluminum was removed from siliceous Y zeolite by leaching with 4 N HCl solution at 80 $^{\circ}$C for several times displays high thermal and hydrothermal stability. After aged at 1200°C for 4 hours, siliceous Y zeolite shows specific surface area as high as 510 m^2/g. Even steamed at 1000 $^{\circ}$C for 4 hours, it still keeps its framework perfectly.

Kung and coworkers (Kung et al.,1999) declared that ultrastable Y (H–USY) zeolite, prepared by steam treatment of Y zeolite, is a very active hydrocarbon cracking catalyst. However, the extent of enhancement in activity compared to a non – steam sample depends on the reaction condition. A model that has been proposed to explain this behavior is summerized. The model incorporates the three different mechanisms for hydrocarbon cracking, and the dependence of their rates on the partial pressures of reactants and product temperature. Depending on the reaction condition, such as hydrocarbon pressure, temperature, and conversion, the predominant cracking reaction mechanism may differ. The change in the predominant mechanism may also be a result of the proportionally small increase in external surface area caused by the steaming-induced structural destruction of the zeolite particles. However, these relatively small changes can lead to a much larger overall effect on the cracking rate because of the sensitive dependence of oligometric cracking, and to a lesser extent, bimolecular cracking on the alkene partial pressure.

Williams and coworkers (Williams et al.,1999) declared that steamed HY or ultrastable Y (H-USY) zeolites are active hydrocarbon cracking catalysts. The high activity of H-USY compared to HY zeolite has been previously explained by the generation of unusually strong and active BrØnsted acid sites, or an crease in the

number of accessible sites in a micropore diffusion controlled reaction. However, neither model explains the accumulated literature observations. A model was proposed that incorporate a change in the predominant cracking reaction mechanism as a function of alkane conversion and the very different rates of these mechanisms. Additionally, an oligometric cracking mechanism is introduced to explicitly account for coking and deactivation of the catalyst. The model is capable of accounting for must literature results. It concludes that the large enhancement in cracking activity by steaming is due to a proportionally smaller increase in external surface area of the zeolite crystals and possibly a small increase in the specific initiation activity of each site. These small changes lead to a much larger overall effect because of the sensitive dependence of oligometric cracking and, to a lesser extent, bimolecular cracking on the alkene partial pressure.

Vaughan and coworkers (Vaughan et al., 2000) insisted that the present invention relates to a method for preparing novel high silica zeolitic catalyst compositions having a high silica to alumina ratio and a crystallinity of at least about 70%. The method involves cation exchanging an as synthesized faujasite material having a silica to alumina ratio greater than about 4 with a component selected from the group consisting of ammonium ions and mineral acids, then steam calcining said cation exchanged faujasite in a single steam calcination step at a temperature from about 900°F to about 1500°F.

CHAPTER 2

THEORY

Zeolites are a well defined (Dyer,1988) class of crystalline naturally occurring aluminosilicate minerals. They have three–dimensional structures arising from a framework of $[SiO_4]^{4-}$ and $[AlO_4]^{5-}$ coordination polyhedral as shown in Figure 2-1, linked by all their corners. The frameworks generally are very open and contain channels and cavities in which are located cations and water molecules as shown in Figure 2-2. The cations often have a high degree of mobility giving rise to facile ion exchange and the water molecules are readily lost and regained: this accounts for the well-known desiccant properties of zeolites.
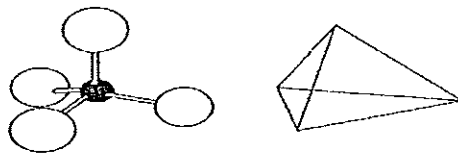
Figure 2-1 Representations of $[SiO_4]^{4-}$ or $[AlO_4]^{5-}$ tetrahedral (Dyer,1988)

The word "zeolite" has Greek roots and means "boiling stones" an allusion to the visible loss of water noted when the natural zeolites are heated. This property, of course, illustrates their easy water loss and is described as "intumescence".

Many of the natural zeolites can be produced synthetically and several crystalline aluminosilicates with framework structures with no known natural counterpart have been made in the laboratory. The best known example of a synthetic zeolite is a zeolite A, which can be related structurally to naturally occurring zeolites and so justify its inclusion as a zeolite mineral. It, like other synthetic zeolites, exhibits the definitive zeolitic properties of ion exchange and reverse water loss.

Another characteristic zeolite property arises from their molecular framework structures in that the assemblages of tetrahedral creating their porous structure happen to create regular arrays of apertures. These apertures are of such a site as to be able to

15
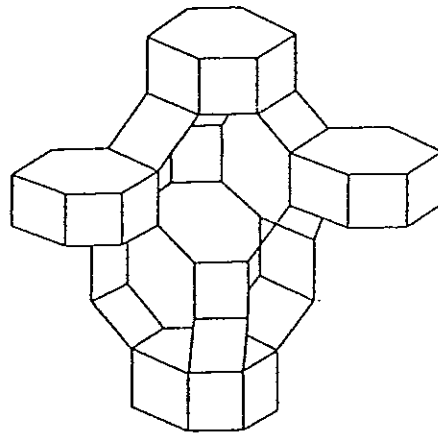
Figure 2-2 The framework structure of chabazite. Each line represents an oxygen atom and each junction a silicon or aluminum (Water molecules fill the space in the cages and cations float in this aqueous environment) (Dyer,1988)

selectivity take up some molecules into their porous structure, whilst rejecting others on the basis of their larger effective molecular dimensions. This is the property of "molecular sieving", largely unique to zeolites and responsible for their first commercial success.

2.1 Natural zeolites and their occurrence

In 1756 a Swedish mineralogist, Cronstedt, recognized a new mineral species which he called " zeolite " on the basis of its intumescence. He found zeolites in relatively small cavities in rocks of volcanic origin, a classical zeolite occurrence.

In the short space of 25 years zeolites have become recognized as one of the most abundant mineral species on earth, an unparalleled change from their " rarity "still chronicled in many museum displays. Natural zeolites still await large scale use, but they have some commercial usage. Current literature reflects the high interest shown in the prospects of natural zeolites as a new commodity. A detailed description of the modes and nature of their natural occurrences as follows;

2.1.1 Zeolites of saline alkaline lake origin

The creation of zeolites in a saline alkaline lacustrine environment which is typified by a closed basin in arid, or semi-arid, regions in which lake water of high sodium carbonate/bicarbonate content has gathered to produce a high pH (~9.5). Zeolites are laid down from reactive materials deposited in the lake. These materials are often "glasses" of volcanic origin, wind blown, and described as "vitric tuffs". Other substances forming zeolites under these conditions are biogenic silica, clays, plagioclase (feldspar) and forms of quartz.

Deposits of this type commonly contain phillipsite, clinoptilolite and erionite, but some include chabazite and mordenite. Zeolite locations of this sort are widespread in the Western USA (Figure 2-3) steaming from the Plio-Pleistocene era. Older deposits (Eocene, Cenozoic) often contain analcime, which arises from subsequent alteration of the zeolites in the younger rocks.

Figure 2-3 Locations of clinoptilolite found in the USA and formed in saline lacustrine environments. (Dyer,1988)

2.1.2 Zeolites in soils and land surfaces

Locations of this environment are typified by the San Joaquim valley, California and the Big Sandy Formation in Arizona, USA, as shown in Figure 2-4. Other well-studied sites are those in the Olduvai Gorge, Tanzania, and at Lake Magadi in Kenya.

Again dry, closed basins are required. In California the reactive material is mostly montmorillonite (a clay mineral) and the high pH is caused by evapotranspiration; analcime is the most to form phillipsite, natrolite, chabasite and analcime. Geologically these deposits are young (Pleistocene and Holocene), red-brown in color and very abundant. The zeolite content of the soils is low (15-40%) and a similar occurrence is reported in the Harwell series of soils of Berkshire (UK) which have a high heulandite content.

2.1.3 Zeolites in marine deposits

Marine zeolites readily form at shallow depths and low temperatures as well as at more substantial depths and higher temperatures. This latter condition will be discussed under burial diagenesis.

The *Glomar Challenger* oceanographic survey ship drilled to depths of 400-700 m in the Pacific ocean bed and found abundant occurrences of phillipsite and clinoptilolite as shown in Figure 2-5. Analcime, erionite and mordenite were also present.
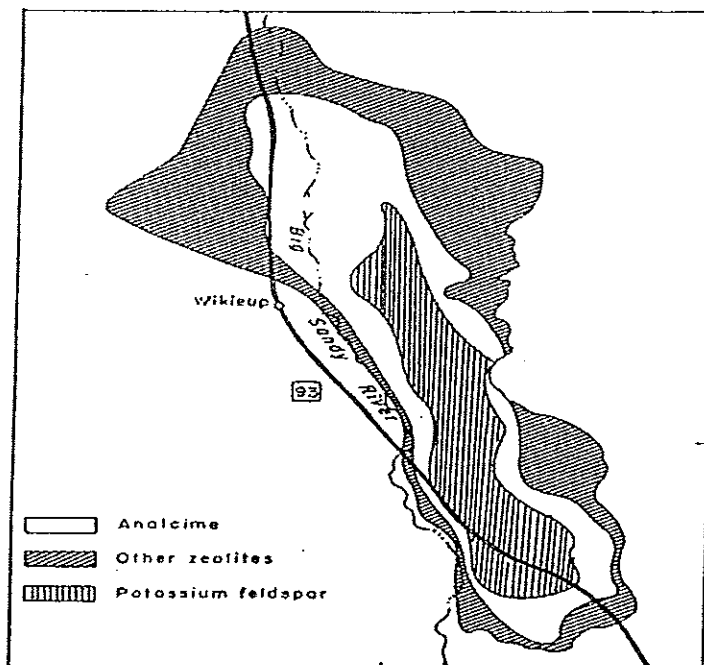
Figure 2-4   Simplified map of the Big Sandy Formation in Arizona, USA, showing zeolite distributions. (Dyer, 1988)

They seemed to have been formed principally from the action of trapped salt solutions (pore fluids) on glasses of underwater volcanic origin. Similar circumstances have formed zeolites under the Indian and Atlantic Oceans. In some cases biogenic silica contributes to clinoptilolite production. Analcime, present again, is thought to arise from slow alteration of other zeolite species over a period of some 100 million years. With further passage of time it is probable that further changes occur to feldspars which emerge as a decrease in zeolite content noted in rocks of marine origin from the Mezozoic and Paleozoic eras.
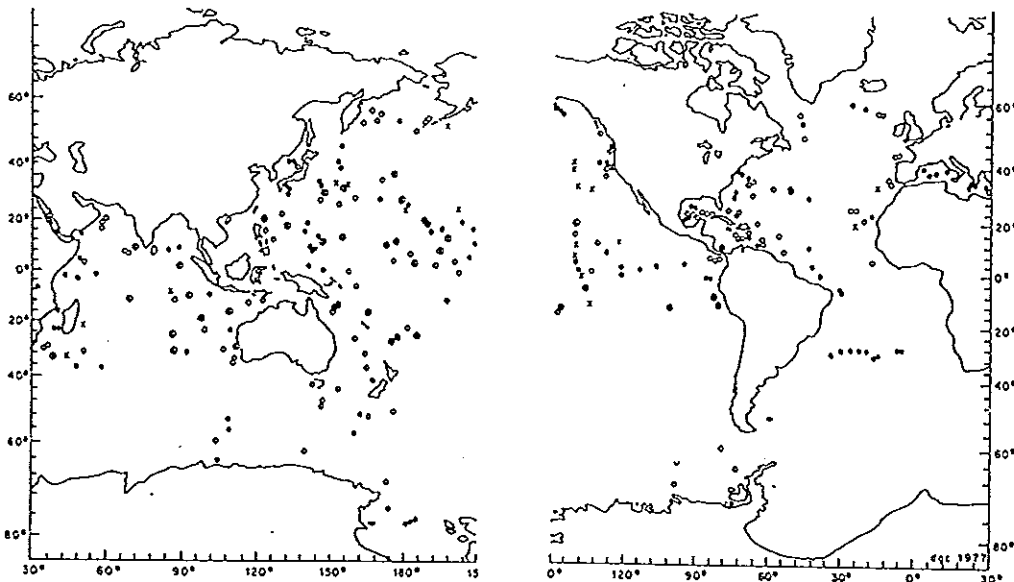
Figure 2-5 Distribution of phillipsite (x) and clinoptilolite (o) in cores from ocean bed analysis. Solid points are core analyses with no zeolites present. (Dyer,1988)

2.1.4 Zeolites from open flowing systems

Zeolites can be formed when flowing waters of high pH and salt content interact with vitric volcanic ash causing rapid crystal formation. Sites demonstrating this genesis have been recorded in Nevada, in the Koko Crater (Hawaii) and in the abundant tuffs in

Southern Italy (typified by the yellow Neopolitan ashes). Tuffs is Southern Italy commonly contain 60% chabazite with some 10% phillipsite.

Evidence suggests that time scales as short (by geological standards) as 4000 years are needed for these formations to occur. The high pH of the system stems from hydrolysis of the volcanic ash by surface water. Clinoptilolite, analcime, phillipssite and chabasite are found in these locations.
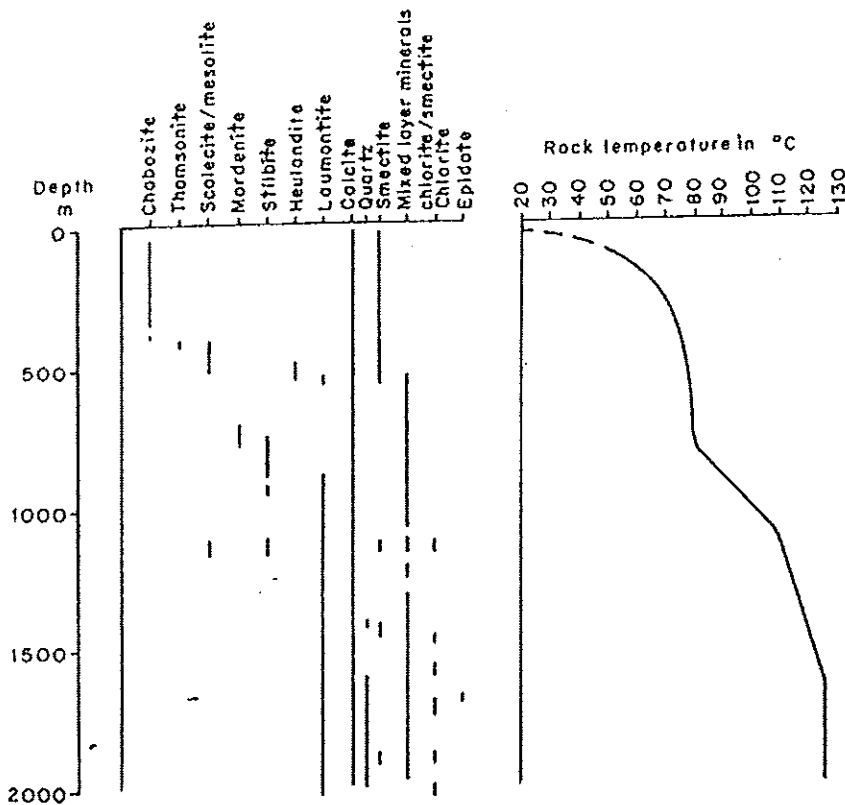
Figure 2-6 Zoning of zeolites with borehole depth in a hydrothermal environment. (Dyer,1988)

2.1.5 Hydrothermally treated zeolites

Zeolites are well known in Yellowstone Park (USA), in Iceland and in Wairakei (New Zealand) where they have formed from geothermal (geyser) action on existing volcanic ash. Often deposits occur in well-defined zones as shown in Figure 2-6, with deeper (hotter) environments containing analcime, heulandite, laumontite and wairakite. Ferrierite, thomsonite, chabazite, mesolite, scolecite and stilbite are also known in hydrothermal zones.

An anachronism of zeolite science is worth nothing here. As yet no true synthesis of laumontite has been reported (although a seeded one exists), but it has been reliably reported as being all too easily formed in the central heating system of a Russian city in Kamchatka, fed by natural hot spring water.

2.1.6 Zeolites formed by burial diagenesis

This classification relates to minerals formed as a result of their depth of burial, by subsequent layers of geologic species, and the consequential geothermal gradient. This group has strong associations with deep-sea and hydrothermal conditions. It reflects decreases in hydration with increased depth, so relatively porous zeolites (clinoptilolite and mordenite) are found above those of a less open nature (analcime, heulandite and laumontite)

Deposits of this nature have been described in the Green Tuff region of Japan and in the John Day formation in Oregon, USA.

2.2 The structure of zeolites

At present some 39 naturally occurring zeolite species have been recorded and their structures determined. In addition more than 100 synthetic species with no known natural counterparts have been reported in the literature. Relatively few of these have been confirmed as new zeolites and the majority awaits full structural determination. This topic will describe the major structural classes of known zeolites together with a more detailed consideration of those zeolites of current commercial significance.

2.2.1 Fundamental zeolite structural units

As stated earlier all zeolites have framework (three-dimensional) structures constructed by joining together $[SiO_4]^{4-}$ and $[AlO_4]^{5-}$ coordination polyhedral. By definition these tetrahedral are assembled together such that the oxygen at each tetrahedral corner is shared with that in an identical tetrahedron (Si or Al), as shown in Figure 2-7.This corner (or vertex) sharing creates infinite lattices comprised of identical building blocks (unit cells) in a manner common to all crystalline materials.
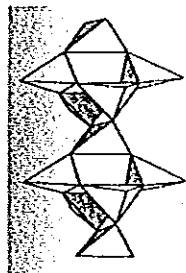
Figure 2-7 Tetrahedral linked together to create a three-dimensional structure.

(Dyer, 1988)

One way to classify zeolite structures would be to relate them to the symmetry of their unit cells. However, this would be cumbersome and is much simplified by the observation that zeolite structures often have identical (or very similar) repeating structural sub-units which are less complex than their repeating unit cells.

These recurring units are called " secondary building units " (SBU) and the simplest, most utilitarian, classification describes all known zeolite frameworks as arrangements linking eight SBU shown in Figure 2-8. These denote only the aluminosilicate skeleton (i.e. the Si, Al and O positions in space relative to each other) and exclude consideration of the cation and water moieties sited within the cavities and channels of the framework. The cation and water sites are complex and only fully defined in certain zeolites as will become apparent later.
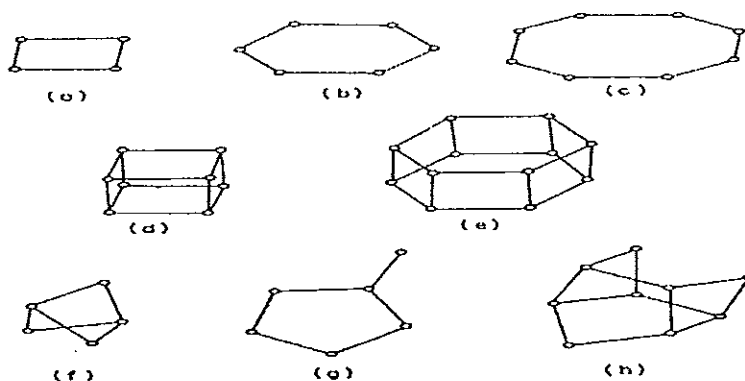
Figure 2-8 The secondary building units (SBU) recognized in zeolite framework; (a) single four ring (S4R), (b) single six ring (S6R), (c) single eight ring (S8R), (d) double four ring (D4R), (e) double six ring (D6R), (f) complex 4-1, (g) complex 5-1 and (h) complex 4-4-1. (Dyer, 1988)

For the present it should be noted that the number of cations present within a zeolite structure is determined by the number of $[AlO_4]^{5-}$ tetrahedral included in the framework. This arises from the isomorphous substitution of Al^{3+} for Si^{4+} into the component polyhedral, causing a residual negative charge on the oxygen framework. This negative charge is compensated by those cations present in the synthesis and held in the interstices of the structure on crystallization. The extent and location of water molecule incorporation depends upon (i) the overall architecture of the zeolite molecular structure, i.e. the size and shape of the cavities and channels present, and (ii) the number and nature of the cations in the structure.

The aluminosilicate skeleton can be represented in a number of ways, as for example in the traditional " ball and stick " model as shown in Figure 2-9. The most favoured is the use of tetrahedral arrays, adopted by organic chemists, where the oxygen atoms are drawn as single bonds joining together tetrahedral centers depicting silicon and aluminum. This is the method used in Figure 2-8. Further perusal of Figure 2-8 shows that each SBU contains rings of tetrahedral which are equivalent to rings of oxygen atoms described as "single four rings", "single six rings", etc. as shown in Figure 2-10.
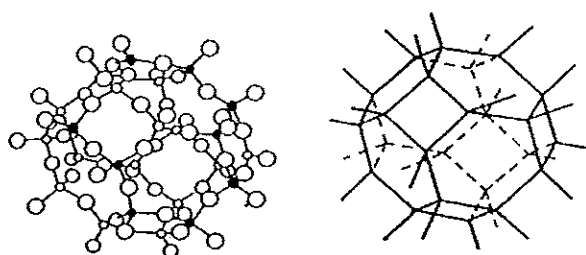
Figure 2-9 A "ball and stick" representation of the structure of the sodalite unit (left) with a framework diagram (like Figure 2-2) for comparison. (Dyer, 1988)
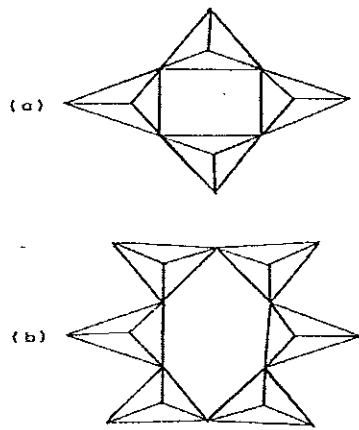
Figure 2-10 The arrangement of tetrahedrals in the (a) S4R and (b) S6R SBU.

(Dyer, 1988)

When the SBU are joined to create the infinite lattices they can proscribe larger rings containing 8, 10 or 12 linked tetrahedral (i.e. rings of 8, 10 or 12 oxygen atoms). These rings are obviously important structural features and are often called ' oxygen windows '.

2.2.2 Classification of zeolite structures

The zeolites comprise the largest group of aluminosilicate with framework structures since there are over 35 known different framework topologies and an infinite number possible.

Early interpretations of the physical and chemical properties of zeolites were based upon fragmentary structural information. As a result of investigations during the last ten years, there is extensive information on the crystal structure of over 35 different zeolites; this is detailed in a few instances and cursory in others. Nearly 100 synthetic types have been reported. Zeolites are classified into groups according to common features of the aluminosilicate framework structures. Important properties now have a structural interpretation. The properties, which are structural-related, include:

1. High degree of hydration and the behavior of ' zeolitic' water.

2. Low density and large void volume when dehydrated.

3. Stability of the crystal structure of many zeolites when dehydrated and when as much as 50 vol% of the dehydrated crystal are void.

4. Cation exchange properties.

5. Uniform molecular-sized channels in the dehydrated crystals.

6. Various physical properties such as electrical conductivity.

7. Adsorption of gases and vapors.

8. Catalytic properties.

In order to understand and relate these properties, new concepts were needed concerning the spatial arrangement of the basic structural components, i.e., the tetrahedral, cations, and H_2O molecules.

The classification used in this topic is based on the framework topology of the zeolites for which the structures are known. The classification consists of seven groups; within each group, zeolites have a common sub unit of structure which is a specific array of (Al, Si)O_4 tetrahedral. In the classification, the Si-Al distribution is neglected. For example, the two simplest units are the ring of four tetrahedral (4-ring) and six tetrahedral (6-ring) as found in many other framework aluminosilicate. These subunits have been called *secondary building units* (SBU). (The primary units are of course the SiO_4 and AlO_4 tetrahedral). In some cases, the zeolite framework can be considered in terms of polyhedral units, such as the truncated octahedron. Some of the SBU are probably involved in crystal growth processes.

The classification, which follows, is based on seven groups. Although, in other classifications, each group has been named after a representative member, an arbitrary designation by number is preferable since no single member is more representatives than any other.

In many instances aperture sizes determined for hydrated zeolites are not consistent with the molecular sieve properties of the dehydrated crystals; this is due to distortion of the framework upon dehydration and the presence of cations in channels. Accurate data on the positions of cations and water molecules are available for some of the hydrated zeolites; positions of cations in some dehydrated zeolites are known. Upon dehydration some of the cations assume different positions in the structure.

Zeolites A, X, Y, ZK-5, faujasite, and paulingite have frameworks consisting of linked truncated octahedral (β-cages) characteristic of the structure of sodalite. Some of the synthetic zeolites are structurally related to minerals and are included in this classification; however, for most of the synthetic zeolites the structures are not known (Table 2.2).

Table 2-1 Shows the zeolites classification based on the secondary building unit (SBU) into 7 groups (Breck,1974)

Group	Secondary Building Unit (SBU)
1	Single 4-ring, S4R
2	Single 6-ring, S6R
3	Double 4-ring, D4R
4	Double 6-ring, D6R
5	Complex 4-1, T_5O_{10} unit
6	Complex 5-1, T_8O_{16} unit
7	Complex 4-4-1, $T_{10}O_{20}$ unit

2.2.3 Classification of zeolite structure by SBU content

Tables 2-3 to 2-7 list known zeolite structures classified by (i) their sbu content, (ii) structure type (IUPAC nomenclature), (iii) name (prefix " zeolite " means that the material is known only as a synthetic material) and (iv) typical unit content.

Table 2-2 Some synthetic zeolites with unknown structures (Breck,1974)

Name	Typical Composition or Unit Cell Contents	Crystal Data [f]	Density g/cc [a]	Void Volume cc/g	Approximate Pore Size, A [c]
Li-A	$Li_2Al_2Si_2O_8 \cdot 4 H_2O$ [b]	Orthorhombic	--	0.15	2.6
F	$K_{11}[(AlO_2)_{11}(SiO_2)_{11}] \cdot 16 H_2O$	Tetragonal a = 10.4, c = 13.9	2.28	0.16	2.6+
Z	$K_2Al_2Si_2O_8 \cdot 3 H_2O$ [b]	--	--	0.14	2.6
H	$K_{14}[(AlO_2)_{14}(SiO_2)_{14}] \cdot 28 H_2O$	Hexagonal a = 13.4, c = 13.2	2.18	0.22	2.6
Li-H	$Li_2Al_2Si_8O_{20} \cdot 5 H_2O$ [b]	Tetragonal	--	0.16	2.6
J	$K_7[(AlO_2)_7(SiO_2)_7] \cdot 4 H_2O$	Tetragonal a = 9.45, c = 9.92	2.22	0.08	2.6
E	$(K,Na)_2Al_2Si_2O_8 \cdot 3.3 H_2O$	--	--	0.21	2.6+
M	$K_{14}[(AlO_2)_{14} (SiO_2)_{14}] \cdot 12 H_2O$	Tetragonal a = 13.1, c = 10.5	2.37	0.10	2.6
Q	$K_{40}[(AlO_2)_{40}(SiO_2)_{44}] \cdot 86 H_2O$	Tetragonal a = 13.5, c = 35.2	2.11	0.23	2.6
W	$K_{42}[(AlO_2)_{42}(SiO_2)_{76}] \cdot 107 H_2O$	Cubic, a = 20.1	2.18	0.22	3.6
N [d]	$(Na,TMA)_2O \cdot Al_2O_3 \cdot 1.8\text{-}2.2 SiO_2 \cdot Y H_2O$	Cubic, 37.2	--	0.16	2.6
ZSM-2	$Li_2O \cdot Al_2O_3 \cdot 3.3\text{-}4.0 SiO_2 \cdot Y H_2O$	Tetragonal, a = 27.4, c = 28.1	--	0.22	6+
ZSM-3	$(Na,Li)_2O \cdot Al_2O_3 \cdot 2.8\text{-}4.5 SiO_2 \cdot 9 H_2O$	Hexagonal, a = 17.5	--	0.30	6+
ZSM-4	$(TMA,Na)_2O \cdot Al_2O_3 \cdot 6\text{-}15 SiO_2 \cdot 5 H_2O$	Cubic, a = 22.2	--	0.14	6+
ZSM-5 [e]	$(TPA,Na)_2O \cdot Al_2O_3 \cdot 5\text{-}100 SiO_2 \cdot Y H_2O$	Tetragonal a = 23.2, c = 19.9	--	0.10	6
ZSM-10 [g]	$(R,K_2)O \cdot Al_2O_3 \cdot 5\text{-}7SiO_2 \cdot 9 H_2O$	--	--	0.14	6+
BETA [h]	$(TEA,Na)_2O \cdot Al_2O_3 \cdot 5\text{-}100 SiO_2 \cdot 4 H_2O$	Cubic, a = 12.04	--	0.20	6+
Z-21	$Na_2O \cdot Al_2O_3 \cdot 1.7\text{-}2.1 SiO_2 \cdot 9 H_2O$	Cubic, a = 36.7	--	0.14	2.6

[a] Density measured for fully hydrated zeolite.
[b] Unit cell constants not determined.
[c] Pore size determined by adsorption. Value of 2.6 A, for example, indicates water and ammonia adsorbed by dehydrated zeolite.
[d] TMA = tetramethylammonium

[e] TPA = tetrapropylammonium
[f] Cell dimensions from x-ray powder data are uncertain.
[g] R = $[1,4\text{-dimethyl-1,4-diazoniabicyclo} (2,2,2) octane]^{2+}$
[h] TEA = tetraethylammonium.

Comments on Tables 2-3 to 2-7

As with all classifications there are queries and possible anomalies in the lists of structures given in these tables. It can be seen (Table 2-7) that barrerite is the sodium form of stellerite and that they have the same framework. There are other equally obvious examples of the same resemblance (see the natrolites in Table 2-5). The justification for their inclusion rather than the quotation of the frameworks alone is that the list includes all the known zeolite minerals recorded and confirmed in the literature. Omitted from the tables are (a) some synthetic zeolites unlikely to be of commercial interest, (b) ' new zeolites ' whose structures have not yet been determined, (c) zeolite-like minerals and (d) zeotypes. Table 2-8 lists examples from these categories with comments.

Other points to note are the following:

(1) Zeolite Y is isostructural with zeolite X (and faujasite). It differs in its higher Si: Al ratio (in the relatively lower amount of isomorphous substitution of Al for Si into tetrahedral framework position) and this caused a drop in the number of cations present in the framework and an increase in the number of water molecules present.

(2) Zeolite A also has a structural isotype described as ZK-4.

(3) Mazzite is the first recorded example of a zeolite known initially as a synthetic material (zeolite Omega) and later found in nature.

(4) Mordenite is described in various publications as " large and small port ". This distinction relates to two types of mordenite having different molecular sieve properties. There is no firm evidence for any framework structural variation between these two varieties.

(5) Varieties of sodalite and cancrinite have been included despite the fact that, mineralogically speaking, they are not zeolites but felspathoids. They are in the tables because their cage structures (Figure 2-11) play important roles in some zeolite frameworks. When synthesized with the unit cell compositions quoted, they possess zeolitic properties. In nature they contain salt molecules trapped inside their cages hence the mineralogical distinction. The salts can be washed out leaving materials of zeolitic type. Sodalite hydrate often is describe d as " hydroxy sodalite " (HS).

(6) Two variations in notation commonly arise. Analcime is often referred to as 'analcite ' and levynite as ' levyne'. Early literature had many synonyms for the natural zeolites and some of the more common examples are listed in Table 2-8.

Table 2-3 Zeolite structures based upon single oxygen ring SBU. (Dyer,1988)

Secondary building unit (SBU)	Structure type	Name	Typical unit cell content
S4R	ANA	Analcime	$Na_{16}Al_{16}Si_{32}O_{96}10H_2O$
	ANA	Wairakite	$Ca_8Al_{16}Si_{32}O_{96}16H_2O$
	GIS	Gismondine	$Ca_4Al_8Si_8O_{32}16H_2O$
	GIS	Amicite	$K_4Na_4Si_8O_{32}10H_2O$
	GIS	Garronite	$NaCa_{2.5}Al_6Si_{10}O_{32}14H_2O$
	GIS	Gobbinsite	$Na_5Al_5Si_{11}O_{32}11H_2O$
	GIS	Zeolite NaP-1	$Na_6Al_6Si_{10}O_{32}12H_2O$
	LAU	Laumontite	$Ca_4Al_8Si_{16}O_{48}16H_2O$
	MER	Merlionite	$K_5Ca_2Al_9Si_{23}O_{64}24H_2O$
	PAU	Paulingite	$(K_2,Na_2,Ca,Ba)_{76}Al_{152}$
	PHI	Phillipsite	$Si_{520}O_{1244}700H_2O$
	PHI	Harmotome	$K_2Ca_{0.5}NaAl_6Si_{10}O_{32}12H_2O$
	YUG	Yugawaralite	$Ba_2Ca_{0.5}Al_5Si_{11}O_{32}12H_2O$
			$Ca_4Al_4Si_{12}O_{32}8H_2O$
S6R	CAN	Cancrinite hydrate	$Na_6Al_6Si_6O_{24}8H_2O$
	ERI	Erionite	$Na_3K_2Mg_{0.5}Ca_2Al_9Si_{27}O_{72}27H_2O$
	LEV	Levynite (Levyne)	$NaCa_3Al_7Si_{11}O_{36}18H_2O$
	LTL	Zeolite L	$K_6Na_3Al_9Si_{27}O_{72}21H_2O$
	LOS	Zeolite Losod	$Na_{12}Al_{12}Si_{12}O_{48}19H_2O$
	MAZ	Mazzite (Zeolite Omega)	
		Offretite	$Mg_2K_3Ca_{1.5}Al_{10}Si_{26}O_{72}$ $28H_2O$
	OFF	Sodalite hydrate(HS)	$KCa_2Al_5Si_{13}O_{36}15H_2O$
	SOD		$Na_6Al_6Si_6O_{24}8H_2O$

S8R   Occurs in many structures but with other SBU (see structure of zeolite A, chabazite, etc.)

Table 2-4 Zeolite structures based upon double oxygen ring SBU. (Dyer,1988)

Secondary building unit (SBU)	Structure type	Name	Typical unit cell content
D4R	LTA	Zeolite A	$Na_{12}Al_{12}Si_{12}O_{48}27H_2O$
D6R	CHA	Chabazite	$Ca_2Al_4Si_8O_{24}13H_2O$
	CHA	Wilhendersonite	$K_2Ca_2Al_6Si_6O_{24}10H_2O$
	FAU	Faujasite	$Na_{12}Ca_{12}Mg_{11}Al_{58}Si_{134}O_{384}235H_2O$
	FAU	Zeolite X	$Na_{88}Al_{88}Si_{104}O_{384}220H_2O$
	GME	Gmelinite	$Na_8Al_8Si_{16}O_{48}24H_2O$
	KFI	Zeolite ZK-5	$Na_{30}Al_{30}Si_{66}O_{192}98H_2O$
	RHO	Zeolite Rho	$(Na,Cs)_{12}Al_{128}Si_{56}O_{55}46H_2O$

Table 2-5 Zeolite structures based upon the 4-1 SBU. (Dyer,1988)

Secondary building unit (SBU)	Structure type	Name	Typical unit cell content
4-1	EDI	Edingtonite	$Ba_2Al_4Si_6O_{20}8H_2O$
	NAT	Natrolite	$Na_{16}Al_{16}Si_{24}O_{80}16H_2O$
	NAT	Tetranatrolite	$Na_{16}Al_{16}Si_{24}O_{80}16H_2O$
	NAT	Paranatrolite	$Na_{16}Al_{16}Si_{24}O_{80}16H_2O$
	NAT	Mesolite	$Na_{16}Ca_{16}Al_{48}Si_{72}O_{240}64H_2O$
	NAT	Scolecite	$Ca_8Al_{16}Si_{24}O_{80}24H_2O$
	THO	Thomsonite	$Na_4Ca_8Al_{20}Si_{20}O_{80}24H_2O$
	THO	Gonnardite	$Na_5Ca_2Al_9Si_{11}O_{40}14H_2O$

Table 2-6 Zeolite structures based upon the 5-1 SBU. (Dyer,1988)

Secondary building unit (SBU)	Structure type	Name	Typical unit cell content
5-1	BIK	Bikitaite	$Li_2Al_2Si_4O_{12}2H_2O$
	DAC	Dachiardite	$Na_5Al_5Si_{19}O_{48}12H_2O$
	EPI	Epistilbite	$Ca_3Al_6Si_{18}O_{48}16H_2O$
	FER	Ferrierite	$NaCa_{0.5}Mg_2Al_6Si_{30}O_{72}20H_2O$
	MFI	Zeolite ZSM-5	$Na_nAl_nSi_{96-n}O_{192}\sim16H_2O$ (n~3)
	MOR	Mordenite	$Na_8Al_8Si_{40}O_{96}24H_2O$

Table 2-7 Zeolite structures based upon the 4-4-1 SBU. (Dyer,1988)

Secondary building unit (SBU)	Structure type	Name	Typical unit cell content
4-4-1	BRE	Brewsterite	$Sr_2Al_4Si_{12}O_{32}10H_2O$
	HEU	Heulandite	$Ca_4Al_8Si_{28}O_{72}24H_2O$
	HEU	Clinoptilolite	$Na_6Al_6Si_{30}O_{72}24H_2O$
	STI	Stilbite	$Na_2Ca_4Al_{10}Si_{26}O_{72}34H_2O$
	STI	Stellerite	$Ca_4Al_8Si_{28}O_{72}28H_2O$
	STI	Barrerite	$Na_8Al_8Si_{28}O_{72}26H_2O$

Table 2-8 (a) Other natural and species cited in zeolite literature. (Dyer,1988)

Natural species	Comment
Afghanite(AFG)	
Liottite(LIO)	
Franzinite	All variations on cancrinite or sodalite structures
Sacrofanite	
Giuseppettite	Multiply twinned and highly faulted dachiardite
Svetlozarite	Analcime with a high magnesium content
Doranite	A beryllium silicate similar to bikitaite(zeotype)
Chiarennite	A beryllium silicate (another zeotype)
Hsianghualite	$Li_{16}Ca_{24}Be_{24}Si_{24}O_{96}F_2$(zeotype)
Lovdarite(LOV)	$Na_{0.5}K_{0.5}Ca_{5.5}Ba_{3.5}Si_{11}Al_9O_{41}(OH_2)(SO_4)_3H_2O$
Wenkite(WEN)	$Ca_{16}(Al_{16}Si_{32}O_{88}OH_{16})[OH]_{16}26H_2O$
Roggianite(ROG)	$Ca_8Al_{16}Si_{16}O_{64}16H_2O$
Partheite(PAR)	May be isostructural with Zeolite L
Perlialite	$Na_2Ca_{10}(Al_{20}Si_6P_{10}O_{60}(OH)_{32})_{16}H_2O$
Viseite	(a natural zeotype with analcime framework)
	Naturally occurring phosphoaluminate with the analime
Keoheite	framework(another natural zeotype)
Leucite	Felspathoid with analcime framework($K_{16}Al_{16}Si_{32}O_{96}$)
	Caesium felspathoid with analcime framework ($Cs_{16}Al_{16}Si_{32}O_{96}$)
Pollucite	Chabazites with pseudo-hexagonal crystal habits
	Partially dehydrated laumontite
Herschelite, phacolite	Barium variety of phillipsite
Leonhardite	Ca6Al2Si12O3210H2O Structure of 4-, 6- and 8- membered rings
Wellsite	with some resemblances to brewsterite but not allocated as yet
Goosecreekite(GOO)	to the groupings in Table IV
	$Ca_6Al_2Si_{18}O_{60}36H_2O$ (structure unknown)
Cowlesite	

Table 2-8 (contd.)

(b) Outmoded names for zeolites

Natural species	Old names
Chabazite	Acadialite, haydenite
Epistilbite	Parastilbite, orizite, reissite
Gismondine	Zeagonite
Laumontite	Caporcianite, lomontite, scheiderite, sloanite
Mordenite	Ptilolite, arduinite, pseudo natrolite
Natrolite	Galaktite
Phillipsite	Christianite
Stellerite	Epidesmine
Stilbite	Desmine, foresite
Thomsonite	Fareolite, comptonite

(c) Synthetic zeolite phases[a]

Name	Comment
Li-A(BW)(ABW)	Structure known
TMA-E(AB)(EAB)	Structure known
Linde type N(LTN)	Structure known
Na,K-F	Isostructural with zeolite F,Rb-D,edingtonite
P[b],Q	ZK-5 structures
Nu, Fu	Structure known
Theta-1 (TON)	The only' two-dimensional zeolite' structure known Offretite phase
O	Gismondine structure
B	Merlionite structure
K-M, W	Isotype of zeolite L
Ba-G	Generic names for the ZSM-5(MFI), ZSM-11(MEL) family of
Pentasils	structures
Dodecasils	Phases of silica[c] with some significant zeolite properties(also called 'clathrosils' because of their structural similarities to clathrate hydrates)
ZSM-39(MTN)	
Silicate	
Nonasil(NON)	Structure known
ZSM-23(MTT)	Structure known
ZSM-12(MTW)	Polymorph of faujasite
ZSM-3	Mazzite structure
ZSM-4	Ferrierite structure
ZSM-21	Offerite/erionite structure intergrown
ZSM-34	

Noted of Table 2-8 (c)

[a] Not a comprehensive list, excludes many species not yet defined.

[b] Not to be confused with Na-P.

[c] Melanophlogite(MEP) is a naturally occurring phase of silica with zeolite properties (not yet synthesized).

Comments on Table 2-8

(1) The atlas of known zeolite structures also lists structure types associated with silica phases and related materials, e.g. NON (nonasil), DOH (dodecasil-1H) and DDR (deca-dodecasil-3R).

(2) Lovdarite, wenkite and roggianite have been included in the most recent atlas of structures.

Figure 2-11 The cancrinite (left) and sodalite cages. (Dyer,1988)

2.2.4 Specific zeolite topologies

The International Zeolite Association (IZA) has published a handbook, which presents a further, more detailed, view of zeolite frameworks. The handbook describes some 40 currently known zeolite topologies and assigns all known zeolite into these topological categories. Each framework has a code (see Tables 2-3 to 2-7) and a full list is given in Table 2-9.

Table 2-9 Zeolite frameworks recognized by the Structure Commission of IZA[a] (Dyer,1988)

Structure	Code	Structure	Code
Li-A(BW)	ABW	Linde type A	LTA
Afghanite	AFG	Linde type L	LTL
Analcime	ANA	Linde type N	LTN
Bikitaite	BIK	Mazzite	MAZ
Brewsterite	BRE	ZSM-11	MEL
Cancrinite	CAN	Melanophlogite	MEP
Chabazite	CHA	Merlionite	MER
Dachiardite	DAC	ZSM-5	MFI
Deca-dodecasil-3R	DDR	Mordenite	MOR
Dodecasil-1H	DOH	ZSM-39	MTN
TMA-E(AB)	EAB	ZSM-23	MTT
Edingtonite	EDI	ZSM-12	MTW
Epistilbite	EPI	Natrolite	NAT
Erionite	ERI	Nonasil	NON
Faujasite	FAU	Offretite	OFF
Ferrierite	FER	Partheite	PAR
Gismondine	GIS	Paulingite	PAU
Gmelinite	GME	Phillipsite	PHI
Goosecreekite	GOO	Rho	RHO
Heulandite	HEU	Roggianite	ROG
ZK-5	KFI	Sodalite	SOD
Laumontite	LAU	Stilbite	STI
Levyne	LEV	Thomsonite	THO
Liottite	LIO	Theta-1	TON
Losod	LOS	Wenkite	WEN
Lovdarite	LOV	Yugawaralite	YUG

[a] Not all these structures have yet been allocated to the formal groupings based upon sbu as listed in Table 2-3.

Each example chosen will include descriptions of the sites of cations and water molecules within the frameworks. It must be stressed that cation and water sittings in any zeolite framework are a function of temperature, water content, cation type and

silica to alumina ratio. In discussing this structural detail it has been decided to use the Angstrom (Å) unit rather than the correct SI unit (pm) to describe dimensional parameters. This decision has been taken in recognition of the fact that most of the zeolite literature (past and present) still used Å rather than pm.

2.2.5 Zeolites of group 4

The framework structures of the zeolites of group 4 are characterized by the double 6-ring, D6R, as the secondary building unit in their structural frameworks (Figure 2-8).

These include the minerals chabazite, gmelinite, and R (related to chabazite), S (related to gmelinite), and zeolites X and Y (related to faujasite). Zeolites L and ZK-5 have no known mineral relatives. Considerable information on the structures of these zeolites has been reported.

a) Faujasite – Type structures (Table 2-10, 2-11, and 2-12)

Zeolites X and Y and faujasite have topologically similar aluminosilicate framework structures, although they are distinct zeolite species with characteristic differences. The unit cells are cubic with a large cell dimension of nearly 25 Å and contain 192 (Si, Al)O_4 tetrahedral. The remarkably stable and rigid framework structure contains the largest void space of any known zeolite and amounts to about 50 vol % of the dehydrated crystal.

Chemical composition

The chemical composition of faujasite is given in Table 2-10. The published data indicate a complex cation distribution including calcium, sodium and variable amounts of potassium and magnesium.

The chemical compositions of zeolites X and Y are related to the synthesis method. The zeolites are distinguished on the basis of chemical composition, structure, and their related physical and chemical properties. Differences are found in the cation composition and distribution, the Si/ Al ratio and possible Si-Al ordering in tetrahedral sites.

In zeolites X and Y the relation between the number of tetrahedral Al atoms, N_{Al}, and the Si/Al ratio is:

$$N_{Al} = 192/\ (1+R) \qquad\qquad (2\text{-}1)$$

Where $R = N_{Si}/\ N_{Al}$

The aluminum ions (N_{Al}) in the unit cell of X vary from 96 to about 77. In zeolite Y N_{Al} is about 76 to 48. The value of R varies from 1 to 1.5 for zeolite X and from greater than 1.5 to about 3 for zeolite Y. For the hydrated zeolites as synthesized in the sodium form, a_0 increases from about 24.6 to 25.0 Å. (See Figure 2-12). The cell constant of faujasite, 24.67 Å (N_{Al} = 59) does not fit this relation. It is about 0.04 Å too small.

Framework structure (Figure 2-13)

The aluminosilicate framework consists of a diamond-like array of linked octahedral which are joined tetrahedral through the 6-rings. The linkage between adjoining truncated octahedral is a double 6-ring (D6R) or hexagonal prism, containing 12 (Si, Al)O_4 tetrahedral. The framework structure can also be described in terms of the D6R units. The aluminosilicate framework as illustrated by a model using skeletal tetrahedral is shown in Figure 2-13.
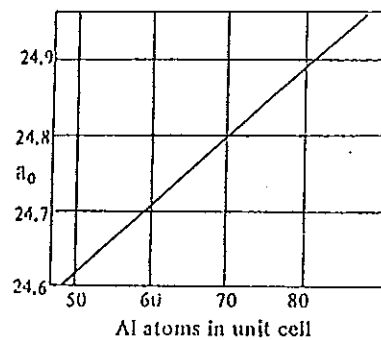
Figure 2-12 Relation between the cell constant, a_0, and aluminum atom density in number/ unit cell for hydrated sodium X and Y zeolites. The linear relation is $a_0 = 0.00868\ N_{Al} + 24.191$ which was established by least squres treatment of 37 experimental points. The Si/Al ratio was determined by wet chemical analysis of 37 pure preparations. Analytical error$\pm$0.5% in SiO_2 and Al_2O_3. Error in a_0 determination estimated to be less than$\pm$ 0.005.$a_0 = (192b/(1+(N_{Si}/N_A)) + c$ where b and c are the slope (0.00868) and intercept (24.191), respectively, of the linear relation (Breck,1974)
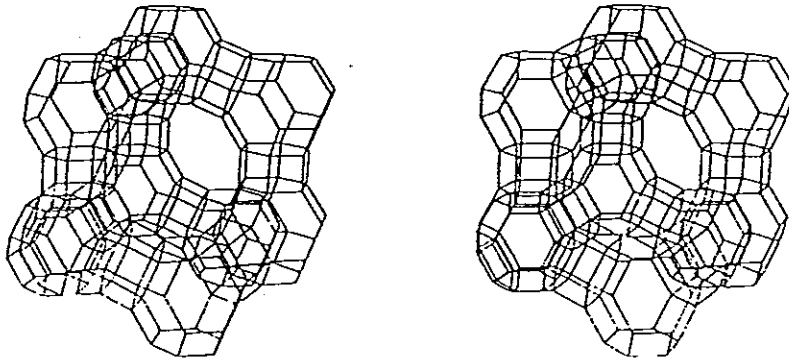
Figure 2-13 The structure of faujasite as a stereopair (Dyer,1988)

Models illustrate more clearly the nature of the internal surface of the zeolite (Figure2-14).
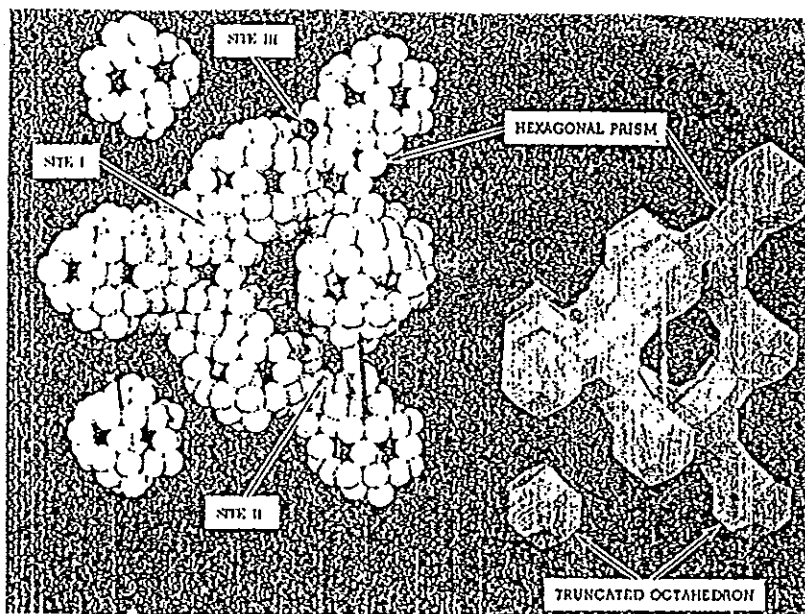
Figure2-14 The structure of zeolites X and Y, and faujasite as depicted by a model showing the spacial arrangement of truncated octahedral units in a diamond-type array. The space- filling model showing the approximate location of oxygen atoms in the framework is also pictured. The arrangement of truncated octahedral in one unit cell is shown. The larger 12 ring is visible as well as the smaller 6-rings which form apertures into the β-cages. The cation positions typical of zeolite X are illustrated as site I within the hexagonal prism unit, site II adjacent to the single 6-rings, and site III within the main cavities (Breck,1974)

Six cation sites have been defined as shown in Figure 2-15. Approximate locations of sites II, III, and I are also shown in the model in Figure 2-14. During initial

crystal structure studies on hydrated zeolite X, 48 out of 80 Na$^+$ ions (per unit cell) were located in site II and I position. Considerable evidence suggests that the remaining cations and the water molecules behave as a strong electrolyte solution and float freely through the framework. This concept is supported by the infrared spectrum which shows the stretch and deformation frequencies of normal water molecules, the heat of adsorption of water which in zeolite X is comparable to the heat of vaporization of water, self-diffusion studies which show that the sodium ions undergo exchange very rapidly, and electrical conductivity studies which have shown that the cations in hydrated zeolite X behave in the same way as they do in salt solutions. The cations must move upon dehydration from positions where they are coordinated with water positions near framework oxygens. In sodium-enriched faujasite crystals, the sites I position are vacant.
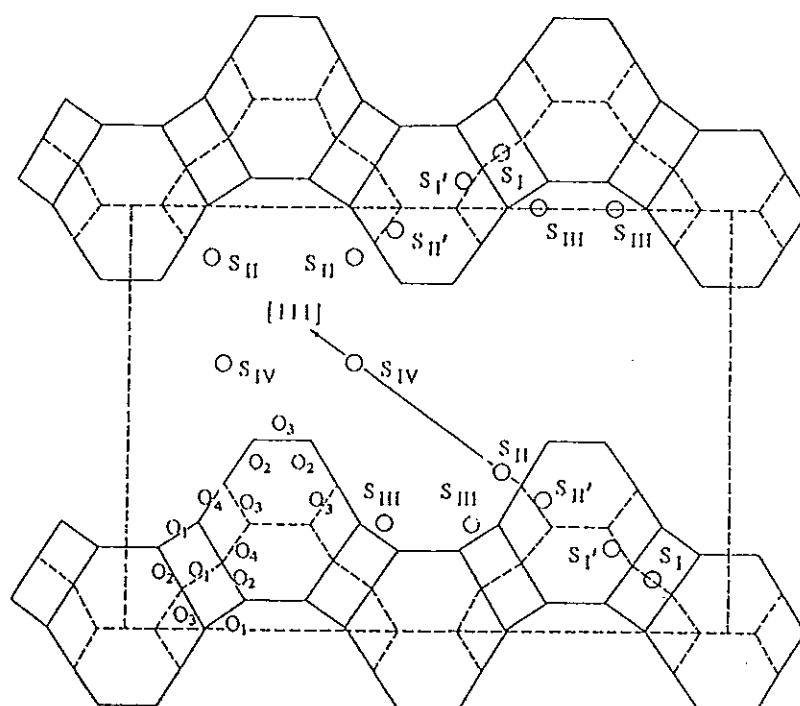
Figure 2-15 The cation sites and their designation in zeolites X, Y, and Faujasite. Starting at the center of symmetry and proceeding along the 3-fold axis toward the center of the unit cell, site I is the 16-fold site located in the center of the double 6-ring (hexagonal prism). Site I' is on the inside of the β-cages adjacent to the D6R. Site II' is on the inside of the sodalite unit adjacent to the single 6-ring. Site II approaches the single 6-ring outside of the β-cage and lies within the large cavity opposite site II'. Site III refers to positions in the wall of the large cavity, on the 4-fold axis in the large 12-ring aperture. The 4 different types of oxygen's O (1), O (2), O (3), O (4) are also indicated in their relative positions (Breck, 1974).

Cation positions in hydrated faujasite-type zeolites (Table 2-13 to 2-15)

Faujasite, when fully hydrated, contains about 235 water molecules distributed in the large supercages and the small β-cages. Structural investigations on hydrated faujasite of undetermined cationic composition, but assuming a total of 43 sodium and calciums ions per unit cell, have shown that 17 cations are located within the β-cages near site I (Figure 2-14) in a tetrahedral arrangement with 4 water molecules. There are four such cation positions within each cage. Each cation is surrounded by a distorted octahedron of three framework oxygens and three water molecules. The remaining 26 cations were not definitely located, but may occupy sites next to the single 6-rings inside the β-cages.

The difference in positions of sodium ions should be noted; site I in faujasite is not occupied by cations; in hydrated NaX, site I is occupied by nine Na^+ ions.

The location of Ca^+ ions in hydrated Ca exchanged faujasite are given in Table 2-13. Nearly all of the Ca^{2+} ions are located in the β-cages in site I' and site II'. Some appear to sit in the 12-rings at site IV. Distributions of other cations in the hydrated zeolites are given in Tables 2-13, 2-14, and 2-15.

Cation positions in dehydrated zeolites (Table 2-13, 2-14, and 2-15)

The Na^+ ions in dehydrated zeolite Y occupy three sites. On an average, 7.5 Na^+ ions were found in site I, 30 Na^+ ions in site II, and 20 Na^+ ions in site I'. Similar site occupancies in K exchanged and Ag exchanged zeolite Y were found.

From Tables 2-13, 2-14, and 2-15 it is apparent that the distribution of cations in the faujasite-type zeolites is dependent upon the presence of adsorbed water or residual OH groups. For example, the distribution of sodium changes from location in site I' and site II' to site I and site II upon hydration (Table 2-13). With polyvalent ions the situation is more complex and site I is preferred by calcium and nickel ions (Breck,1974).

The classification into seven groups should be extended to nine with the addition of the melanophlogite group based on the aluminosilicate analogs of the gas hydrates and the lovdarite group based on 3, 5 and 9-rings.

The nine groups of zeolites identified on the basis of their framework structure are given in Table 2-16 with idealized cell contents and crystallographic data and channel systems (Kokotailo,1983).

2.3 Modified Y – type zeolites involving proton – zeolite interactions. (Rabo,1974)

Most of the zeolite alterations and modifications we have considered represent fairly general phenomena that occur in a wide variety of zeolites. This is probably true also of the complex set of reactions that can occur between protons and a zeolite framework, but, Y-type zeolites have been the only ones for which many of these phenomena have been investigated to any great degree. This follows from the commercial importance that Y-type zeolites have attained and to their unique combination of properties, including a relatively high degree of thermal stability, a large open pore structure, and a reasonable tolerance to acid attack. Consequently, the remainder of our discussion will be centered on modifications of Y-type zeolites.

Structures and reactions related to proton-zeolite interactions in Y-type zeolites.

Several terms have been used to describe the complex maze of reactions and products from these zeolites, but unfortunately, the same or similar terms have been used by different authors with different meanings. The complexity of communication is

Table 2-10 Zeolite: Faujasite (Breck,1974)

Structure Group:	4
	Chemical Composition
Typical Oxide Formula:	$(Na_2,Ca,Mg,K_2)O \cdot Al_2O_3 \cdot 4.5SiO_2 \cdot 7H_2O$
Typical Unit Cell Contents:	$Na_{12}Ca_{12}Mg_{12}[(AlO_2)_{59}(SiO_2)_{133}] \cdot 235H_2O$
Variations :	K observed in variable amounts
	Mg observed in variable amounts
	Crystallographic Data
Symmetry: Cubic	Density: 1.91 g/cc
Space Group: Fd 3m	Unit Cell Volume:15,014 Å^3
Unit Cell Contents:	a = 24.67 Å
	Structural Properties
Framework:Figure 2-13	Truncated octahedra, β-cages, linked tetrahedrally through D6R's in arrangement like carbon atoms in diamond. Contains eight cavities,~ 13Å in diameter in each unit cell
SBU:	D6R, 16/uc Void volume: 0.47cc/cc

(Table 2-10, contd.)

Cage type:	β, 8/uc, 26-hedron(II). Framework density: 1.27 g/cc
Channel System:	Three-dimensional, II to $[110]$

Hydrated-

Free Apertures:	12 ring, 7.4Å, 6 ring, 2.2Å
Cation Locations:	Table 2-13

Dehydrated-

Cation Locations:	Table 2-13
Effect of Dehydration:	Stable and Reversible

Location of H_2O Molecules: 4 in each β-cage

Largest Molecule Adsorbed: $(C_4F_6)_3N$

Kinetic Diameter, σ, Å: 8.0

Table 2-11 Zeolite: X (Breck, 1974)

Structure Group:	4

Chemical Composition

Typical Oxide Formula:	$Na_2O \cdot Al_2O_3 \cdot 2.5SiO_2 \cdot 6H_2O$
Typical Unit Cell Contents:	$Na_{86}[(AlO_2)_{86}(SiO_2)_{106}] \cdot 264H_2O$
Variations :	Ga substitution for Al; Si/Al=1 to 5
	Na/Al=0.7 to 1.1

Crystallographic Data

Symmetry: Cubic	Density: 1.93 g/cc
Space Group: Fd 3m	Unit Cell Volume:15,362-15,670A³
Unit Cell Contents:	a = 25.02-24.86Å

Structural Properties

Framework: Figure 2-13	Truncated octahedra, β-cages, linked tetrahedrally through D6R's in arrangement like carbon atoms in diamond. Contains eight cavities,~ 13Å in diameter in each unit cell
SBU:	D6R, Void volume: 0.50cc/cc
Cage type:	β,26-hedron(II) Framework density: 1.31 g/cc
Channel System:	Three-dimensional, II to $[110]$

Hydrated

Free Apertures:	12 ring, 7.4Å, 6 ring, 2.2Å
Cation Locations:	Table 2-14

Dehydrated

Free Apertures:	7.4 Å
Cation Locations:	Table 2-14
Effect of Dehydration:	Stable and Reversible

Location of H_2O Molecules: See Table 2-14

Largest Molecule Adsorbed: $(C_4H_9)_3N$

Kinetic Diameter, σ, Å: 8.1

Table 2-12 Zeolite: Y (Breck,1974)

Structure Group:	4
Chemical Composition	
Typical Oxide Formula:	$Na_2O \cdot Al_2O_3 \cdot 4.8SiO_2 \cdot 8.9H_2O$
Typical Unit Cell Contents:	$Na_{56}[(AlO_2)_{56}(SiO_2)_{136}] \cdot 250H_2O$
Variations :	Na/Al 0.7to1.1: Si/Al => 1.5 to about 3
Crystallographic Data	
Symmetry: Cubic	Density: 1.92 g/cc
Space Group: Fd 3m	Unit Cell Volume:14,901 to 15,347 A^3
Unit Cell Contents:	a = 24.85-24.61Å
Structural Properties	
Framework: Figure 2-13	Truncated octahedra, β-cages, linked tetrahedrally through D6R's in arrangement like carbon atoms in diamond. Contains eight cavities,~ 13Å in diameter in each unit cell
SBU:	D6R, Void volume: 0.48cc/cc
Cage type:	β,26-hedron(II) Framework density: 1.25-1.29 g/cc
Channel System:	Three-dimensional, II to $[110]$
Hydrated	
Free Apertures:	12 ring, 7.4Å, 6 ring, 2.2Å
Cation Locations:	Table 2-15
Dehydrated	
Free Apertures:	~7.4 Å
Cation Locations:	Table 2-15
Effect of Dehydration:	Stable and Reversible
Location of H_2O Molecules: Not specifically located	
Largest Molecule Adsorbed:	$(C_4H_9)_3N$
Kinetic Diameter,σ,Å:	8.1

Table2-13 Cation distribution in faujasite (Breck, 1974).

[111]	Site		Na^{+a}	K^{+g}	Ca^{2+b}	Ba^{2+h}	Ni^{2+c}	Ce^{3+d}	La^{3+e}	Cs^{+f}, Na^+
	16 I	De	10	8.6	14.2	7.3	10.6	$3.4\ Na^+$	11.8	.
		Hy	.	.	.		.	.	.	
	32 I′	De	9	12.9	2.6	5.0	3.2	11.5	2.6	.
		Hy	14		9.7		.	$18\ Na^+$	3.3	17
	32 II′	De	.		.		1.9	$16. O_x$	$1.4, O_x$	.
		Hy	15		11.5		.	$32. O_x$	$25.3, O_x$	$32. O_x$
	32 II	De	32	31.7	11.4	11.3	6.4	$10.7, Na^+$	1.5	.
		Hy	11		$23.4, O_x$		.	$26. O_x$	$14.2, O_x$	$11. O_x$
	48 III	De	.							
		Hy	.							
	16 IV	De	.		.			.		
		Hy	.		2.2			6	10.3	

[a] Data based on Na- and Ca- enriched faujasite from Kaiserstuhl. Dehydration *in vacuo* at 350°C. Si/Al = 2.27. Degree of exchange assumed to be > 80%.

[b] Data on Ca^{2+} form from a completely exchanged crystal; composition: $Ca_{27}[(AlO_2)_{56}(SiO_2)_{133}] \cdot xH_2O$. Dehydration *in vacuo*; temp. raised to 475°C over 4-days and held at 475°C for 12 hr before cooling to RT.

[c] Ni^{2+} faujasite obtained by treatment with 1.0 M $NiCl_2$ at 90°C. Dehydrated *in vacuo* at 400°C for 7 hr, 1 × 10^{-6} torr. Intensity data collected at RT. Composition: $Ni_{22}Ca_4[(AlO_2)_{58}(SiO_2)_{134}]$. Two site I′ peaks assigned to Ni. Location of site II is further from the 6-ring than usual site I.

[d] Ce^{3+} faujasite uc contents given as: $Ce_{12}Ca_{16}Na_{28}[(AlO_2)_{59}(SiO_2)_{133}] \cdot 270\ H_2O$. Data on hydrated crystal at RT. Dehydration *in vacuo* at 350°C. Six Ce^{3+} in hydrated crystal (site IV) located at random in supercages. Residual H_2O or OH shown as O_x.

[e] La^{3+} faujasite completely exchanged except for possible hydrolysis. Residual Na, Mg, Ca < 0.1%. Dehydrated *in vacuo* at 475°C for 7 hr. Data collected at RT. 19 La atoms expected but 15.9 found. The La in site I is displaced along the 3-fold axis, half-atoms 0.17 A from site I. Structure (420°C) showed same distribution of La^{3+} 11.7 site I, 2.5 site I′, 1.4 site II.

[f] Structure determined on hydrated crystal of mineral; Na-Ca cations assumed to be dominant; 17 located. H_2O molecules shown by O_x.

[g] 33 K^+ ions per unit cell.

[h] 23.1 Ba^{2+} ions per unit cell.

Table 2-14 Cation distribution in zeolite X (Breck, 1974).

[111]	Site		Na^+	Ca^{2+}	K^+	Sr^{2+}	La^{3+}_{25o}	La^{3+}_{25o}	La^{3+}_{425o}	La^{3+}_{735o}	Ce^{3+}
	16 I	De	4	13.3	8	11.2	—	$32.1, O_x$	5.0	5.2	4.2
		Hy	9	—	8.9	2.1	—	—	—	—	$11.4, O_x$
	32 I′	De	32	5.0		7.0	30	13.8	15.2	14.1	22.8
				8 13							
		Hy	12 H_2O	16 H_2O	7.2	11.1	12	—	—	—	9
	32 II′	De	—	6.0		$4.2; 5.40, O_x$	$32, O_x$	$24.3, O_x$	—	—	
				$26, O_x$							
		Hy	26 H_2O	—		$32, O_x$	$32, O_x$	—	—	—	$32, O_x$
	32 II	De	32	25	.	19.5	—	13.2	4.9	6.3	
		Hy	24,	27 ·	23.2	15	17	—	—	—	21
			8 H_2O	H_2O							
	48 III	De	4	.	—	—	—	—	—	—	
	16 IV	De	—	—	—	—	—	3.4	—	—	2.6
		Hy	32	—	—	—	—	4	—	—	
	8 U	De	—	—	—	—	—	$8, O_x$	$3.3, O_x$	—	

| | Footnote | a | b | g | e | c | d | d | d | f |

[a] NaX of composition $Na_{80}[(AlO_2)_{80}(SiO_2)_{112}] \cdot xH_2O$. 32 Na^+ ions in hydrated zeolite not located. Assignment in dehydrated zeolite postulated as most probable. Probably space group Fd3 for NaX single crystal; 47 Na^+ not located.

[b] Single crystal, composition $Ca_{40}[(AlO_2)_{80}(SiO_2)_{112}] \cdot 235\ H_2O$ activated by heating in vacuum at 500°C.

[c] Data for LaX on powder; uc contents: $La_{29}Na_{24}[(AlO_2)_{86}(SiO_2)_{105.1}] \cdot 270\ H_2O$. Reported to be calcined (specific conditions not published) and "equilibrated to atmospheric conditions." Readsorption of H_2O from atmosphere may have occurred.

[d] This data obtained on powder; uc contents: $Na_{46}La_{24.6}Al_{82}Si_{110}O_{385} \sim 260\ H_2O$. Dehydration by heating in dry He at 100 μ.

[e] Data for hydrated SrX obtained on hydrated powder; uc contents: $Sr_{42}Na_2[(AlO_2)_{85}(SiO_2)_{107}] \cdot 2\ H_2O$. ·

[f] CeX powder, composition $Ce_{26}Na_{0.6}[(AlO_2)_{88}(SiO_2)_{104}] \cdot n\ H_2O$. Activation by heating in N_2 at 540° for 2 hr. 9 deficient cations.

[g] KX powder, composition: $K_{85}Na_2[(AlO_2)_{85}(SiO_2)_{105.5}]$ activated by heating *in vacuo* at 500°C.

Table 2-15 Cation distribution in zeolite Y (Breck, 1974).

Site		Na+	K+	Ag+	Cu2+	La3+_H	Ni2+	La3+_725°
16 I	Dc	7.5	12	16	3.4	13.1,Ox	12	5.2
	Hy	–	–	–	–	--	3.5	–
32 I'	Dc	19.5	14.2	10.7	10.4	16.0	1.1	8.9
	Hy	–	13.6	–	–	–	6	–
32 II'	Dc	–	--	--	–	–	–	–
	Hy	–	--	–	–	29.1,Ox	–	–
32 II	Dc	30	30	28.3	21 Na	–	1.9	–
	Hy	–	17.8	–	–	–	21.3 Na	5.5
8 U	Dc	–	--	--	4.6 OH	--	23.6 Na	--
	Hy	–	–	--	–	--	--	--
Footnote		a	a,c	a	d	b	c	b

(Site diagram at left: [111] with framework positions labeled S_II, S_II', U, S_I', S_I, S_I', U, S_II', S_II, S_III, S_IV)

[a] Na, K, Ag, Y. Composition of NaY powder given as Na$_{57}$[(AlO$_2$)$_{57}$(SiO$_2$)$_{135}$]. The K+ and Ag+ forms prepared by cation exchange; complete exchange assumed. Dehydration at 350°C to 10^{-5} torr. Data are at room temperature.

[b] LaY. Data on powder sample of composition: Na$_{13.3}$La$_{16.3}$(Al$_{55}$Si$_{137}$O$_{384}$) 270 H$_2$O, (Na + 3 La) = 62.3 which is 7.3 equivalents in excess of the 55 Al. Presence of some La OH^{2+} is indicated. Dehydration in vacuum at 350°C, data collected at room temperature and at 725°C with sample under dry He. The U site is in the center of the β-cage and is occupied by residual oxygen (H$_2$O or OH). This is removed at 725°C with

movement of La^{3+} in site I' to site I and site II. This effect appears to be reversible. i.e., on cooling to room temperature, La^{3+} in site I and site II returns to site I' and site II'. One La is equivalent to 6.5 Na or Ox. Assignment of Na not made.

[c] KY powder, composition: K$_{47.5}$Na$_{0.7}$[(AlO$_2$)$_{48.2}$(SiO$_2$)$_{143.8}$]. References include structure data on intermediate compositions of Si/Al ratio = 2.51 and 1.75 (69.8 and 54.7 K+ ions per unit cell).

[d] Cu, NaY powder, composition: Cu$_{16}$Na$_{24}$[(AlO$_2$)$_{56}$(SiO$_2$)$_{136}$]. Activated in vacuum at 500°C.

[e] NiY powder, composition: Ni$_{14}$Na$_{23}$H$_5$[(AlO$_2$)$_{56}$(SiO$_2$)$_{136}$]. Activation by heating O$_2$ at 600°C and vacuum for 12 hr.

Table 2-16 Classification and crystallographic data for zeolites (Kokotailo, 1983).

	Typical Unit Cell Contents	Crystal Data	Framework Density	Channel System
Analcite Group				
Analcite	Na$_{16}$(AlO$_2$)$_{16}$(SiO$_2$)$_{32}$·16H$_2$O	Cubic Ia3d a=13.7A	18.6[c]	
Laumontite	Ca$_4$(AlO$_2$)$_8$(SiO$_2$)$_{16}$·16H$_2$O	Monoclinic Am or A$_2$ a=7.6, b=14.8, c=13.1A, γ=112°	17.7	10[b](4.0x5.6)1[c,d]
Natrolite Group				
Natrolite	Na$_{16}$(AlO$_2$)$_{16}$(SiO$_2$)$_{24}$·16H$_2$O	Orthorhombic Fdd2 a=18.3, b=18.6, c=13.2A	17.8	8(2.6x3.9)3
Thomsonite	Na$_4$Ca$_8$(AlO$_2$)$_{20}$(SiO$_2$)$_{20}$·24H$_2$O	Orthorhombic Pnn2 a=13.1, b=13.1, c=13.2A	17.7	8(2.6x3.9)3
Edingtonite	Ba$_2$(AlO$_2$)$_4$(SiO$_2$)$_6$·8H$_2$O	Orthorhombic P2,2,2, a=9.6, b=9.7, c=6.5A	16.6	8(3.5x3.9)3
Chabazite Group				
Chabazite	Ca$_2$(AlO$_2$)$_4$(SiO$_2$)$_8$·13H$_2$O	Trigonal R3m a=13.2, c=15.1	14.6	8(3.6x3.7)3
Gmelinite	Na$_8$(AlO$_2$)$_8$(SiO$_2$)$_{16}$·24H$_2$O	Hexagonal P6$_3$/mmc a=13.8, c=10.0A	14.6	12(7.0)1[e] 8(3.6x3.9)2
Erionite	(Ca,MgNa$_2$K$_2$)$_{4.5}$(AlO$_2$)$_9$(SiO$_2$)$_{27}$·27H$_2$O	Hexagonal P6$_3$/mmc a=13.3, c=15.1A	15.6	8(3.6x5.2)3
Offretite	(K$_2$,Ca,Mg)$_{2.5}$(AlO$_2$)$_5$(SiO$_2$)$_{13}$·15H$_2$O	Hexagonal P6m2 a=13.3, c=7.6A	15.5	12(6.4)1[e] 8(3.6x5.2)2
Levynite	Ca$_3$(AlO$_2$)$_6$(SiO$_2$)$_{12}$·18H$_2$O	Trigonal R3m a=13.3, c=23.0A	15.2	8(3.3x5.3)2
Mazzite	Na$_6$K$_{1.9}$Ca$_{1.4}$Mg$_2$ (AlO$_2$)$_{9.8}$(SiO$_2$)$_{26.5}$·28H$_2$O	Hexagonal P6$_3$/mmc a=18.4, c=7.6A	16.1	12(7.4)1
Linde L	K$_6$Na$_3$(AlO$_2$)$_9$(SiO$_2$)$_{27}$·8H$_2$O	Hexagonal P6/mmm a=18.4, c=7.5A	16.4	12(7.1)1
Afghanite	(Na$_2$CaK$_2$)$_{12}$(AlO$_2$)$_{24}$(SiO$_2$)$_{24}$ -(Na$_2$CaK$_2$)$_6$(Cl$_2$,SO$_4$,CO$_3$)$_6$	Hexagonal P6$_3$/mmc a=12.8, c=10.5A	15.9	6
Losod	Na$_{12}$(AlO$_2$)$_{12}$(SiO$_2$)$_{12}$·19H$_2$O	Hexagonal P6$_3$2c a=12.9, c=10.5A	15.8	6
Liottite	(CaNa$_2$K$_2$)$_9$(AlO$_2$)$_{18}$(SiO$_2$)$_{18}$ -(CaNa$_2$K$_2$)$_n$(SO$_4$,CO$_3$,Cl)$_8$·2H$_2$O	Hexagonal P6m2 a=12.8, c=5.1A	15.7	6
TMA-E (AB)	(Me$_4$N)$_2$Na$_7$(AlO$_2$)$_9$(SiO$_2$)$_{27}$·26H$_2$O	Hexagonal P6$_3$/mmc a=13.3, c=15.2A	15.4	8(3.7x4.8)2
Cancrinite	Na$_8$(AlO$_2$)$_6$(SiO$_2$)$_6$·CaCO$_3$·2H$_2$O	Hexagonal P6$_3$ a=12.8, c=5.1A	16.7	12(6.2)1

(Table 2-16, contd.)

Phillipsite Group	Typical Unit Cell Contents	Crystal Data	Framework Density	Channel System
Phillipsite	$(KNa)_5 (AlO_2)_5 (SiO_2)_{11} \cdot 10H_2O$	Monoclinic P2$_1$/m $a=9.9$, $b=14.3$, $c=8.7\text{\AA}$ $\beta=124°$	15.8	8(4.2x4.4)1[e] 8(2.8x4.8) 8(3)1
Gismondite	$Ca_4 (AlO_2)_8 (SiO_2)_8 \cdot 16H_2O$	Monoclinic P2$_1$/a $a=9.8$, $b=10.0$ $c=10.6\text{\AA}$, $\gamma=90°$	15.4	8(3.1x4.4)1[e] 8(2.8x4.9)1
Yugawaralite	$Ca_4 (AlO_2)_8 (SiO_2)_{20} \cdot 16H_2O$	Monoclinic Pc $a=6.7,b=14.0,c=10.0\text{\AA},\beta=112°$	18.3	8(3.1x3.5)1[e] 8(3.2x3.3)1
Li A(BW)	$Li_4 (AlO_2)_4 (SiO_2)_4 \cdot 4H_2O$	Orthorhombic Pna2 $a=10.3$, $b=8.2$, $c=5.0\text{\AA}$	19.0	8(3.6x4.0)1
Heulandite Group				
Heulandite	$Ca_4 (AlO_2)_8 (SiO_2)_{28} \cdot 24H_2O$	Monoclinic Cm $a=17.7,b=17.9,c=7.4\text{\AA},\beta=116°$	17.0	8(4.0x5.5)1[e] 10(4.4x7.2)1 8(4.1x4.7)
Brewsterite	$(Sr,Ba,Ca)_2 (AlO_2)_4 (SiO_2)_{12} \cdot 10H_2O$	Monoclinic P2$_1$/m $a=6.8,b=17.5,c=7.7\text{\AA},\beta=95°$	17.5	8(2.3x5.0)1[e] 8(2.7x4.1)1
Stilbite	$Na_2Ca_4 (AlO_2)_{10} (SiO_2)_{26} \cdot 32H_2O$	Monoclinic F 2/m $a=13.6,b=18.2,c=17.8\text{\AA},\beta=91°$	16.9	10(4.1x6.2)1[e] 8(2.7x5.7)1
Mordenite Group				
Mordenite	$Na_8 (AlO_2)_8 (SiO_2)_{40} \cdot 24H_2O$	Orthorhombic Cmcm $a=18.1,b=20.5,c=7.5\text{\AA}$	17.2	12(6.7x7.0)1[e] 8(2.9x5.7)1
Ferrierite	$Na_{1.5}Mg_2 (AlO_2)_{5.5} (SiO_2)_{30.5} \cdot 18H_2O$	Orthorhombic Immm $a=19.2,b=14.1,c=7.5\text{\AA}$	17.7	10(4.3x5.5)1[e] 8(3.4x4.8)1
Dachiardite	$Na_5 (AlO_2)_5 (SiO_2)_{19} \cdot 12H_2O$	Monoclinic C2/m $a=18.7,b=7.5,c=10.3\text{\AA},\beta=108°$	17.3	10(3.7x6.7)1[e] 8(3.6x4.8)
Bikitaite	$Li_2 (AlO_2)_2 (SiO_2)_4 \cdot 2H_2O$	Monoclinic P2$_1$ $a=7.6,b=8.6,c=5.0\text{\AA},\gamma=114°$	20.2	8(3.2x4.9)1
Epistilbite	$Ca_3 (AlO_2)_6 (SiO_2)_{18} \cdot 16H_2O$	Monoclinic C2/m $a=8.9,b=17.7,c=10.2,\beta=124°$	18.0	10(3.5x5.3)1[e] 8(3.7x4.4)1
ZSM-5	$Na_n (AlO_2)_n (SiO_2)_{96-n} \cdot 16H_2O$ $n<27$	Orthorhombic Pnma $a=20.1,b=19.9,c=13.4\text{\AA}$	17.9	10(5.4x5.6)2[e] 10(5.1x5.5)3
ZSM-11	$Na_n (AlO_2)_n (SiO_2)_{96-n} \cdot 16H_2O$ $n<27$	Tetragonal I$\bar{4}$m2 $a=20.1$, $c=13.4\text{\AA}$	17.7	10(5.1x5.5)3

Faujasite Group	Typical Unit Cell Contents	Crystal Data	Framework Density	Channel System
Faujasite	$Na_{12}Ca_{12}Mg_{11} (AlO_2)_{59} (SiO_2)_{133} \cdot 260H_2O$	Cubic Fd3m $a=24.7\text{\AA}$	12.7	12(7.4)3
Linde A	$Na_{12} (AlO_2)_{12} (SiO_2)_{12} \cdot 27H_2O$	Cubic Fm3c (Pm3m) $a=24.6\text{\AA}$ ($a=12.3\text{\AA}$)	12.9	8(4.1)3
ZK-5	$Na_{30} (AlO_2)_{30} (SiO_2)_{66} \cdot 98H_2O$	Cubic Im3m $a=18.7\text{\AA}$	14.7	8(3.9)3[f] 8(3.9)3
ZSM-3	$((LiNa)_2)AlO_2)_2 (SiO_2)_{3.2} \cdot 8H_2O)_m$	Hexagonal $a=17.5$, $c=129\text{\AA}$		
Zeolite Rho	$(Na,Cs)_{12} (AlO_2)_{12} (SiO_2)_{36}n \cdot H_2O$	Cubic I$\bar{4}$3m $a=15.1\text{\AA}$	14.3	8(3.9x5.1)3
Paulingite	$(K_2,Na_2,Ca,Ba)_{76} (AlO_2)_{152} (SiO_2)_{525} \cdot 700H_2O$	Cubic Im3m $a=35.1\text{\AA}$	15.5	8(3.9)3[f] 8(3.9)3
Merlinoite	$(K_5,Ca_2) (AlO_2)_9 (SiO_2)_{23} \cdot 24H_2O$	Orthorhombic Immm $a=14.1,b=14.2,c=10.0\text{\AA}$	16.0	8(3.1x3.5)1[e] 8(3.5x3.5)1 8(3.4x5.1)1
Linde N	$Na_{384} (AlO_2)_{384} (SiO_2)_{384} \cdot 518H_2O$	Cubic Fd3 $a=36.93$		6-rings
Sodalite	$Na_6 (AlO_2)_6 (SiO_2)_6 \cdot 2NaCl$	Cubic P$\bar{4}$3n $a=8.9\text{\AA}$		6-rings
Melanophlogite Group				
Melanophlogite	$Me_n (AlO_2)_n (SiO_2)_{48-n} \cdot rH_2O$	Cubic P4$_2$32 $a=13.4\text{\AA}$		6-rings
ZSM-39	$(Na,THA,TEA)_{0.4} (AlO_2)_{0.4} (SiO_2)_{135.6} \cdot mH_2O$	Cubic Fd3m $a=19.4\text{\AA}$	18.7	6-rings
Lovdarite Group				
Lovdarite	$X_4Na_{12} (BeO_2)_8 (SiO_2)_{28} \cdot 18H_2O$	Tetragonal Poly type P4$_2$/mnc $a=7.14,b=7.14,c=21.0\text{\AA}$ Poly type I$\bar{4}$m2 $a=7.15,b=7.15,c=42$		8-ring 1 9-ring 2[e] 8-ring 9-ring 2

a. Number of atoms per $1000\text{\AA}^3$.
b. Number of ring members in channel opening.
c. Ring direction.
d. Dimensions of channel system.
e. Channel system intersects.
f. Separate channel systems.

compounded because the true nature of a specific material with which an investigator is working is often unknown or subject to question. When dealing with materials of uncertain character, many authors have applied many of the terms indiscriminately, and it is often not clear to which specific substance or reaction an author is referring.

A generally accepted terminology will probably have to await the firmer establishment of the validity of the presently postulated structures and reactions. Hopefully, a move toward standardization of terminology in the entire zeolite area will be made by IUPAC in the near future.

Various terms have been used in discussions of modified Y-type zeolites. This topic is briefly outline the meaning of some of these terms as used by various authors and describe their role in zeolite modification. However, a full characterization of any particular material or process described by an individual author may involve one or several of these descriptive terms. In this topic do not attempt to establish any preferred usage since this has been and is being considered by others, but in this topic use the set of terms as a focal point for discussing the various structures and reactions that are postulated.

Hydrogen Y and Protonated Y. These terms have been used interchangeably to denote the hydrogen-exchanged form of the zeolite. There is disagreement among authors as to what materials should be properly given these labels. Some feel that the term hydrogen should be reserved for only those materials made by a direct hydrogen-ion exchange. Others have applied the description to include the products of low-temperature thermal decomposition of ammonium and other nitrogenous-base-exchanged zeolites.

Regardless of nomenclature, the hydrogen form of zeolite can exist, in contradiction to earlier doubts, as equilibrium between a BrØnsted acid and the hydroxyl form as represented in equation 1 of Figure 2-16.
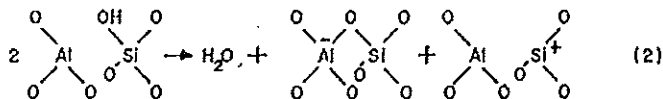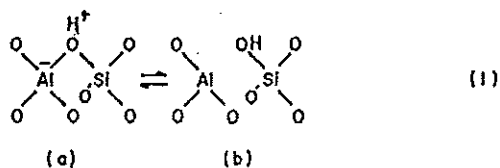
Figure 2-16 (1) Equilibrium between the Brønsted and hydroxyl forms of a hydrogen zeolite and (2) the reaction of dehydroxylation in zeolites. (Rabo,1974)

For Y type zeolites, the equilibrium at room temperature strongly favors the hydroxyl form. Hydrogen ions can be introduced into Y-type zeolites by a carefully controlled exchange or by the indirect route of the thermal decomposition of the ammonium-exchanged form. The hydrogen form is extremely active and unstable at elevated temperatures and plays an important part in subsequent reactions such as dealumination, decationation, and stabilization.

Ammonium Y. This term signifies simply an ammonium-exchanged form of the zeolite. Many authors have failed to specify the degree of exchange, and the term has been widely applied to zeolites containing appreciable quantities of other ions, particularly sodium. The term has also been used to describe materials that actually no longer contain nitrogen, such as calcined ammonium Y. The term is quite prevalent in the zeolite literature because of the importance of ammonium-exchanged zeolites as intermediate products in the preparation of other materials.

Deaminated Y. The term deamination has been used to describe the liberation of NH_3 from the ammonium-exchanged form of the zeolite by heating. The deamination reaction is shown in the Figure 2-17.
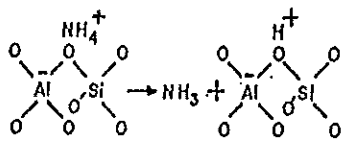
Figure 2-17 The reaction of deamination in zeolites. (Rabo,1974)

Reactions involving the liberation of NH_3 from ammonium-exchanged zeolite when subjected to thermal treatment have received much attention because of their role in preparing other products, including decationated, hydrogen, and stabilized zeolites.

Decationated Y and decationized Y. These terms, unfortunately, have not been used consistently by different authors. Barrer applied the term decationization in referring to the removal of aluminum from a zeolite structure, or dealumination. This is quite justified, of course, since the removal of an aluminum atom is necessarily accompanied by the removal of the associated cation. Rabo favors the term decationized to designate those zeolites, which have been heat-treated following an ammonium exchange. Others have used the term to denote that the equivalent number of metal cations is less than that of aluminum. This use is based on the fact that non-metal ions and, in particular, hydrogen ions are often not included in the chemical analysis of a zeolite.

Cationated Y and partially cationated Y. The term cationated has been used to refer to zeolites containing ions other than hydrogen. This usage reflects that there is generally no analysis for protons or hydrogen in zeolites and, hence, they are not included as cations. The term partially cationated has in the same manner been used to describe zeolites that may be considered to contain both protons and a metal ion such as NaHY, KHY, etc. Thus, the term partially cationated is synonymous with the term decationated used by some authors.

Deprotonated Y. This term designates a reaction wherein a hydrogen zeolite has been heated, with a resulting decrease in exchange capacity. The term has been used

synonymously with decationation. Although it may appear less ambiguous, it does not specify any particular mechanism or product.

Aluminum Y and aluminum-hydrogen Y. These terms have been used to signify that the zeolite is at least partially in the aluminum cationic form. Many earlier references to aluminum-exchanged zeolites are probably misleading since a high degree of aluminum exchange by direct methods does not, in general, occurs. The exchanged aluminum may have been deduced from the decrease in other cations upon treatment with solutions of aluminum salts. Such decrease is largely accounted for by hydrogen-ion exchange in the acidic aluminum-salt solution. More recent work has been reported where aluminum-hydrogen Y zeolites have been prepared and characterized. Recently, the existence of Y-type zeolites containing cationic aluminum derived from a partial extraction of framework aluminum has been demonstrated.

Amorphous Y. This term has been applied to the amorphous degradation products resulting from the destruction of Y-type zeolites. It is, of course, a contradiction in terms since Y-type zeolites are, by definition, crystalline materials. Since the possible products resulting from destruction of crystallinity are indefinite and varied, there is little justification for the use of this term.

Metal-hydrogen Y. Such terms as sodium-hydrogen Y, rare earth hydrogen Y, etc., have been used to designate materials that were believed to contain significant amounts of both hydrogen and metal cations. In some instances there have been proper grounds for such belief; in most instances, however, the amount of hydrogen ion has been inferred from the difference between the aluminum and metal cation analyses. These terms have most often been applied to the calcination products of mixed ammonium-metal forms of the zeolite. Thus, the term metal-hydrogen Y is synonymous with the terms partially cationated and decationated used by some authors. Many zeolites used in commercial catalytic applications have received such treatment.

Dehydroxylated Y. This term has been widely used as a result of the work of Uytterhoeven et al. (Uytterhoeven,1965) to signify the elimination of water from hydroxyl groups that originated from the hydrogen form of the zeolite. Their concept of the

process of dehydroxylation is shown in Figure 2-16 in which present evidence for the existence of an equilibrium between the Brønsted acid form (A) of zeolite with hydroxylated acid form (B) as shown in equation 1 by showing the extensive presence of hydroxyl groups. Equation 2 illustrates the elimination of water from two such hydroxyl groups, a process that results in trigonally coordinated aluminum and silicon atoms. The reaction in equation 2 has been termed dehydroxylation.

Aluminum deficient Y and dealuminated Y. These terms have been used interchangeably to denote products resulting from a partial extraction of aluminum from the structural framework of a Y-type zeolite without collapse of the structure. An aluminum-deficient framework structure appears to be characteristic of ultrastable zeolites. Although it has not been the practice, these terms can be properly applied to those zeolites that have had aluminum extracted from the framework but not removed from the crystal. These structures are certainly aluminum deficient, even though it is not obvious from the chemical analysis.

Aluminum-deficient Y-type zeolites have been prepared by two distinct methods: (1) removal of aluminum with a chelating agent, e.g., EDTA, and (2) heat treatment of the ammonium or hydrogen form of the zeolite followed by removal of the extracted aluminum by ion exchange or by complexing agents. Both of these methods appear to require a prior step of hydrogen exchange of the zeolite.

Kerr first proposed and demonstrated that aluminum extraction from the tetrahedral positions occurs in the preparation of ultrastable zeolites. He also demonstrated an alternate method of aluminum extraction from Y-type zeolites by treatment of sodium Y and ammonium Y with the acid form of EDTA.

Stabilized Y, Ultrastable Y, and Z-14-US. Y-type zeolites can undergo a transformation that results in structures with gross structural properties similar to those in the parent zeolite but with greatly enhanced stability and drastically different other properties. The chemical composition of these unusually stable structures is almost indistinguishable from that of the acid exchanged zeolites, which are extremely unstable. Although the extract nature of these ultrastable zeolites is not yet fully

understood, our understanding of their structure and the reactions involved in their formation has recently increased greatly.

Highly stable zeolites of this sort have been referred to by various authors as stabilized Y, ultrastable Y, and Z-14-US. The term stabilized Y is rather broad and has been also employed to describe zeolites whose stability is associated with a metal cation. The term ultrastable Y or ultrastable structure has been generally accepted to describe the zeolites of our discussion.

Metastable Y, Stabilizable Y, and Unstable Y. These terms apply to the low-sodium ammonium or hydrogen zeolite which upon heating to temperatures above 650 $^{\circ}$C will either convert to the ultrastable structure with shrinkage in unit cell size or will collapse to an amorphous phase.

Ultrastable zeolites. Since ultrastable zeolites were first described by McDaniel (McDaniel,1968), several methods have been reported for preparing, from Y-type zeolites, materials that have ultrastable properties. A complex set of reactions either causes or accompanies the stabilization of the structure and some of these reactions may vary depending on the method of preparation. However, all of the methods described involve certain common reactions and structures. Consequently, the ultrastable properties common to these materials follow from a single stabilization phenomenon.

The ultrastable structure is characterized by a significant contraction in unit cell dimensions of the order of 1% to 1.5% compared with the parent sodium zeolite. This contraction is shown graphically in Figure 2-18. The parent sodium zeolites have a definite relationship between silica to alumina ratio and unit cell dimension. When converted to the ultrastable structure, the unit cells size decreases to some point within the range indicated. The exact amount of decrease depends on several factors, including sodium content, degree of aluminum extraction, and calcination conditions. The full relationship between this contraction of the structure and stabilization is not completely clear, but certain things are apparent.

The contraction of the structure is accomplished only when a significant number of the aluminum atoms have left their position in the framework. This was proposed and demonstrated by Kerr when he first showed that after stabilization by thermal treatment, cationic aluminum was present in the ultrastable structure and could be removed by ion exchange. Kerr later showed that ultrastable zeolites could be prepared by an alternate method wherein aluminum was extracted from the structure by use of a chelating agent such as EDTA.

The ion exchange capacity of the ultrastable zeolite is substantially lower than that of the parent zeolite. This, of course, follows from the extraction of framework aluminum. The presence of residual cations limits the thermal stability. Nevertheless, the cell shrinkage with accompanying stabilization can be achieved when an appreciable amount of sodium is present especially in the process described by Kerr (Kerr,1968).

2.4 Preparation and physicochemical properties of zeolite-molecular sieve component

The zeolite is primarily responsible for the catalyst's activity, selectivity, and stability (catalytic, thermal, and hydrothermal). The zeolites frequently used in octane-enhancing catalysts are modified Y zeolites, in which some of the aluminum has been removed from the framework (dealuminated or high-silica Y zeolites). Dealumination results in an increase in the silica to alumina ratio of the zeolite framework, which, in turn, affects the physicochemical properties of the zeolite. Such changes in zeolite composition and properties have a significant impact on catalytic activity, selectivity, stability, and FCC gasoline octane rating. This has led to the development of several preparation methods of high-silica Y zeolites, which resulted in materials with different physicochemical and catalytic properties.
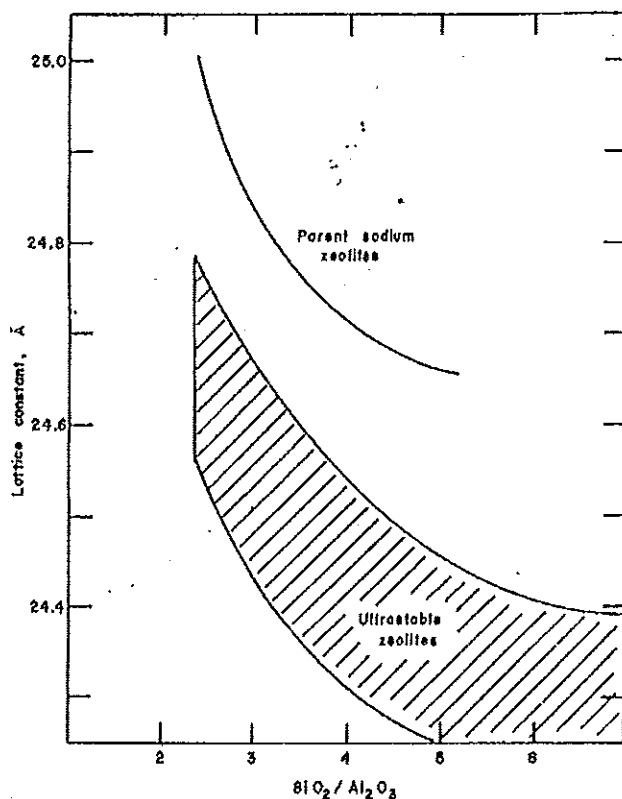
Figure 2-18 Unit cell contraction in ultrastable zeolites (Rabo,1974)

Structural characteristics of Y zeolites

The structure of Y zeolites consists of a negatively charged, three-dimensional framework of SiO_4 and AlO_4 tetrahedral, joined to form an array of truncated octahedral. These truncated octahedral (β-cages or sodalite cages) are joined at the octahedral faces by hexagonal prisms resulting in tetrahedral stacking. This type of stacking creates large cavities (α-cages or supercages) with a diameter of $\sim$ 13 Å. The supercages can be entered through any of four tetrahedral distributed opening (12-membered rings), each having a diameter of 7.4 Å. The supercages, connected through 12-membered rings, form the large-pore system of the zeolite as shown in Figure2-19. The structure comprises also a small - pore system, made up of sodalite cages and the connecting hexagonal prisms. The six-member rings of the sodalite cages have a diameter of $\sim$ 2.4 Å.

Each tetrahedral coordinated aluminum atom in the framework carries a negative charge. These negative charges in the framework are compensated by cations located in specific non-framework positions, as shown in Figure 2-19. In the dehydrated form, charge-balancing protons occupy certain preferred positions in the zeolite and form two types of acidic hydroxyl groups: α-cages hydroxyls, which are very acidic and are directly accessible to adsorbates: and β-cages hydroxyls, which are less acidic but sufficiently mobile to interact with α-cage restricted adsorbates. In the hydrated form, the ions and the water molecules in the supercages have considerable freedom of movement, which permits ion exchange, as well as reversible dehydration and sorption (Scherzer,1989).
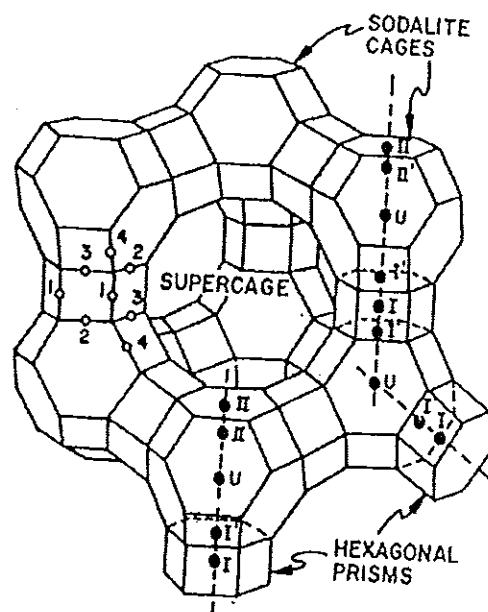
Figure 2-19 Faujasite framework showing oxygen type (O) nonframework locations (●) and Brønsted acid sites(Scherzer,1989).

Preparation methods of high-silica Y (HSY) zeolites.

The following methods have been used to increase the silica to alumina ratio in Y zeolites (Table 2-17) (Scherzer,1984):

1. Thermal and hydrothermal modification.

2. Chemical modification.

3. Combination of hydrothermal and chemical modification.

Table 2-17 Preparation of high-silica Y zeolites (Scherzer,1984)

I.   Hydrothermal treatment of NH_4Y zeolites (formation of ultrastable Y zeolites)
II.   Chemical treatment
A. Dealumination with silicon enrichment
1. Reaction with $(NH_4)_2SiF_6$ in solution
2. Reaction with $SiCl_4$ vapors
B. Dealumination without silicon enrichment
1. Reaction with chelating agents(e.g., EDTA)
2. Reaction with F_2 gas
3. Reaction with volatile, nonsiliceous halides (e.g., $COCl_2$, BCl_3)
III   Hydrothermal and chemical treatment. Reaction of ultrastable Y zeolites with:
A. Acids (e.g., HCl, HNO_3)
B. Bases (e.g., NaOH)
C. Salts (e.g.,KF)
D. Chelating agents (e.g.EDTA)
E. Volatile halides (e.g., $COCl_2$)

1. Thermal and hydrothermal modification.

Calcination of an ammonium-exchanged Y zeolite in the presence of steam results in the explusion of tetrahedral aluminum from the framework into nonframework positions. This process, which consists essentially in a high temperature hydrolysis of Si-O-Al bonds, leads to the formation of nonframework aluminum species, while increasing the framework silica to alumina ratio and decreasing the zeolite unit cell size. The defect sites left by dealumination are filled to a large extent by silica, which leads to a very stable, highly siliceous framework. An example of such hydrothermal dealumination is

the formation of ultrastable Y zeolites (USY zeolites), first reported by McDaniel and Maher (McDaniel and Maher,1968). While McDaniel and Maher used in their preparation the steam generated by the wet zeolite 'cake' (deep bed calcination), Eberly et al. (Eberly,1971) prepared USY zeolites by calcining ammonium Y zeolites in flowing steam.

Ultrastable Y zeolites are thermally and hydrothermally more stable than conventional Y zeolites. They maintain their structural integrity up to about 1000° C. USY zeolites have significantly fewer exchange sites, since the number of exchange sites in the zeolite is equivalent to the number of framework aluminum atoms. Furthermore, the number of BrØnsted acid sites in USY zeolites is also smaller than in conventional rare earth exchanged Y zeolites. Such differences in acidity have an impact on the catalytic activity and selectivity of USY zeolites.

2. Chemical modification

High silica Y zeolites can be prepared by partial dealumination of conventional Y zeolites with different reagents. Dealumination can be accomplished by reacting the zeolite with a suitable reagent in solution or by passing the reagent in vapor phase over the zeolite at high temperature. Depending upon the reagent used, dealumination can be carried out (a) with silicon enrichment or (b) without silicon enrichment of the dealuminated zeolite. In the former case, silicon from an external source (i.e., the reagent) is inserted into the framework vacancies left by dealumination. In the later case, no such insertion of silicon occurs.

a. Dealumination with silicon enrichment

i. Dealumination with $(NH_4)_2SiF_6$. Skeels and Breck (Skeels and Breck,1985) have shown that treatment of Y zeolites with solutions of ammonium fluorosilicate (AFS) under controlled pH conditions is an effective dealumination method. Aluminum is removed from the zeolite in the form of soluble fluoroaluminate salts, while most of the created framework vacancies are filled by silicon from the fluorosilicate. The rate of

aluminum removal from the zeolite framework is higher than that of silicon insertion into the vacant tetrahedral sites, resulting is some framework vacancies.

ii. **Dealumination with SiCl₄.** According to Chang (Chang,1981), by reacting Y zeolites with $SiCl_4$ vapors at high temperatures (between 450° and $550^\circ C$), aluminum is removed from the zeolite framework and replaced by silicon. The degree of dealumination depends upon reaction temperature and reaction time. The resulting high silica zeolites have high thermal and chemical (acid) stability.

b. Dealumination without silicon enrichment

i. **Dealumination with chelating agents.** Kerr(Kerr,1968) has shown that treatment of Y zeolites with solutions of EDTA under reflux conditions results in zeolite dealumination. Using this EDTA method, Kerr was able to prepare high-silica Y zeolites in which up to about 50% of aluminum was removed in the form of a water-soluble chelate, without any appreciable loss in zeolite crystallinity. Later work has shown that up to 80% of framework aluminum can be removed with EDTA, resulting in a zeolite with about 60 – 70% of its initial crystallinity. According to the proposed reaction mechanism, aluminum is extracted in the form of a soluble aluminum-EDTA chelate.

ii. **Dealumination with volatile nonsiliceous halides.** Zeolite dealumination can be achieved by react Y zeolites at high temperature with different volatile, nonsiliceous halides (e.g., $COCl_2$). Nonaqueous solutions of inorganic halides or oxyhalides can also be used for zeolite framework dealumination.

iii. **Dealumination with fluorine.** According to Lok et al.(Lok,1982), treatment of Y zeolites with a fluorine-and-air mixture at ambient temperature results in zeolite framework dealumination. The suggested reaction mechanism involves the formation of different aluminum-fluorine compounds along with zeolites containing hydroxyl and fluorine nests.

3. Combination of hydrothermal and chemical treatment

This two-step treatment consists in the initial conversion of a conventional, ammonium-exchanged Y zeolite into the ' ultrastable' form by hydrothermal treatment,

followed by a chemical treatment designed to remove the nonframework aluminum. The chemical treatment can be carried out with solutions of acids (e.g., HCl), bases (e.g., NaOH), salts (e.g., KF), or chelating agents (e.g., EDTA). Nonframework aluminum can also be removed by gas-solid reactions with volatile halides at high temperature. At high concentrations most of these reagents will react with the remaining framework aluminum.

Direct synthesis. Attempts have been made to increase the silica to alumina ratio of Y zeolites by direct synthesis. Most commercial Y zeolites are crystallized with silica to alumina ratios between 5.0 and 5.5. Attempts to crystallize Y zeolites with higher silica to alumina ratios have encountered difficulties. The silica to alumina ratio of the crystallized zeolite can be influenced by numerous factors, such as type of raw material used, ratio between reaction components, aging conditions of the sodium aluminosilicate gel, crystallization temperature and time, the presence of zeolite 'seeds' and so forth.

2.5 Preparation and physicochemical properties of matrix component

In a zeolitic FCC catalyst, the zeolite is embedded in the catalyst matrix. The matrix composition and catalyst preparation conditions are selected to convey specific physical and catalytic properties to the catalyst particles.

A. Functions and classification of matrices

1. Physical functions

The catalyst matrix fulfills several important physical functions:

Binder. One of the major functions of the matrix (or of some of its components) is to bind the zeolite particles together in spray-dried microspheroidal catalyst particles, hard enough to survive interparticle and reactor wall collisions.

Diffusivity. The matrix serves as a diffusion medium for the feed stock molecules and their cracking products. This requires a pore structure that allows the diffusion of hydrocarbon molecules in and out the catalyst particles. Furthermore, the pore structure should not deteriorate during severe hydrothermal treatment of the catalyst. By favoring

or inhibiting the diffusion of certain large hydrocarbon molecules, the pore structure will also affect the activity and selectivity characteristics of the catalyst.

Diluting medium. The matrix serves as a diluting medium for the zeolite particles. This moderates zeolite activity and avoids excessive cracking (overcracking).

Sodium sink. Matrices can act as sinks for sodium ions. Through solid-solid ion exchange, the sodium ions migrate from the zeolite into the matrix, thus increasing the thermal and hydrothermal stability of the zeolite.

Heat transfer. The matrix acts as a heat carrier in the FCC unit. It facilitates heat transfer during cracking and regeneration, thus protecting the zeolite from structural damage.

2. Classification

Catalyst matrices can be classified by different criteria: by chemical composition, by the origin of their components (synthetic, semisynthetic, natural), by their catalytic role (e.g., low, medium, and high activity), by some physical or chemical property (e.g., low and high surface area, low and high density), and so forth.

Most matrics contain two or more components. One component is the catalyst binder, usually consisting of amorphous silica, alumina, silica-alumina, or silica-magnesia. Another component is clay, usually kaolinite, halloysite, or montmorillonite. Thermally or chemically modified clays are also used in catalyst formulations. The clay generally improves the mechanical strength of the catalyst. It also serves as filler. Other inorganic oxides such as TiO_2, ZrO_2, P_2O_5, B_2O_3, etc., are also present in some catalysts. Matrices consisting of a synthetic component (binder) and a natural component (clay) are called semisynthetic matrices.

The matrix components described in this section are present in most zeolitic FCC catalysts, including octane catalysts. Firstly, describe the major synthetic matrix components commonly found in FCC catalysts: amorphous silica, alumina, silica-alumina, and silica-magnesia. Subsequently, the natural matrix components, such as clays and modified clays, are described (Scherzer,1989).

B. Synthetic components

1. Amorphous silica

Silica derived from a silica hydrosol can be used as an effective, low activity binder in the preparation of spray-dried FCC catalysts. A silica sol can be prepared by one of several methods; for example, by reacting a sodium silicate solution with an acid under controlled conditions, by passing a dilute sodium silicate solution over an acid ion exchange resin, by peptizing a silica gel, by hydrolysis of silicon compounds, by electrodialysis, and so forth. The usual commercial source of sodium silicate used in the preparation of silica sols or gels is a sodium 'water glass' solution, with a SiO_2 / Na_2O mole ratio of about 3.3 and containing silicate anions of varying degrees of polymerization. A silica sol is most effective as a binder when freshly prepared, since at that point the silica has a low degree of polymerization and no gelation has set in yet. Such sols are generally unstable and, in time, gelation occurs through aging. An increase in pH will also cause rapid gelation. Silica sol binders form matrices with low catalytic activity, due to the absence of acidic OH groups. However, in combination with clay, such matrices can have high surface areas and relatively high pore volumes (Scherzer,1989).

2. Alumina

This is an important component of many zeolitic catalysts. Depending upon the type, amount, and mode of incorporation into the matrix, its presence can serve several roles: (a) increases the catalytic activity of the matrix: (b) improves the attrition resistance of the catalyst; (c) improves the hydrothermal stability of the catalyst.

Of the different commercial aluminas available, pseudoboehmite is more frequently used in catalyst formulations. Pseudoboehmite is a high surface area (200 – 300 m^2/g) alumina monohydrate that can be prepared by a variety of methods: by hydrolysis of Al-alkoxides, by reacting sodium aluminate with aluminum sulfate, by acidifying an alkali aluminate, or by adding a base to a cationic aluminum salt under controlled process conditions. The presence of pseudoboehmite-derived alumina in the catalyst not only increases its catalytic activity and stability, but also improves its attrition

resistance. Pseudoboehmite is usually dispersed in water with an acid (peptized), mixed with the other catalyst components. To be effective as a binder, the pseudoboehmite should be easily peptized (high peptizability index) (Scherzer,1989).

3. Silica – alumina gels

Amorphous silica-alumina is an active matrix component encountered in many commercial FCC catalysts. The physical and catalytic properties of the catalyst are strongly affected by the composition, preparation conditions and incorporation method of this synthetic matrix component into the catalyst. Its activity is due to the presence of BrØnsted and Lewis acid sites. The formation of meso- and macropores in the gel is favored by synthesizing the gel at high pH, in concentrated solution, in the presence of pore-regulating agents. Similar to other amorphous components, steaming of amorphous silica-alumina results in a partial loss of activity, loss of surface area, collapse of micropores and increase in the average pore radius. Amorphous silica-alumina matrices can serve as a source of volatile silica species that are transported under steam from the matrix to zeolite, where they replace the expelled aluminum atoms in the zeolite framework (Scherzer,1993).

C. Natural components

1. Natural clays

Clays are used in almost all-commercial catalyst formulations. They are used in finely divided hydrous form or in a form modified by chemical or thermal treatment. Hydrous clays have poor catalytic activity, but their presence in the catalyst affects its physical properties. In general, clay-containing catalysts are harder, denser, and have better attrition resistance than catalysts with synthetic matrices. The hydrous clay also serves as a filler, since it is usually less expensive than other matrix components.

Clay is commonly used in FCC catalyst formulations are kaolinite and halloysite. The use of other clays such as montmorillonites, illites, bentonites etc. The clays used in FCC formulations are usually purified and have a small average particle size. Purification removes impurities that have a deleterious effect on the catalyst's performance (e.g., iron) or that can create environmental problems (e.g., quartz). The small particle size

and a high degree of dispersion improve the attrition resistance of the catalyst. Kaolin clays with no synthetic additive have been used as binders for Y zeolites.

2. Modified clays

Acid treatment of natural clays such as kaolinite, halloysite, or montmorillonite results in materials catalytically more actives than the corresponding raw clay. Mild leaching of the raw clay with a mineral acid, such as dilute sulfuric acid, removes most of the contaminating iron, which has a deleterious effect on the catalyst (due to excessive formation of coke and hydrogen). Furthermore, mild leaching removes some of the aluminum, magnesium, and alkaline earth ions, increasing the clays porosity and surface area, and exchanging some of the metal cations with protons. This results in a catalytically more active clay (Scherzer,1989).

2.6 Instrumental methods for characterized the physical properties of faujasite zeolites.

A great variety of instrumental methods are capable of revealing information of value to some aspect of catalysis. Methods of surface characterization are of particular importance, but many of these techniques are highly specialized and are of use mostly for fundamental research. Many methods that can be applied to plane surfaces lose much of their usefulness when confronted by porous catalysts. Spatial resolution is frequently of importance in practice and may be a primary consideration in choosing one or more optimum surface characterization methods. The following is intended to give a brief introduction to a few of the better-developed techniques that have been of particular value in working with technical catalysts.

Microscopy

Light microscopy helps to characterize materials and to define problems by revealing such features as size, shape, surface marking, occurrence of occlusions or other discontinuities, and color. It is particularly helpful to identify the characteristics of single particles and to determine particle size distribution (Satterfield,1991).

In the field of electron optical instrumentation a wide range of techniques is available giving information concerning crystal habit and crystal size and other more

specific characteristics. The main techniques used in zeolite research are connected to transmission electron microscopy (TEM), whereby the technique yielding most information is connected with the use of the scanning electron microscope (SEM) accompanied by a scanning micro-probe analysis. A microscope is usually used as a first means of identification by looking at the crystal shape of some specific zeolites.

A. Characterization of zeolites by scanning electron microscopy (SEM)

The most powerful method in the investigation of zeolite problems is the scanning electron microscopy (SEM). This method has above all the advantage of a simple preparation of the samples and gives quick information on the shape and the distribution of the size of the crystals and also of the presence of amorphous material.

In the scanning electron technique a fine beam of electrons is scanned over the surface of the sample using a system of deflection coils. The various signals produced by the interaction of the electron with the surface, such as secondary electrons, back-scattered electrons, or X-rays can be used to form an image. Magnifications in the range of 20 – 50,000 are available with a resolution of about 100 Å. Non-metallic samples are usually covered with a thin film of carbon and gold to ensure a sufficient electric conductivity to prevent surface charge, which leads to distorted pictures. Another effect is the protection of heat sensitive material.

The output of the secondary electron varies according to the accelerating voltage of the beam (5-50 kv) and the structural characteristics of the sample as well as the particular angle of the incident beam with respect to the surface features. The change in the secondary electron current induced by these features exhibit therefore a 3-dimensional character of the image.

The back-scattered electrons give a signal varying with the respective atomic number. Measuring the wavelength of the induced characteristic X-ray radiation with special detectives an elementary analysis of the area hit by the beam can be carried out. This technique is known as electron micro-probe analysis (Lechert, 1984).

B. Characterization of zeolites by thermal analysis

Thermoanalytical methods are among the most important tools of the characterization of zeolites.

Generally, thermal analysis describes a group of methods whereby the dependence of the parameters of any physical property of a substance on temperature is measured.

The two techniques measuring the change of heat and the change of weight are the methods used preferably for the characterization of zeolite properties.

These methods are called differential thermal analysis (DTA) and thermogravimetric analysis (TGA).

In both methods the sample and possibly a reference sample are heated or cooled at a controlled rate. In the DTA technique the difference in temperature between a substance and a reference material against either time or temperature is recorded. If any heat releasing or heat consuming process takes place in the sample, the temperature of the sample increases or remains behind the temperatures of the reference. If the process is finished the temperatures of both specimen become equal again. The peak, obtained in the recorded curve can be evaluated to get the kinetics and the amount of the heat transfer.

In the thermogravimetric analysis the weight of the sample is recorded in dependence on the temperature.

In modern devices both principles of measurement are often realized in one apparatus.

The DTA method has a sensivity of about 10^{-4} Joule. With the TGA method weight changes of about 10^{-8} g can be detected.   .

In the typical behaviour of a zeolite being heated and subjected to differential thermal analysis three typical regions can be distinguished. The first region begins slightly above room temperature, has its maximum mostly near 500 K and is finished at about 750 K. this region expresses itself as an endotherm in the DTA curves and is

caused by the evolution of water and possibly other volatile substances in the zeolite cavities.

Between about 900 and 1500 K often two exotherms can be observed which are associated with the collapse of the zeolite lattice and sometimes at much higher temperatures recrystallization to a new phase.

In the first region often a stepwise evolution of water can be observed. Figure 2-20 shows DTA curves for A zeolites containing different cations.
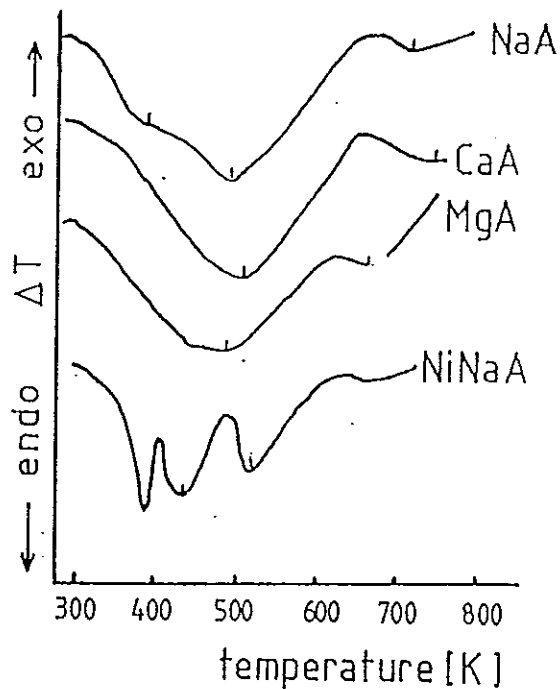
Figure 2-20 DTA curves in the region of dehydration for A zeolite with different cations (Lechert,1983).

Changing the cations characteristic changes in the DTA curves are observed which depend on the degree of the exchange and may often be explained by the typical complexes with these ions. Some typical exothermic effects of A zeolites with different cations are shown in Figure2-21.
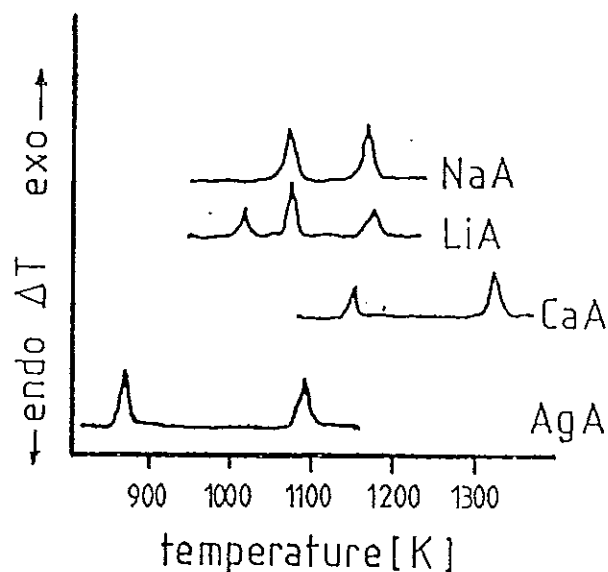
Figure 2-21 High temperature effects in the DTA curves of different A zeolites (Lechert,1983).

The process of the dehydration of faujasite zeolites is more complicated. This is also due to the fact that at higher temperatures dehydroxylation occurs. Special attention has been devoted to the deammoniation and the formation of the hydrogen form. In dependence on the composition of the sample for the end of the deammoniation of various zeolite temperatures between 570 and 770 K are reported, so that the deammoniation and the dehydroxylation often cannot be resolved. The process can only be studied exactly by analyzing the released substances simultaneously to the DTA measurement. Furthermore, the high temperature effects influencing of ultrastabilization can be detected.

For the two methods a large number of variations have been reported giving answers to questions about different properties of zeolites and zeolite catalysts.

Finally, a special method shall be mentioned with which centers of different acid strength can be characterized. The acid form of the zeolite in question is exposed to ammonia at temperatures near 500 K, where no more physical adsorption occurs and the sorbed ammonia is then desorbed by programmed heating at higher temperatures

near 850 K detecting the amount in a TGA experiment. The temperature at which an evolution of ammonia is observed, is then a good measure of the acidity of the respective site.

Although thermal analysis gives valuable information on a series of properties of zeolites and zeolite catalysts, it has not successfully provided a reproducible and standard method for measuring thermal properties because too many factors of the particular instrument and the conditions of the experiment influence the measured parameters. Although it is often quite useful for direct comparisons, it is difficult to compare results reported by different authors (Lechert,1984).

C. Characterization of zeolites by Brunauer-Emmett-Teller (BET) method

The most common method of measuring surface area, and one used routinely in most catalyst studies, is that developed by Brunauer, Emmett, and Teller (1938). Early's descriptions and evaluations are given by Emmett (1948,1954). In essence, the Langmuir adsorption isotherm is extented to multilayer adsorption. As in the Langmuir approach, for the first layer the rate of evaporation is considered to be equal to the rate of condensation, and the heat of adsorption is taken to be independent of coverage. For layers beyond the first, the rate of adsorption is taken to be proportional to the fraction of the lowest layer still vacant. The rate of desorption is taken to be proportional to the amount present in that layer. The heat of adsorption for all layers except the first layer is assumed to be equal to the heat of liquefaction of the adsorbed gas. Summation over an infinite number of adsorbed layers gives the final expression as follows:

$$P / V(P_0 - P) = 1/V_m C + (C-1)P/V_m CP_0 \qquad (2\text{-}2)$$

Where V = volume of gas adsorbed at pressure P

       V_m = volume of gas adsorbed in monolayer, same unit as V

       P_0 = saturation pressure of adsorbate gas at the experimental temperature

       C = a constant related exponentially to the heats of adsorption and liquefaction of the gas

$$C = e^{(q_1 - q_L)/RT} \qquad (2\text{-}3)$$

Where q_1 = heat of adsorption on the first layer

q_L = heat of liquefaction of adsorbed gas on all other layers

R = the gas constant

The larger the value of C, the sharper is the curve in the region of the B point (according to type II of adsorption isotherm) and the more accurately the surface area can be determined.

If the equation (2-2) is obeyed, a graph of $P / V (P_0 - P)$ versus P/P_0 should give a straight line, the slope and intercept of which can be used to evaluate V_m and C. Many adsorption data show very good agreement with the BET equation over values of the relative pressure P/P_0 between approximately 0.05 and 0.3, and this range is usually used for surface area measurements. At higher P/P_0 values, complexities associated with the realities of multilayer adsorption and/or pore condensation cause increasing deviation. With microporous substances such as zeolites, the linear region on a BET plot occurs at much lower values of P/P_0, typical around 0.01 or less.

From equation (2-2), $V_m = 1/(s+l)$, where S is the slope, equal to $(C-1)V_mC$ and I is the intercept, equal to $1/V_mC$. This proceeds from the fact that

$$S+I = (1/V_mC)[(C-1) + 1] = 1/V_m \qquad (2-4)$$

The surface area of the catalyst may then be calculated from V_m if the average area occupied by an adsorbed molecule is known.

Any condensible inert vapor can be used in the BET method, but for the most reliable measurements, the molecules should be small and approximately spherical. The vapor should also be easy to handle at the required temperatures; for example, P/P_0 values of 0.05 to 0.3 should be conveniently attainable. Liquid nitrogen is a readily available coolant, and nitrogen is usually used as the adsorbate since it is relatively cheap and readily available in high purity.

A standard test method for determining the BET surface area of catalysts based on nitrogen adsorption has been published as ASTM D3663-84. For a catalyst containing zeolites, and hence both micropores and mesopores, a method of determining the zeolite content (or the microporous portion of the total) by nitrogen

adsorption has been developed by Johnson (1978) and published as ASTM D4365. The method basically involved determining the area of mesopores by the *t*-plot method and subtracting this from the BET total area to obtain the zeolite area. This method was apparently developed for faujasite-type zeolites (zeolite X and Y), that have relatively large zeolite pores. Its degree of applicability to other zeolites is uncertain.

D. Diffractive Analysis

Powder XRD (X-ray Diffraction)

X-ray diffraction may be used to obtain information about the structure and composition of crystalline material. Common compounds can be identified using tabulations of reference patterns. The minimal limit of detection is approximately 5 percent for compounds and approximately 1 percent for elements. With calibration procedures it is possible to obtain quantitative information and thus determine the approximate amount of a particular phase in a sample. Phases for which reference patterns are not available can sometimes be identified by other X-ray procedures.

XRD patterns can be of great importance in identifying specific crystal structures or crystal planes within a complex catalyst if these are responsible for a desired specificity. Indeed a patented composition of matter useful as a catalyst may be identified primarily through a stated XRD pattern combined with a composition claim.

XRD is of particular importance in characterization of zeolite catalysts. ASTM procedure D3906-85a provides a method for determining the percentage of zeolite Y in a catalyst sample based on the intensity of a portion of the X-ray diffraction pattern of the sample relative to that of a reference zeolite Y. ASTM D3942-85 gives a standard test method for determining the unit cell dimension of a faujasite-type zeolite. This makes possible a determination of zeolite framework composition (e.g., Si / Al ratio) which cannot be done by elemental analysis when the zeolite is incorporated into a matrix (Satterfield,1991).

An explanation of the principle of the technique is illustrated in Figure2-22. The crystalline compound forms a series of repeating planes with a spacing of a few tenths of a nanometer. The radiation is scattered by each atom in the plane. Part of the wave is

reflected, but most goes through to the next plane where part is reflected, etc. The wave front interacts with the electrons associated with each atom on the plane. Each atom re-emits a spherical wavelet. The re-emitted waves will be in phase and will give a peak at the detector for a particular angle, 2ϑ, such that the distances traveled by the wavelets differ by an integral wavelength. At any other angles, even ones only slightly different, the amplitude of the wave reflected from neighboring atoms will be slightly out of phase, the wave from second neighbors will be twice as much out of phase, and finally the negative amplitude of the reflected wave from some nth neighbor will cancel the reflection from the first and so on until there is a net cancellation. Consequently, the angel 2ϑ is a measure of the distance between planes, and the intensity of the signal is a measure of the scattering power (number of electrons) and the density of the atoms in the diffracting plane. For a given material, the intensity is a measure of how much material there is and of how perfectly the planes are ordered.
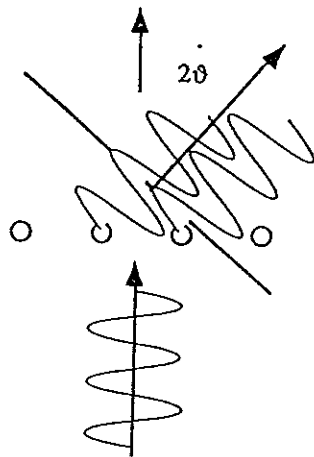
Figure2-22 Pictorial representation of X-ray scattering intensity reinforcements responsible for the distinctive X-ray patterns of crystalline materials (Peters,1993).

Identification of crystalline materials

The basis of the XRD technique is that crystalline materials have peaks at values of 2ϑ such that both the values of 2ϑ and the intensities are characteristics of the structure of the material. Figure 2-23 shows the powder patterns of two zeolites, faujasite and ZSM-5, used in cracking catalysts as well as a pattern characteristic of clay (kaolin) often used as filler. Crystalline or amorphous alumina may also form a part of the matrix of the cracking catalyst. The XRD scan of a cracking catalyst may show peaks due to all or several of these components. Amorphous materials, of course, do not have an X-ray pattern and cannot be identified by XRD.

A major feature of current XRD systems is the existence of search routines capable of identifying zeolites, clays, or other catalytic components from an XRD scan. Although currently only two zeolites, faujasite and ZSM-5, are being used commercially, other zeolites will almost certainly be used in the future.

Quantitative Analysis

XRD intensities can be used to estimate the amount of a material present in a catalyst. The XRD intensities are compared to some standard defined as 100% crystallinity. There is a procedure defined as a standard test, ASTM D3906, for the measurement of crystallinities of faujasite containing material. This technique is often used to measure the relative amounts of zeolite such as faujasite in either a fresh catalyst or in commercial or lab deactivated catalysts. The stability of the zeolite is the percent zeolite retention. The presence of varying amounts of exchange cations such as sodium or rare earth can significantly alter intensity relationships. Further, the recently observed presence of an extensive system of internal surface defect structures (mesopores) in the framework of hydrothermally dealuminated zeolites is expected to cause an intensity loss. Atoms near the internal surface will be slightly displaced from their ideal lattice positions and so there will be some interference of amplitudes.

Unit cell size measurement in Faujasite

In a zeolite framework consisting of silicon and aluminum, the aluminum is the catalytically active ingredient. The activity, selectivity, and stability of the zeolite are all

related to the framework aluminum content of the zeolite. Chemical analysis will give the aluminum content of the framework in a pure zeolite sample if there is no other source of alumina. However, the aluminum removed from the framework by dealumination, either during manufacture or during deactivation, remains within the structure in some form as nonframework alumina. Further the catalyst will contain other sources of alumina including clay and matrix components. It is desirable to be able to measure the amount of framework alumina in a zeolite independently of the occurrence of other forms of alumina in the catalyst or the zeolite. A number of instrumental methods of measuring framework aluminum content have been developed.

The most common method of measuring the aluminum content of the framework and the only one directly applicable to the catalyst is based on the measurement of the unit cell by XRD. Since the Si-O-Al bond is longer than the Si-O-Si bond, the unit cell increases slightly with aluminum content. Consequently the unit cell size is a very important parameter. The measurement of unit cell size by XRD has been standardized as ASTM Test D-3942. In the case of faujasite there are several correlation's of unit cell size and alumina content in current use, one developed by Breck and Flannigan, and another more recently by Fichtner-Schmittler and by Sohn (Peters,1993).

In general, as the zeolite framework is dealuminated, unit cells size (a_0) decreases. The number of aluminum atoms per unit cell (N_{Al}) can be estimated from the unit cell size according to the Breck-Flanigan relationship:
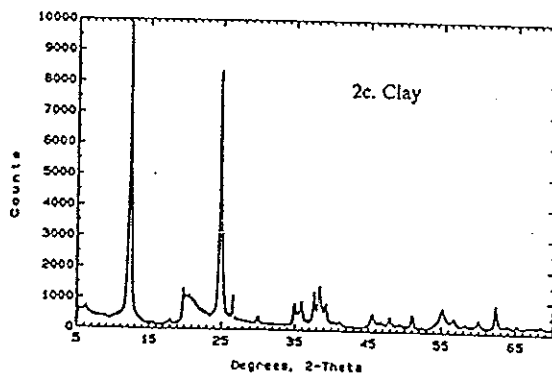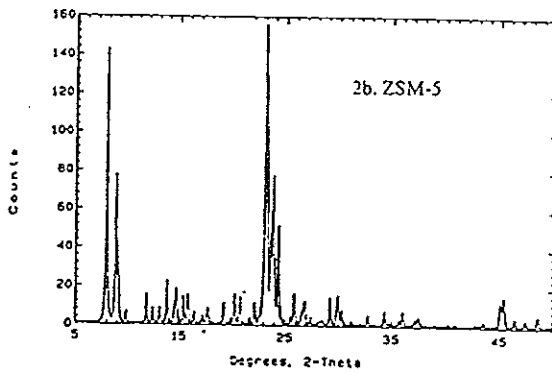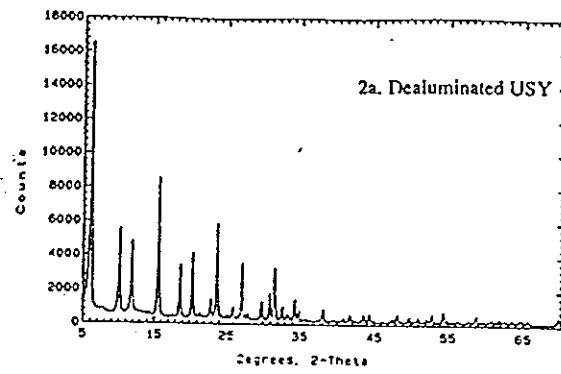
Figure 2-23 X-Ray patterns for a) dealuminated USY, b) ZSM-5 and c) Clay (Kaolin) (Peters,1993).

$$a_0 \text{ (Å)} = 24.191 + 0.00868 \, (N_{Al}) \qquad (2\text{-}5)$$

Because of the total number of aluminum and silicon atoms $(N_{Al}+N_{Si})$ is constant, according to:

$$N_{Al}+N_{Si} = 192 \qquad (2\text{-}6)$$

Then, the framework silica to alumina mole ratio can be expressed as:

$$SiO_2/Al_2O_3 = 2\left[1.6704/ \, (UCS - 24.19) -1) \, \right] \qquad (2\text{-}7)$$

Where UCS is the unit cell size in Angstroms equivalent to a_0 (Å) of Equation 2-5 (Dai,1996)

It is possible also, to calculate the number of aluminum atoms per unit cell from the chemical analysis, and to compare the results with an estimation of the aluminum content in framework, Table2-18

By chemical analysis

$$R = Si/ \, Al = (\% \, SiO_2 X51) \, / \, (\%Al_2O_3 x60) \qquad (2\text{-}8)$$

$$SiO_2 \, / \, Al_2O_3 = 2R \qquad (2\text{-}9)$$

$$Al \, / \, unit \, cell = 192 \, / \, (R+1) \qquad (2\text{-}10)$$

Table 2-18 The measurement of aluminum content per unit cell in faujasite by XRD analysis using the published unit cell correlation's, where a_0 is the unit cell in Angstroms (Peters,1993).

	Breck	F-S	Sohn
Al / unit cell =	$1152(a_0 - 24.191)$	$1124(a_0 - 24.233)$	$1071(a_0 - 24.238)$

There is no single correct correlation since cation exchange and even the degree of hydration can significantly affect the unit cell size (Peters,1993).

X-ray diffraction unit cell size measurements can therefore be used to estimate the framework silica to alumina mole ratios. The unit cell size of the zeolite may also predict zeolite properties such as hydrothermal stability, total acidity, and acid strength.

CHAPTER 3

EXPERIMENTAL

The experiments in this work can separate into 6 parts in which mainly focus on the ion exchanges condition and hydrothermal treatment (steam calcination) steps.

1. Study the ion exchange conditions for prepared NH_4Y zeolite

2. Study the hydrothermal treatment conditions for prepared USY zeolite

3. Preparation the USY zeolite by hydrothermal treatment combined with acid leaching method

4. Preparation of a HY zeolite

5. Preparation the Y zeolite catalysts

6. Evaluation the performance of the Y zeolite catalysts to cracking the gas oil by microactivity test (MAT) unit.

The experimental details

3.1 Study the ion exchange conditions for prepared NH_4Y zeolite

The ion exchange conditions were studied for prepared NH_4Y zeolite as follows:

1) The influence of ion exchange temperatures in the range of room temperatures to 90 $^\circ$C.

2) The influence of ion exchange times in the range of 1 to 3 hours.

3) The influence of various weight ratio of NaY zeolite: NH_4Cl: H_2O, 1: 0.5:20, 1: 1: 20, and 1: 1.5: 20

3.1.1 Equipment

a. Stainless steel stirring vessel, volume1, 10 and 15 liters.

The vessel shown in Figure F-1 (see Appendix F) was used to mix the materials.

b. Heater (Fisher Scientific made in U.S.A.)

The heater shown in Figure F-2 (see Appendix F) was used to heating the reaction mixtures and control the reaction's temperature.

c. Electric mixer with stirring rod (Heidolph made in Germany)

The electric mixer type R2R1 with stirring rod shown in Figure F-3 (see Appendix F) was used to mix the reaction mixtures.

d. Vacuum pump (Eyela made in Japan)

The vacuum pump model A-3S shown in Figure F-4 (see Appendix F) was used for vacuum filtration the zeolite slurry.

e. Hot air oven (Eyela made in Japan)

The hot air oven model NDO-600N shown in Figure F-5 (see Appendix F) was used to dried the prepared zeolite.

f. Furnace

The furnace shown in Figure F-6 (see Appendix F) was used to calcined the prepared zeolite.

g. Thermometer

h. Mortar

The morta shown in Figure F-7 (see Appendix F) was used to grind the zeolite.

3.1.2 Reagents

The using reagents in this works were shown as follows:

a. A parent NaY zeolite raw material, from RIPP.,China.

b. Ammonium chloride (NH_4Cl),G.R. Grade, Merck, Germany.

c. Deionized water, from Faculty of Natural resource and Faculty of Agro-industry, PSU.

Procedures:

1) The influence of ion exchange temperatures

A parent commercial NaY zeolite (a_0, 24.66 Å and crystallinity,89.32 %) was supplied by Research Institute of Petroleum Processing (RIPP), China. The solid content was determined by using NaY zeolite about 1.5 to 3 grams to calcinate in the furnace at $800^{\circ}C$ for an hour.

The ion exchange was performed, using NaY zeolite (dry basis), NH_4Cl and deionized water ratio 1: 1: 20 by weight. By mixing all three parts together in a stirring vessel, using various ion exchange temperatures from room temperature to $90^{\circ}C$, the ion exchange time was carried on for an hour with continuous stirring. Then the NH_4Y zeolite slurry was filtered by a Vacuum pump. The filter cake was then washed with hot deionized water ($60^{\circ}C$) until the filtrate was substantially chlorine free, and finally dried at $120^{\circ}C$ in the oven for 2 hours. After that, the samples were calcined at $350^{\circ}C$ for 2 hours in the furnace. In the next steps, calcined samples were taken to continue ion exchange for the prepared NH_4Y zeolite (second ion exchange). After that, the NH_4Y zeolite (second ion exchange) was calcined at $550 ^{\circ}C$ for 2 hours in the furnace. Finally, calcined samples were taken to do third ion exchange for the prepared NH_4Y zeolite (third ion exchange). The Na_2O exchange degree was determined by Atomic Absorption Spectrometry Model GBC 3000,Avanta; the percent of crystallinity retention was determined by X-Ray Diffractometer (XRD) Model X' Pert-MPD, Type 3040/00NC, Philips.

2) The influence of ion exchange times.

A starting material commercial NaY zeolite (a_0, 24.66Å and crystallinity,89.32 %) was supplied by Research Institute of Petroleum Processing (RIPP), China. The solid content was determined by using NaY zeolite about 1.5 to 3 grams to calcinate in the furnace at $800^{\circ}C$ for an hour.

The ion exchange was performed, using NaY zeolite (dry basis), NH_4Cl and deionized water ratio 1: 1: 20 by weight. By mixing all three part together in a stirring vessel, using various ion exchange times from 1 to 3 hours, the ion exchange temperatures was carried on for $90^{\circ}C$ with continuous stirring. Then the NH_4Y zeolite slurry was filtered by a Vacuum pump. The filter cake was then washed with hot deionized water ($60^{\circ}C$) until the filtrate was substantially chlorine free, and finally dried at $120^{\circ}C$ in the oven for 2 hours. After that, the samples were calcined at $350^{\circ}C$ for 2 hours in the furnace. In the next steps, calcined samples were taken to continue ion exchange for the prepared NH_4Y zeolite (second ion exchange). After that, the NH_4Y

zeolite (second ion exchange) was calcined at 550 $^\circ$C for 2 hours in the furnace. Finally, calcined samples were taken to do third ion exchange for the prepared NH_4Y zeolite (third ion exchange). The Na_2O exchange degree was determined by Atomic Absorption Spectrometry Model GBC 3000,Avanta; the percent of crystallinity retention was determined by X-Ray Diffractometer (XRD) Model X' Pert-MPD, Type 3040/00NC, Philips.

3) The influence of various weight ratio of NaY zeolite: NH_4Cl: H_2O, 1: 0.5:20, 1: 1: 20, and1: 1.5: 20

A raw material commercial NaY zeolite (a_0, 24.66Å and crystallinity,89.32%) was supplied by Research Institute of Petroleum Processing (RIPP), China. The solid content was determined by using NaY zeolite about 1.5 to 3 grams to calcinate in the furnace at 800°C for an hour.

The ion exchange was performed, using NaY zeolite (dry basis), NH_4Cl and deionized water in the various ratio from1: 0.5: 20 to 1: 1.5: 20by weight. By mixing all three parts together in a stirring vessel, using ion exchange for an hour, the ion exchange temperatures were carried on for 90°C with continuous stirring. Then the NH_4Y zeolite slurry was filtered by a Vacuum pump and the filter cake was washed with hot deionized water (60°C) until the filtrate was substantially chlorine free, dried at 120 $^\circ$C in the oven for 2 hours. After that, the samples were calcined at 350°C for 2 hours in the furnace. In the next steps, calcined samples were taken to continue the ion exchange for the prepared NH_4Y zeolite (second ion exchange). After that, the NH_4Y zeolite (second ion exchange) was calcined at 550 $^\circ$C for 2 hours in the furnace. Finally, calcined samples were taken to do third ion exchange for prepared NH_4Y zeolite (third ion exchange).The Na_2O exchange degree was determined by Atomic Absorption Spectrometry Model GBC 3000,Avanta; the percent of crystallinity retention was determined by X-Ray Diffractometer (XRD) Model X' Pert-MPD, Type 3040/00NC, Philips.

3.2 Study the hydrothermal treatment conditions for prepared USY zeolite.

The steam calcination conditions were studied for prepared USY zeolite as follows;

1) The influence of temperatures in the range of 400 to 700 $^{\circ}$C.

2) The influence of the ratios of water to zeolite in the range of 2.25 to 9.

3) The influence of times in the range of 1 to 4 hours.

    3.2.1 Equipment

        a. Hydrothermal Aging Unit (CLY-1 made in China)

        The hydrothermal aging unit model CLY-1 shown in Appendix B was used to steam calcination.

    3.2.2 Reagent

        a. Deionized water

        The deionized water was used as steam in steam calcination process.

Procedures:

1) The influence of temperatures in the range of 400 to 700 $^{\circ}$C.

NH_4Y zeolites (third ion exchange) were taken to steam calcination. Firstly, the samples were put into micro reactor, then placed in the furnace of hydrothermal aging unit model CLY-1 (see Appendix B) and the amount of samples to steam in the ratio of 1:3 by weight. Next step, the inert gas flows through the micro reactor and heats the furnace to attain each desired temperature. When the temperature was stable, steam flowed steam through the micro reactor for 2 hours. Finally, the inert gas flows to expel the volatile matters for 15 minutes. The unit cells size and percent of the crystallinity retention were analyzed by X-Ray Diffractometer (XRD) Model X' Pert-MPD, Type 3040/00NC, Philips.

2) The influence of water to zeolite ratios in the range of 2.25 to 9.

NH_4Y zeolites (third ion exchange) were taken to steam calcination. Firstly, the samples were put into micro reactor, then placed in the furnace of hydrothermal aging unit model CLY-1 (see Appendix B) .The amount of samples to steam were varied from the ratio of 1: 2.25 to 9 by weight. Next step, the inert gas flows through the micro reactor and heats the furnace temperature to 600°C. When the temperature became

stable, the steam is allowed to flow through the micro reactor for 2 hours. Finally, the inert gas flows to expel the volatile matters for 15 minutes. The unit cells size and percent of the crystallinity retention were analyzed by X-Ray Diffractometer (XRD) Model X' Pert-MPD, Type 3040/00NC, Philips.

3) The influence of times in the range of 1 to 4 hours.

NH_4Y zeolites (third ion exchange) were taken to steam calcination. Firstly, the samples were put into micro reactor then, placed in the furnace of hydrothermal aging unit model CLY-1 (see Appendix B) .The amount of samples to steam ratio was 1:3 by weight. Next step, flowing the inert gas through the micro reactor to heat the furnace temperature to $600^{\circ}C$. When the temperature was stable, steam flowed through the micro reactor from1 to 4 hours. Finally, the inert gas flows to expel the volatile matters for 15 minutes. The unit cells size and percent of the crystallinity retention were analyzed by X-Ray Diffractometer (XRD) Model X' Pert-MPD, Type 3040/00NC, Philips.

3.3 Preparation the USY zeolite by hydrothermal treatment combined with acid leaching method.

3.3.1 Equipment

a. Hydrothermal Aging Unit (CLY-1 made in China)

The hydrothermal aging unit model CLY-1 shown in Appendix B was used to steam calcination.

b. Heater (Thermolyne made in U.S.A.)

The heater shown in Figure F-2 (see Appendix F) was used to heating the reaction mixtures, stirring and control the reaction's temperature.

c. Beaker and magnetic bar

d. Thermometer

e. Vacuum pump (Eyela made in Japan)

The vacuum pump model A-3S shown in Figure F-4 (see Appendix F) was used for vacuum   filtration the zeolite slurry.

f. Hot air oven (Eyela made in Japan)

The hot air oven model NDO-600N shown in Figure F-5 (see Appendix F) was used to dried the prepared zeolite.

g. Mortar

The morter shown in Figure F-7(see Appendix F) was used to grind zeolite

3.3.2 Reagents

a. USY zeolite, from steam calcination step.

b. Deionized water

c. Hydrochloric acid (HCl), G.R. Grade, Merck, Germany.

A zeolite of the faujasite type, NH_4Y zeolite of a suitably lower sodium content, dealuminated by steam calcination and followed by acid leaching .In this experiment the influence of various concentration of mineral acid, using hydrochloric acid in the concentrations of 1 to 4 Normal were studied. Firstly, prepared USY zeolite by hydrothermal treatment method, using suitable conditions as previously studied as follows; the treat temperature of 600 $^{\circ}$C, the ratio of water to zeolite of 3:1 and the treat time of 2 hours. Then the USY zeolite were treated with 1 to 4 Normal of hydrochloric acid solutions for studies the influence of the concentration of mineral acid to USY zeolite.

The procedure of acid leaching

The USY zeolites were treated with hydrochloric acid in each concentration; ratio 1:10 by weight in the stirring vessel for 2 hours at 90 $^{\circ}$C with stirring. The USY-Ex zeolite slurry was filtered by vacuum pump and washed by hot deionized water until substantially chloride free. Then the filtered cake was dried in the oven at 120 $^{\circ}$C for 2 hours. The USY-Ex zeolite were analyzed and the percent of crystallinity retention and the unit cell size by X-Ray Diffractometer, Model X'Pert-MPD, Type 3040/00NC,Philips, the surface area by Brunauer-Emmett-Teller (BET), the thermal stability by Differential Thermal Analyser (DTA) Model DTA7, Perkin Elmer and physical morphology by Scanning Electron Microscope (SEM), Model JSH-35CF,Jeol.

3.4 The procedure for prepared HY zeolite.

   3.4.1 Equipment

   a. Stainless steel stirring vessel, volume1, 10 and 15 liters.

      The vessel shown in Figure F-1 (see Appendix F) was used to mix the
      materials.

   b. Heater (Fisher Scientific made in U.S.A.)

      The heater shown in Figure F-2 (see Appendix F) was used to heating the
      reaction mixtures and control the reaction's temperature.

   c. Electric mixer with stirring rod (Heidolph made in Germany)

      The electric mixer type R2R1 with stirring rod shown in Figure F-3 (see
      Appendix F) was used   to mix the reaction mixtures.

   d. Vacuum pump (Eyela made in Japan)

      The vacuum pump model A-3S shown in Figure F-4 (see Appendix F) was
      used for vacuum   filtration the zeolite slurry.

   e. Hot air oven (Eyela made in Japan)

      The hot air oven model NDO-600N shown in Figure F-5 (see Appendix F)
      was used to dried the prepared zeolite.

   f. Furnace

      The furnace shown in Figure F-6 (see Appendix F) was used to calcined the
      prepared zeolite.

   g. Thermometer

   h. Mortar

      The morter shown in Figure F-7 (see Appendix F) was used to grind zeolite

   3.4.2 Reagents

   The using reagents in this works were shown as follows:

   a. A parent NaY zeolite raw material, from RIPP.,China.

   b. Ammonium chloride (NH_4Cl),G.R. Grade, Merck, Germany.

   c. Deionized water, from Faculty of Natural resource and Agro-industry, PSU.

Procedure:

A starting material commercial NaY zeolite (a_0, 24.66Å and crystallinity,89.32%) was supplied by Research Institute of Petroleum Processing (RIPP), China. The solid content was determined by using NaY zeolite about 1.5 to 3 grams to calcinate in the furnace at 800°C for an hour.

The ion exchange was performed, using NaY zeolite (dry basis), NH_4Cl and deionized water ratio 1: 1: 20 by weight mixing all three parts together in a stirring vessel, using ion exchange temperature of 90°C, the ion exchange time was carried on for an hour with continuous stirring. Then the NH_4Y zeolite slurry was filtered by vacuum pump and the filter cake was washed with hot deionized water (60°C) until the filtrate was substantially chlorine free, dried at 120°C in the oven for 2 hours. After that, the samples were calcined at 350°C for 2 hours in the furnace. In the next steps, the calcined samples were taken to continue the ion exchange for prepared NH_4Y zeolite (second ion exchange). After that, the NH_4Y zeolite (second ion exchange) was calcined at 550 °C for 2 hours in the furnace followed by a third ion exchange for prepared NH_4Y zeolite (third ion exchange). Finally, calcined NH_4Y zeolite (third ion exchange) at 500 °C for 2 hours. The Na_2O exchange degree was determined by Atomic Absorption Spectrometry Model GBC 3000,Avanta, the percent of crystallinity retention was determined by X-Ray Diffractometer (XRD) Model X'Pert-MPD, Type 3040/00NC, Philips.

3.5 Preparation the Y zeolite catalysts.

The Y zeolite catalysts were prepared in this step. The Y zeolite raw materials were listed in the Table 3-1.

Table 3-1 Y zeolite raw materials used in preparation of catalysts.

Raw materials	Sources
USY zeolite	PSU., Hatyai, Songkhla, Thailand
SRY zeolite	RIPP. Beijing, China
HY zeolite	PSU. Hatyai, Songkhla, Thailand
USY-1N Ex zeolite	PSU. Hatyai, Songkhla, Thailand
USY-2N Ex zeolite	PSU. Hatyai, Songkhla, Thailand
USY-3N Ex zeolite	PSU. Hatyai, Songkhla, Thailand
USY-4N Ex zeolite	PSU. Hatyai, Songkhla, Thailand

3.5.1 Equipment

a. Stainless steel stirring vessel, volume 1 liter.

The vessel shown in Figure F-1 (see Appendix F) was used to mix the materials.

b. Electric mixer with stirring rod (pitched blades turbine joined inside truncated cone) (VOSS model 2020 made in England)

The electric mixer with stirring rod shown in Figure F-3 (see Appendix F) was used to mix the reaction mixtures.

c. Hot air oven (Eyela made in Japan)

The hot air oven model NDO-600N shown in Figure F-5 (see Appendix F) was used to dried the prepared zeolite.

d. Furnace

The furnace shown in Figure F-6 (see Appendix F) was used to calcined the catalysts.

e. Mortar

The morter shown in Figure F-7 (see Appendix F) was used to grind the ingredients of catalyst as shown in Table 3-1.

3.5.2 Reagents

a. Zeolites as shown in Table 3-1

    b. Kaolin clay, from RIPP, China.

    c. Pheudoboemite (PBA), from RIPP, China.

    d. Hydrochloric acid (HCl), G.R. Grade, Merck, Germany.

Procedures:

50 parts (by weight) of fine particles of kaolin clay as filler were dispersed into 2 of 3 parts of deionized water in which the total mixture has a slurry solid content 25 %, with continuous stirring. Followed by the addition of 20 parts by weight of pheudoboemite (PBA) with stirring for 15 to 30 minutes. Then slowly drop the hydrochloric acid in the ratio of 0.1:1 by weight of hydrochloric acid: pheudoboemite to the mixture and stirring for an hour. After that, add 30 parts of that zeolite as listed in the Table 3-1 by mixing with 1 part of the remaining deionized water to the mixture with stirring for 30 minutes. The composition was then dried in the oven at 150 $^{\circ}$C and calcined at 500 $^{\circ}$C for an hour to expel the volatile organic matters.

3.6 Microactivity test method and Test condition

3.6.1 Equipment.

    a. Microactivity Test (MAT) Unit, Model WFS-1D (see Appendix D)

    b. Gas Chromatograph (GC-14 B,SHIMADZU) and Integrater (HP3295, Hellet Packard)

    c. Hydrothermal Aging Unit, Model CLY-1 (see Appendix C)

3.6.2 Test methods and Test conditions.

Catalyst samples reacted with gas oil in the fix-bed reactor of the Microactivity Test Unit and product oil was collected in a glass receiver and thereafter was analyzed by Gas – Chromatograph (see full details of method in Appendix D)

Condition of MAT Unit

Catalyst loading	5 g
Oil weight	1.56 $\pm$ 0.01 g
Catalyst / oil	3.2
Weight hour space velocity (WHSV)	16 hr-1
Feeding rate	1.54 g / min.

Feeding time	70 sec.
Reactor temperature	$460 \pm 1^{\circ}C$
Purging time	90 sec

Liquid produced from MAT unit was then analyzed by the Gas Chromatograph.

<u>Condition of Gas Chromatograph (GC)</u>

Column (Pack column)	OV-I (Methyl silosane)
Detector	Flame Ionized Detector (FID)
Carrier Gas	Nitrogen (Purity 99.99%, OFN)
	Folw rate 35-40 ml/min.
Combustion Gas	Hydrogen , flow rate 40ml / min.
Auxilliary Gas	Air, flow rate 400 ml / min.
Injector Temperature	$280^{\circ}C$
Detector Temperature	$280^{\circ}C$
Column Chamber Temperature	raise from 35 $^{\circ}C$ to 80 $^{\circ}C$ with a rate

of 15 $^{\circ}C$ / min, then raising from 80 $^{\circ}C$ to 235 $^{\circ}C$ with a rate of 8 $^{\circ}C$ / min, hold

at 235 $^{\circ}C$ for 10 min.

Sample injection volume	0.4 μl.

Catalyst samples and feed stock tested by MAT were list in Table 3-2.

3.6.3 Hydrothermal Treatment Procedure and Test Condition

The fresh catalyst must be deactivated (normally by high temperature steaming) to decrease activity of the test catalysts before evaluation by using MAT Unit. In this work the deactivation was performed in hydrothermal aging unit model CLY-1 which manufactured by RIPP. (see full details of the equipment in Appendix C)

The hydrothermal treatment conditions were listed in Table3-2.

Table 3-2 Catalysts used to test by MAT Unit.

Catalysts	Treatment condition	Source of Catalysts
USY zeolite	4hrs.,100%steam,800°C	PSU.,Hat yai, Songkhla,Thailand
SRY zeolite	4hrs.,100%steam,800°C	RIPP.,Beijing , China
HY zeolite	4hrs.,100%steam,800°C	PSU.,Hat yai, Songkhla,Thailand
USY-1N Ex zeolite	4hrs.,100%steam,800°C	PSU.,Hat yai, Songkhla,Thailand
USY-2N Ex zeolite	4hrs.,100%steam,800°C	PSU.,Hat yai, Songkhla,Thailand
USY-3N Ex zeolite	4hrs.,100%steam,800°C	PSU.,Hat yai, Songkhla,Thailand
USY-4N Ex zeolite	4hrs.,100%steam,800°C	PSU.,Hat yai, Songkhla,Thailand

CHAPTER 4

RESULTS AND DISCUSSION

In this experiment, the results and discussion were concentrated on these purposed as follows:

4.1 Study the ion exchange conditions for prepared NH_4Y zeolite

4.2 Study the hydrothermal treatment conditions for prepared USY zeolite

4.3 Preparation the USY zeolite by hydrothermal treatment combined with acid leaching method

4.4 Evaluation the performance of the Y zeolite catalysts to cracking the gas oil by microactivity test (MAT) unit.

4.1 The influence of various factors to the ion exchange for prepared NH_4Y zeolite.

This topic relates to a method of zeolite cation exchange whereby essentially, more than 90 percent of the mobile cations are exchanged. In particular, the method of this invention comprises an initial ion exchange step, whereby, the more easily exchangeable cations are ion exchanged, followed by a heat treatment to provide the necessary activation energy for the redistribution of the redistributed cations that are exchanged.

The forms of zeolites containing alkaline metal ions are inactive in the cracking reaction. At the same time it is found that there is a complete absence of strong acid sites on the surface of the materials. Therefore, the preparation of an active cracking catalysts from zeolites requires the formation of strong acid sites. This is performed by exchanging varying amounts of the originally present sodium ions by ammonium ions or by di- or trivalent cations.

The method of generating acidity on the surface of the zeolite is the replacement of sodium ions by protons. In this experiment, the sodium ion exchange with ammonium chloride, since direct exchange with an acid destroys the crystalline framework of the

89

zeolite. Once the ammonium ions are placed inside the cages and the sodium ions are removed, the zeolites are calcined at a higher temperature, decomposing ammonium ions, driving off ammonia, and leaving protons in the place of the original sodium ions.

In this experiment, the NaY zeolite was used as a raw material. The influence of various factors to ion exchange was studied.

4.1.1 The ion exchange temperature

Carrying out the exchange at an elevated temperature can increase the rate of exchange. Obviously, the ion exchange temperature of the solution must be below the atmosphere boiling point of the solution, unless pressure equipment is used.

The influence of ion exchange temperatures in the range of 30 to $90^{\circ}C$ were studied. The NH_4Y zeolite samples were analyzed the amounts of sodium ion calculated as the oxide of the cation, for example, Na_2O, and the crystallinity retention by Atomic Absorption Spectroscopy (AAS) and X–Ray Diffractometer (XRD) respectively.

The results of the amounts of sodium ion measurements as shown in the form of Na_2O are shown in Table 4-1.

Table 4-1 Illustrate data of the influence of temperatures to Na_2O exchange in each order.

Temperature ($^{\circ}C$)	30	60	90
Exchange Order	Na_2O Content (%)		
NaY zeolite	12	12	12
1	5.86	5.23	1.82
2	4.76	4.28	1.50
3	2.93	1.63	0.90

From table 4-1, it can be observed that the number of sodium ions in the NaY zeolite was decreased along with increasing exchange order in each temperature, indicated that the sodium ions that located in the original sample structure have been replaced by

ammonium. The amounts of sodium ion largely decreased to lower values when the ion exchange temperature was reached $90^\circ C$ so that, the higher ion exchange temperature enhanced the removal of sodium ion from the NaY zeolite.

Parts of the influence of temperatures to Na_2O exchange degree are presented in Figure 4-1. Exchange degree was obtained from:

$$\text{Exchange degree (\%)} = \frac{(\text{initial Na} - \text{final Na})}{\text{Initial Na}} \times 100 \qquad (4\text{-}1)$$
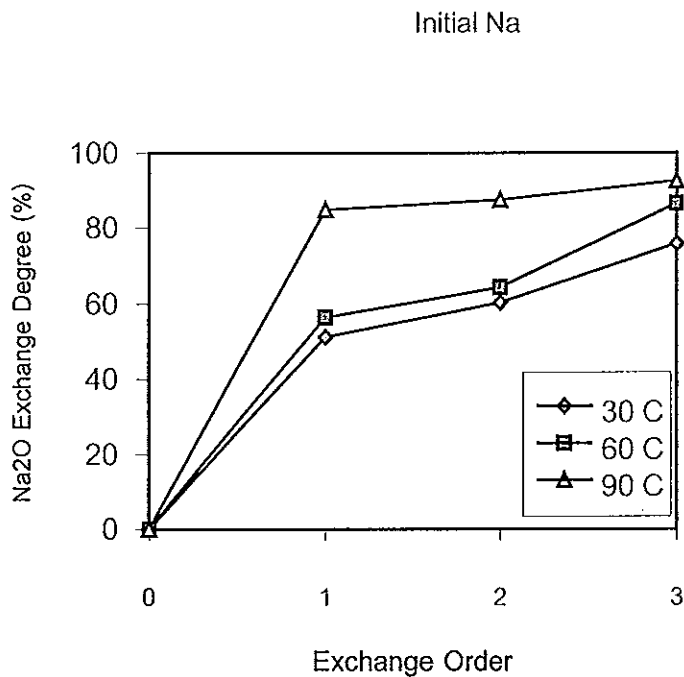
Figure 4-1 Representations of the influence of temperatures to Na_2O exchange in each order.

The ion exchange temperatures can effect the removal of sodium ions from the structure and the vacant position, which left by sodium ions were replaced by ammonium ions from the solution because when increasing the ion exchange temperature, the Na_2O exchange degree was increased. It has been observed in a NaY zeolite that about 85 percent of sodium ions are readily accessible for ion exchange from the original structure in the first exchange order. While the ion exchange temperature of about $90^\circ C$, indicates that the removal of sodium ions from the zeolite

strongly effected from the ion exchange temperature. The Na_2O exchange degrees have higher value in each exchange order than other temperatures.

The results of the influence of temperatures to crystallinity retention in each exchange order are shown in Figure 4-2.
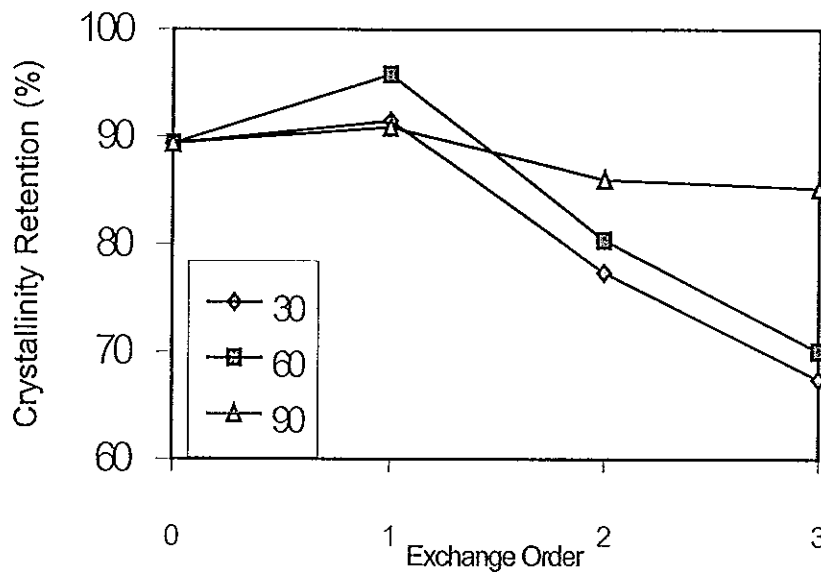
Figure 4-2 Dependence of crystallinity retention to ion exchange temperatures in each exchange order.

The crystallinity retention of NH_4Y zeolite has direct effect from the ion exchange temperature. When they increased, the crystallinity retention of NH_4Y zeolite slightly decreased and remained a higher percent than the low ion exchange temperature (see $90°C$). These results correspond to the amounts of sodium ion (see Table 4-1) that remains in high concentration in the NH_4Y zeolite cage at low ion exchange temperature so that, the higher amounts of sodium ions in the NH_4Y zeolite structure markedly affected to the loss of crystalline structure of the zeolite.

From this data, it is indicated that the desired ion exchange temperature for use to prepare NH_4Y zeolite is $90°C$.

4.1.2 The ion exchange time

The influence of the ion exchange time to the removal sodium ions from NaY zeolite are studied in this step, in the range of 1 to 3 hours and ion exchange temperature $90^{\circ}C$. The NH_4Y zeolite samples were analyzed by the amounts of sodium ion as shown in the form of Na_2O and crystallinity retention by Atomic Absorption Spectroscopy and X-Ray Diffractometer respectively.

The result of the sodium ions measurements as shown in the form of Na_2O are shown in Table 4-2

Table 4-2 Illustrate data of the influence of times to Na_2O exchange in each order.

Time (hour)	1	2	3
Exchange Order	Na_2O Content (%)		
NaY zeolite	12	12	12
1	1.82	2.51	2.24
2	1.50	1.71	1.61
3	0.90	0.75	0.63

From this Table, it can be seen that the rate of ion exchange can be increased by carrying out the exchange at an elevated time. Namely when increasing ion exchange times, the easy amounts of sodium ions was largely removed and only remaining small amounts remained locked in the original zeolite structure.
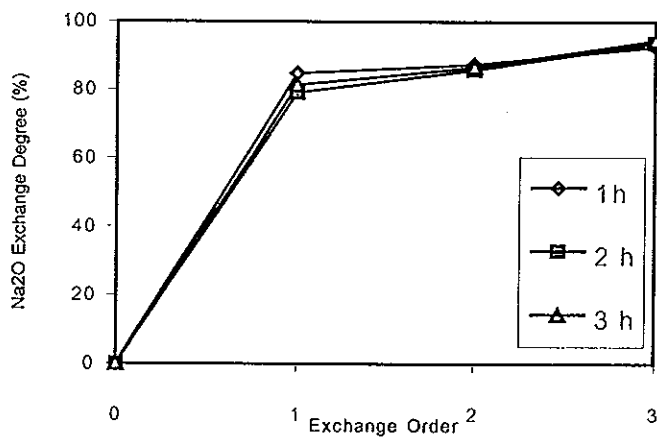
Figure 4-3 Representations of the influence of times to Na_2O exchange in each order.

From this Figure, it was found that the Na_2O exchange degree is similar in each exchange order, eventhough increasing the ion exchange time. Therefore, the difference in ion exchange times has little effect of the removal of sodium ions from the original zeolite structure.

The results of the influence of times to the crystallinity retention in each exchange order are shown in Figure 4-4.
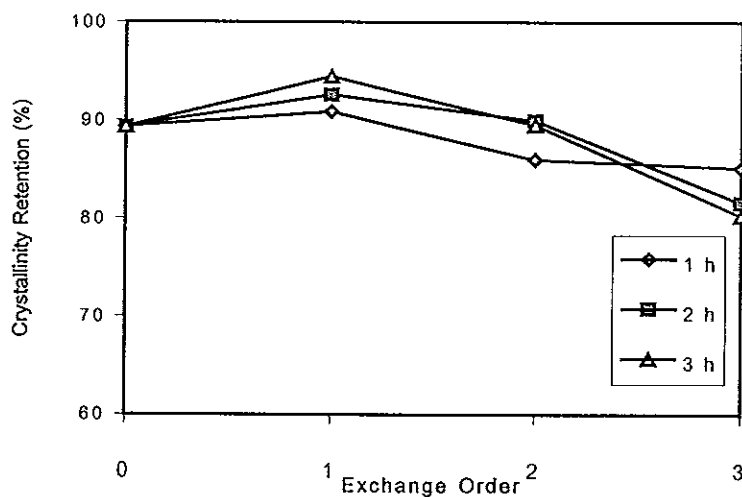
Figure 4-4 Dependence of crystallinity retention to ion exchange times in each exchange order.

This Figure indicates that the crystallinity retention of NH_4Y zeolite depends on the ion exchange time. The exchanged sample, in which contacted to the ion exchange time of 1 hour quite constant in a percent of crystallinity and it maintained about 85% after contacted to the ion exchange solution. Indicated that, although the structure of NH_4Y zeolite has low amounts of sodium ion when increasing the ion exchange time but it could not retained the crystallinity to higher degree. Therefore, the degree of crystallinity of these samples not only depends on the amounts of the caions in the structure but also depends on the ion exchange time.

From this data, the preferred ion exchange time is 1 hour; because of at this time the sample has lower amounts of sodium ion in the structure and retained higher degree of crystallinity.

4.1.3 The weight ratios

The influence of raw material weight ratios to the removal of sodium ions from the NaY zeolite structure were studied by the variations in the amounts of ammonium chloride (NH_4Cl) in each the weight ratios is as follows; NaY zeolite: NH_4Cl: H_2O in the range of 1: 0.5: 20, 1:1: 20 and 1: 1.5: 20 by using ion exchange temperature and time of 90 $^\circ$C, 1 hour respectively. The NH_4Y zeolite samples were determined the amounts of sodium ions and crystallinity retention by Atomic Absorption Spectrometry and X–Ray Diffractometer respectively.

The results of sodium ion measurement as shown in the form of Na_2O are shown in Table 4-3.

Table 4-3 Illustrate data of the influence of weight ratio to Na_2O exchange in each

exchange order.

Weight Ratio	1:0.5:20	1:1:20	1:1.5:20
Exchange Order	Na_2O Content (%)		
NaY zeolite	12	12	12
1	2.18	1.82	1.64
2	1.65	1.50	1.22
3	0.98	0.90	0.88

From this Table, it indicated that carrying out the exchange at different amounts of NH_4Cl could increase the rate of exchange. The sodium ion largely replaced by ammonium when increasing the amounts of NH_4Cl into the exchange solution.

The results of the influence of weight ratios to the Na_2O exchange degree are shown in Figure 4-5.
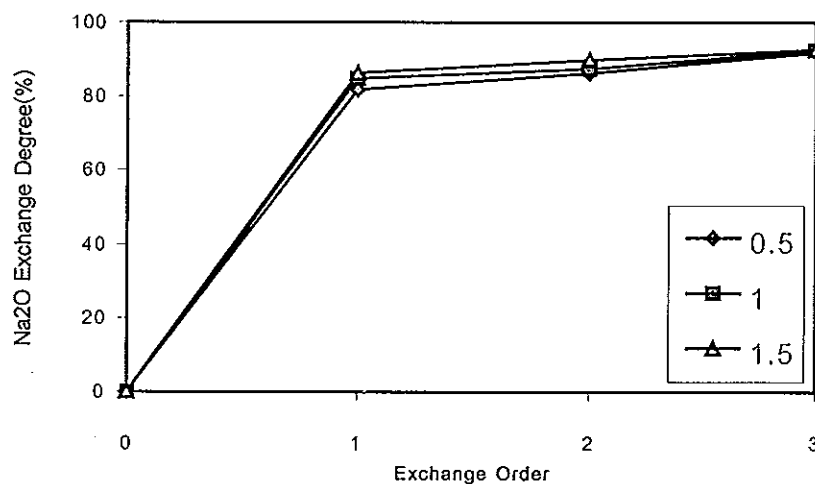
Figure 4-5 Representations the influence of the weight ratios to the Na_2O exchange

degree in each exchange order

From this Figure, it can be seen that the raw material weight ratios can effect the removal of sodium ions from the structure and the vacant position which, left by sodium

ions were replaced by ammonium ions from the solution, because when increasing the weight ratio, the Na_2O exchange degree was increased. It has been observed in these NaY zeolite samples that about 85 percent of sodium ions are readily accessible for ion exchange from the original structure in the first exchange order.

The results of the crystallinity retention of the NH_4Y zeolite samples in each weight ratio are shown in Figure 4-6.
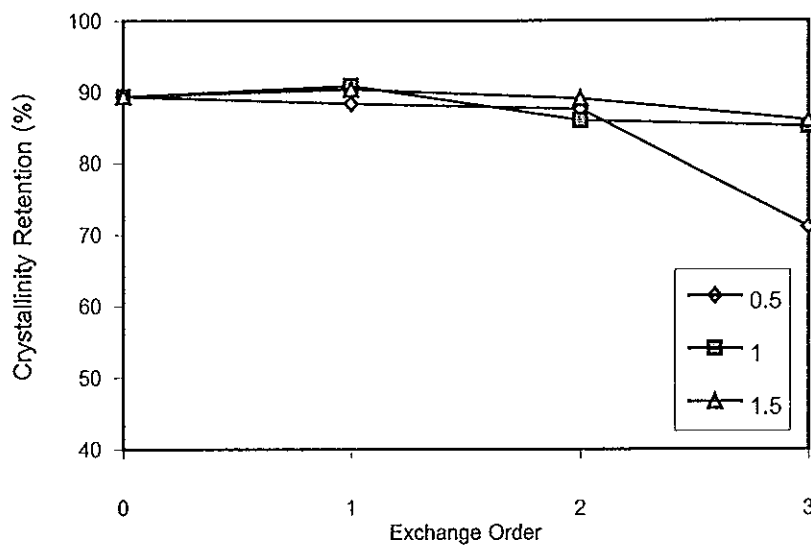
Figure 4-6 Dependence of crystallinity retention to raw material weight ratio in each exchange order.

This Figure shows that the degree of crystallinity stability of NH_4Y zeolite samples were quite constant in each exchange order but the final (third) exchange order of the weight ratio of 1: 0.5: 20 states that there was large decreased in the crystalline to lower degree than others. Because of in this weight ratio, the NH_4Y zeolite had a higher final degree of sodium ions that were still located in the zeolite structure. This cation more affected the crystallinity of zeolite sample.

From these data, it can be found that the desirable of weight ratio is 1:1:20.

4.2 The influence of various factors to hydrothermal treatment (steam calcination) for prepared ultrastable Y (USY) zeolite

The most active component in cracking catalysts is Y zeolite. Zeolite crystals have a regular network of very small diameter pores. The acid sites that catalyze cracking reactions are distributed on the internal and external surface area of the zeolite. The Y zeolite in cracking catalysts is a crystalline framework of these silicon and aluminum tetrahedral connected by shared oxygen atoms. The silicon content exceeds the aluminum content by a ratio of about 2.5 to 1 in conventional Y zeolite. Each aluminum atom is separated from the next aluminum atom by at least one silicon tetrahedron. Ultrastable Y zeolite is relatively poorer in aluminum atoms and enriched in silicon atoms. Its silicon to aluminum ratio is 4 or more. This means that the aluminum atom density and therefore the acid site density are reduced. This aluminum deficient, or dealuminated, Y zeolite has higher thermal and hydrothermal stability than conventional Y zeolite. The added stability is the reason it is called " ultrastable zeolite". The increased isolation of the aluminum acid sites enhances their acidity and reduces their ability to catalyze reactions involving two or more molecules.

No zeolite crystallization conditions are known that will economically produce USY zeolite directly. Instead, catalyst manufacturers crystallize conventional zeolite Y. Following this, high silica, removing aluminum atoms from the crystalline zeolite framework and replacing them with silicon atoms makes dealuminated USY. They are two basic approaches to dealumination of the zeolite framework, namely hydrothermal and chemical treatments.

The hydrothermal approach to dealumination involves treating the zeolite with steam at elevated temperatures. The aluminum–oxygen bonds are broken by the steam and the aluminum atom is expelled from the zeolite framework. The resulting hole is healed by a process that is said to involve insertion of Si $(OH)_4$ into the site vacancy left by the departing aluminum. If the vacancy is not healed it can reduce zeolite stability. Commercial hydrothermal dealumination processes are operated at conditions that minimize zeolite destruction.

The present topic relates to new compositions of matter consisting of crystalline aluminosilicate zeolites of the molecular sieve type having framework silica to alumina ratios substantially higher than has before been obtainable for use in hydrocarbon conversion reactions. More specially, zeolites of the molecular sieve type are subjected to a hydrothermal treatment (steam calcination) in the presence of water to effectuate removal of a substantial portion of alumina from the zeolite crystal structure thereby resulting in a high silica content crystalline zeolite molecular sieve, namely ultrastable Y (USY) zeolite.

The various factors involving the steam calcination were studied for obtained a desirable condition in the preparation of ultrastable Y (USY) zeolite. The results of each factor can be shown that as follows:

4.2.1 The influence of Na_2O exchange degree

Analysis data of the NaY zeolite after ammonium ion exchange at $90^{\circ}C$, 1 hour and NaY zeolite: NH_4Cl: H_2O in the weight ratio of 1: 1: 20 are given in Table 4-4 and a part of Na_2O exchange degree are presented in Figure 4-7.

Table 4-4 Illustrate data of the percent Na_2O in each exchanged order.

Exchange Order	Na_2O (%)
NaY zeolite (Starting material)	12
1	1.50
2	1.07
3	0.31
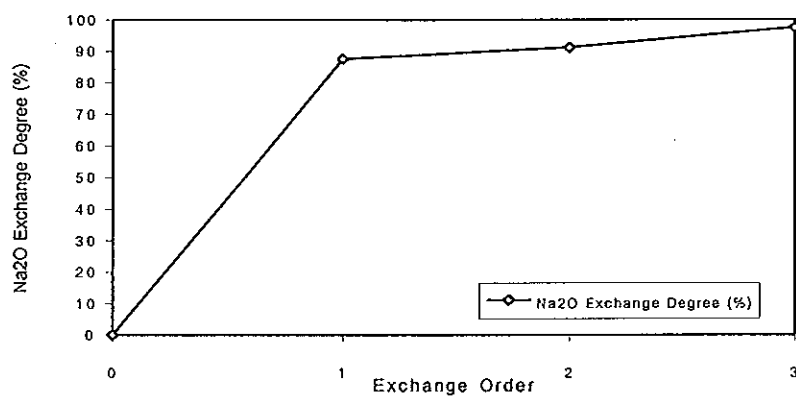
Figure 4-7 Representations of the exchange order to Na_2O exchange degree.

From this data, it is indicated that the amounts of sodium ions largely reduced from the original structure of zeolite in the first ion exchange, about 85 percent of this cation are readily accessible for ion exchange. Because of they are located in the unlocked positions of the zeolite structure, thus they are easily to removed and then, these positions were replaced by ammonium ions. Before the next ion exchange, the zeolite sample should be subjected to heat treatment (calcined) to provide the necessary activation energy for the redistribution of the remaining locked in sodium ions. The calcined temperatures are 350 and 550 °C wherein, used before in the second and third ion exchange respectively.

The results of the crystallinity stability in which were determined by differential thermal analyser (DTA) are shown in Figure 4-8 and Table 4-5.
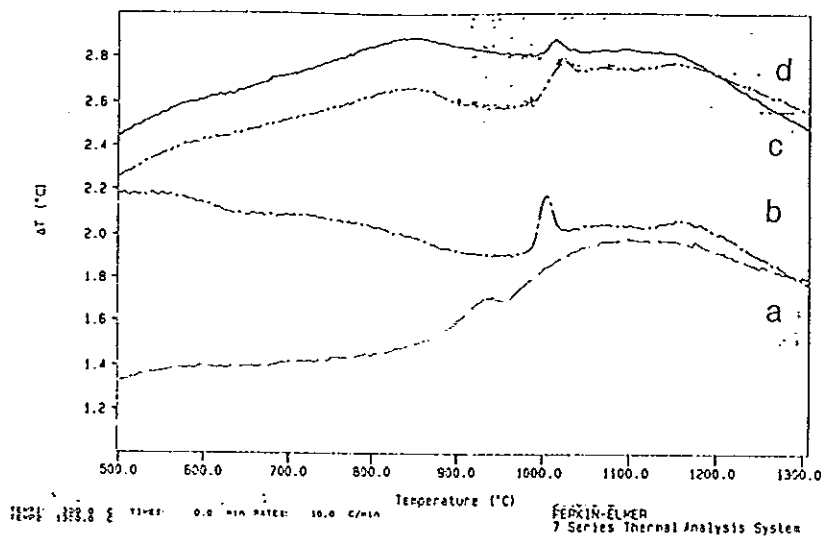
Figure 4-8 Differential thermal analyses of ion exchange-steamed Y zeolites as (a) NaY zeolite, (b) 1st ion exchanged Y zeolite, (c) 2nd ion exchanged Y zeolite and (d) 3rd ion exchanged Y (USY) zeolite.

Table 4-5 Illustrate data of the crystallinity stability and surface area of steamed Y zeolite samples on various exchange order

Exchange Order	Crystallinity Stability, $^\circ$C, (DTA)	Surface area, m^2/g, (BET)
NaY zeolite (Starting Material)	965.27	560
NaY zeolite	930	474
1	1004.23	532
2	1022.27	493
3	1015.2	462

Figure 4-8 shows the differential thermal analysis of the steamed calcination zeolite samples. Each sample showed exotherms between 900 to 1050 °C wherein corresponds to the crystal collapse temperature. The steamed Y zeolite sample, which was subjected to ion exchange and steamed treatment, had a crystallinity stability

excess of 1000°C that is shown in Table 4-5. It has been recognized that the presence of alkali metal ions (normally sodium ions) results in the collapse of the crystalline structure at relatively low temperatures. This is of course, expected from knowledge of the melting points of glasses having similar chemical compositions. The thermal stability of zeolites generally increases with the framework silica to alumina ratio. The amounts of sodium ions in the zeolite structure play important roles to the thermal stability of steamed Y zeolites. The crystalline of Y zeolite retained at higher temperature when the structure had low amount of sodium ions. Apart of surface area decreased when increasing exchange order.
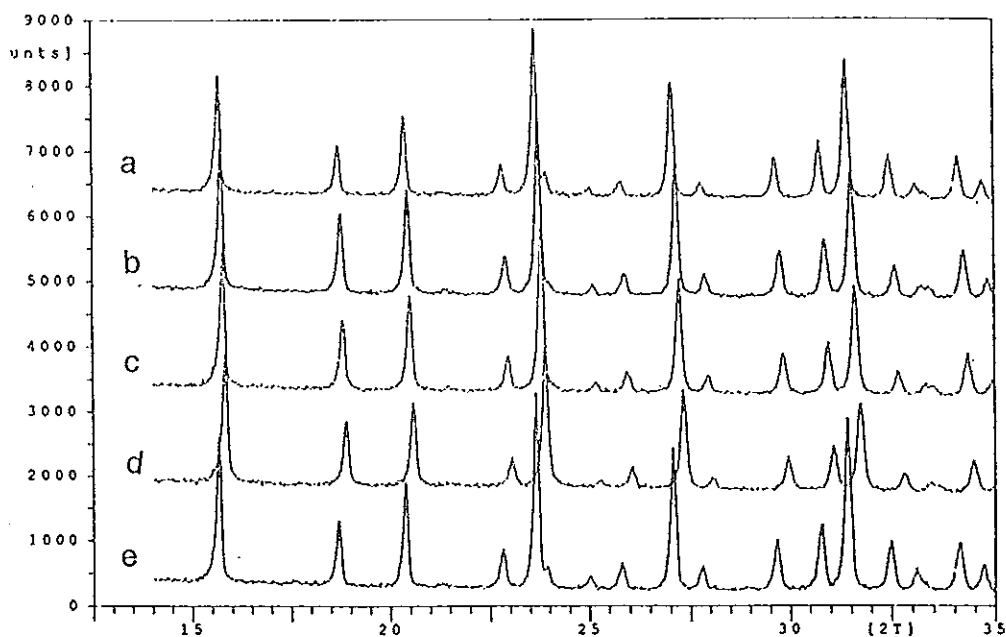
Figure 4-9 Representations of the XRD patterns of steamed Y zeolites as a) NaY zeolite b) 1st ion exchange steamed Y zeolite c) 2nd ion exchange steamed Y zeolite d) 3rd ion exchanged steamed Y (USY) zeolite compared with e) NaY zeolite standard.

Figure 4-9 shows the XRD patterns of steamed Y zeolite in which the spectrum of each sample was shifted to higher 2θ compared to the spectrum of NaY zeolite standard, since the partial removal of the aluminum ions from these samples framework. The zeolite framework has a lower aluminum per unit cell and unit cell shrinked.

A part of the surface morphology of the zeolite samples is shown in Figure 4-10.
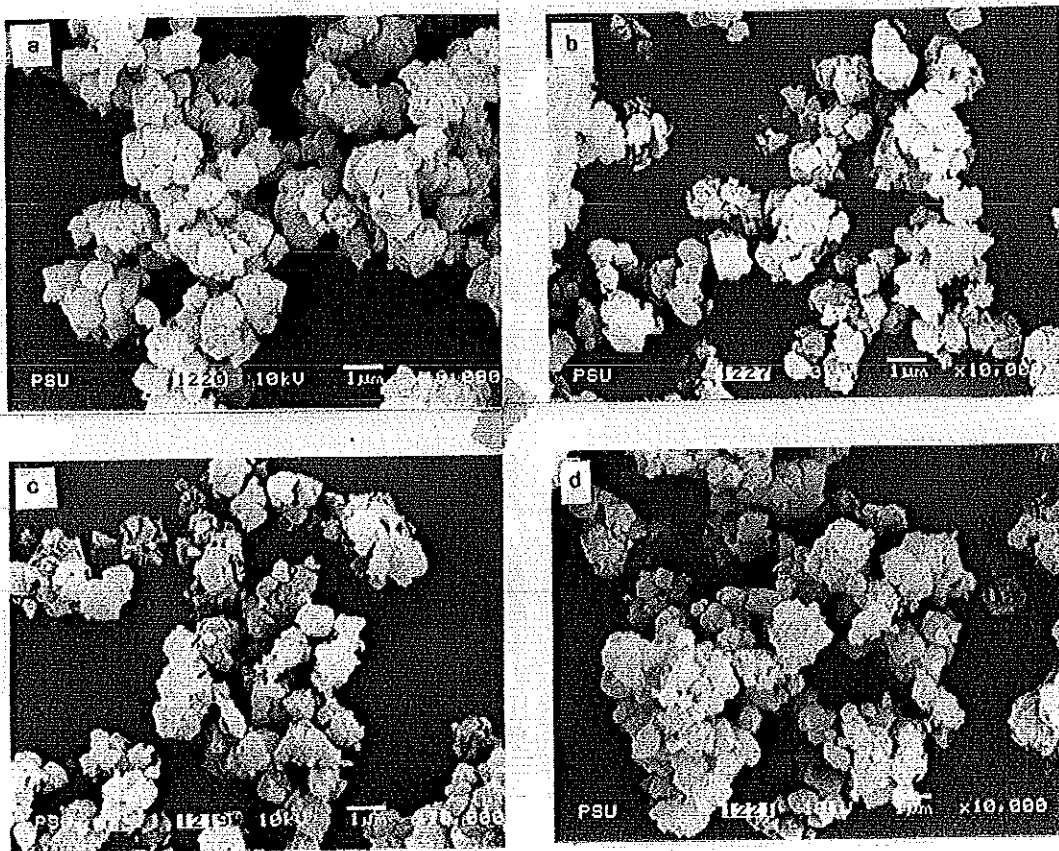
Figure 4-10 Representations of a surface morphology of steamed Y zeolites as a) NaY zeolite b) 1st ion exchange steamed Y zeolite c) 2nd ion exchange steamed Y zeolite d) 3rd ion exchanged steamed Y (USY) zeolite

The surface morphology of the Y zeolites was determined by using a Jeol JSM – 5800LV scanning electron microscope (SEM). Standard gold coating techniques were used to prevent specimen charging. The spatial resolution was therefore limited by the granularity of the gold film to about 5 nm. From this Figure, it can be seen that these zeolites have irregular shape of crystals and an average crystal size of about 1μ. A NaY zeolite has a larger crystal size than the ion exchange steamed Y zeolites. These zeolites were contacted to steam for 2 hours, which lead to the unit cell shrinkage, namely the framework dealumination occurred. These results were shown that the characteristic of crystal zeolite effected by the steam.

4.2.2 The influence of the treated temperature

The influence of the treated temperature to the preparation of a USY zeolite was studied in the range of 400 to 700 °C.

Table 4-6 Physicochemical of steamed Y zeolite samples on various the treated temperatures.

The treated Temp.(°C)	Framework[1] SiO_2/Al_2O_3 ratio	N_{Al}[1]	N_{Si}[1]	% Al removed
400	8.78	35.60	156.4	34.11
500	13.19	25.23	166.77	53.3
600	16.77	20.39	171.61	62.26
700	17.89	19.24	172.76	64.39

1 According to the Breck–Flanigan relationship (Dai,1996).

From Table 4-6, the Breck–Flanigan relationship (Dai,1996) was used to calculate the framework silica to alumina ratio, number of aluminum (N_{Al}) and number of silicon (N_{Si}). It is shown that, when increasing the steam treatment temperature leading to the removal of aluminum from framework into nonframework positions more than the

lower temperature. It can be observed from the percent of Al removed, namely when the temperature attained 500 °C, more than 50 percent of aluminum was removed from the framework into nonframework positions and the framework silica to alumina ratio increased excessively to 10. The formation of USY zeolite has been related to the expulsion of aluminum from the framework into the zeolite cages in the presents of steam and the filling of framework vacancies by silicon atoms in which they migrate with steam.

The results of crystallinity stability of steamed Y zeolite samples are presented in Figure 4-11.

Figure 4-11 Correlation of the treated temperatures to crystallinity retention and unit cell
size of steamed Y zeolite samples.

This Figure shows that the crystallinity retention is quite constant in each steam treatment temperature between 400 – 600 °C and then decreases while the samples contacted to a higher temperature. A part of unit cell size directly relates to the amounts of the aluminum per unit cell. Therefore, when the aluminum was removed from the framework, it effected the reduction of the unit cell size. Originally the NaY zeolite is 24.66 Å of a unit cell size but it decreased to 24.37 Å after the zeolite sample contacted

to steam at the temperature of 600 °C. The USY zeolite prepared in the higher steam calcination temperature had more siliceous framework than those prepared in the lower temperature.

The data from the Table 4-6 and Figure 4-11 indicates that a suitable temperature in the steam calcination treatment is 600 °C, because of a USY zeolite has lower unit cell size about 24.37 Å and the structure retained a high degree of crystalline about 65.5 percent. At the higher steam calcination temperature, the unit cells size slightly decreased but had a large loss of crystallinity.

The steam calcination temperatures play an important role in the preparation of USY zeolite to desired properties, that is to say to a high degree of crystallinity and low unit cell size. It is necessary to keep constant temperature during steam calcination.
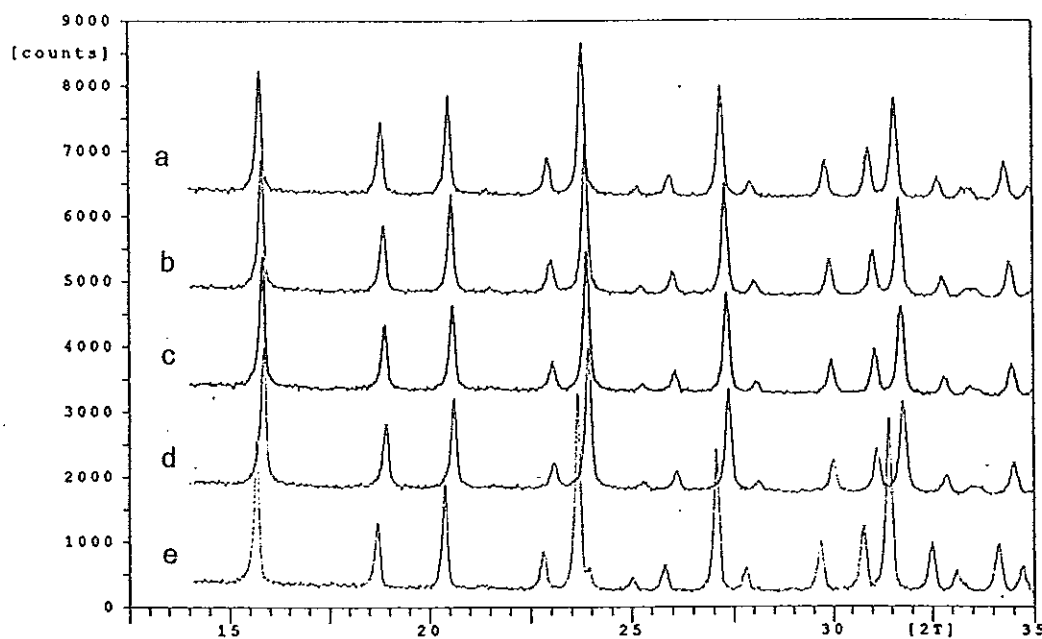
Figure 4-12 Representations of the XRD patterns of steamed USY zeolites which contacted to steam at several temperatures as a) 400°C b) 500°C c)600°C and d)700°C compared to e) NaY zeolite standard

Figure 4-12 shows the XRD patterns of steamed Y zeolite in which the spectrum of each sample was shifted to higher 2θ compared to the spectrum of NaY zeolite standard, since the partial removal of the aluminum ions from the sample framework. The zeolite framework has a lower aluminum per unit cell and unit cell shrinkage.

4.2.3 The influence of the water to zeolite ratio

Steam has an important role in the steam calcination treatment, since it can remove aluminum ions from the zeolite framework and effect to the degree of crystallinity. The effect of steam to zeolite ratio to the preparation of a USY zeolite was studied in the range of 2.25 to 9.

Table 4-7 Physicochemical of steamed Y zeolite samples on various water to zeolite
ratios.

Water to zeolite ratio	Framework[1] SiO_2/Al_2O_3 ratio	N_{Al}[1]	N_{Si}[1]	% Al removed
2.25	14.70	22.93	169.07	57.56
3	16.77	20.39	171.61	62.26
4.5	15.58	21.77	170.23	59.71
9	15.58	21.77	170.23	59.71

1 According to the Breck–Flanigan relationship (Dai,1996).

The Breck–Flanigan relationship (Dai,1996) was used to calculate the framework silica to alumina ratio, N_{Al} and N_{Si} in the unit cell. The difference in the water to zeolite ratio effected the removal of aluminum from the framework into a different degree. The water to zeolite ratio, about 3, give a high framework silica to alumina ratio up to 16.77, because in this ratio the aluminum was removed from the zeolite framework in a high degree about 62.26 percent. From this data, it is indicated that the amount of steam strongly effected to the preparation of a USY zeolite. Only a suitable ratio could remove

aluminum from the zeolite framework in a higher degree. The other ratio could not strongly effect the removal of aluminum into a desired degree.

The results of correlation between water to zeolite ratio to crystallinity stability and unit cell size of steamed Y zeolite samples is shown in the Figure 4-13.
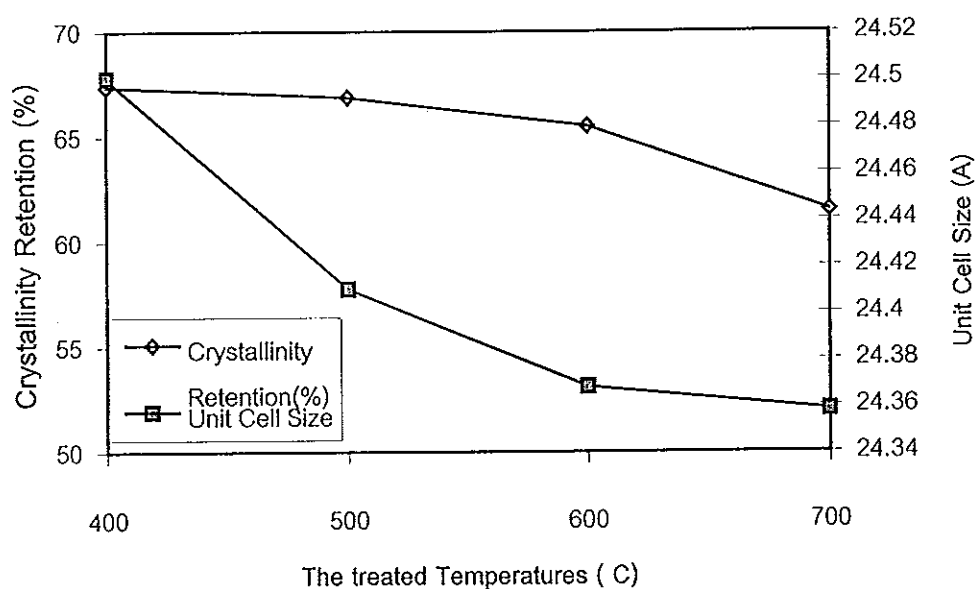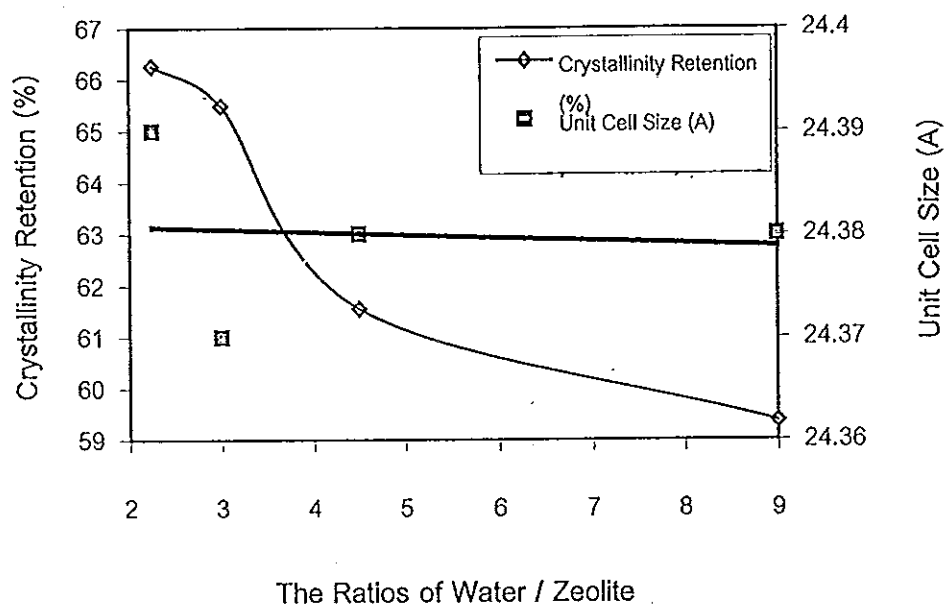

Figure 4-13 Correlation of water to zeolite ratios to crystallinity retention and unit cell size of steamed Y zeolite samples.

This figure shows a little change in the crystallinity at the low ratio of water to zeolite in the range of 1 to 3, but it shows a large decrease when it contacted to the high amount of steam. While, at a constant in the reduction of aluminum from the framework zeolite, which can be observed from the constant in the unit cell size of about 24.38 Å, it indicated that the excess amount of steam could be more affected to the crystallinity retention than the reduced aluminum from the zeolite framework.

The calcination of NH_4Y zeolite in the presence of steam results in the expulsion of tetrahedral aluminum from the zeolite framework into nonframework position. This, process, which consists essentially in a high temperature hydrolysis of Si–O–Al bonds,

leads to the formation of nonframework aluminum species, while increasing the framework silica to alumina ratio and decreasing the zeolite unit cell size, the reaction as shown in Figure4-14. In addition to amorphous alumina, amorphous silica-alumina is also form as shown in Table 4-8 (Scherzer,1989).

A) FRAMEWORK DEALUMINATION

(2) $Al(OH)_3$ + $H^+[Z]$ ———→ $Al(OH)_2^+[Z]$ + H_2O
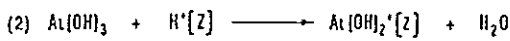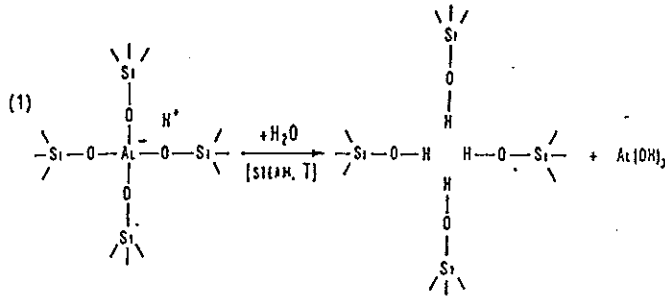
(B) FRAMEWORK STABILIZATION
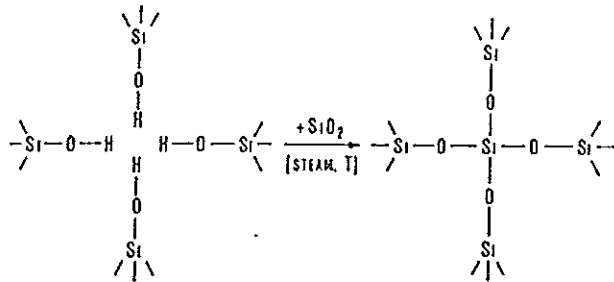
Figure 4-14 Reaction mechanism for hydrothermal dealumination and stabilization of Y Zeolite (Scherzer,1984)

Table 4-8 Framework and nonframework aluminum species in USY zeolites (Scherzer,1984)

Figure 4-15 Representations of the XRD patterns of steamed USY zeolites which
contacted to different amounts of steam to zeolite ratio as a) 2.25 b) 3
c) 4.5 and d) 9 compared to e) USY zeolite and f) NaY zeolite standard.

The progress of framework dealumination can be observed from the X-Ray
Diffraction scan, since the diffraction peaks are shifted to higher 2 θ values (lower–d
spacing) with progressive dealumination. It was shown that the defect sites left by
dealumination are filled to a large extent by silica, which leads to a very stable, highly
siliceous framework (Figure 4-14 (b)).

4.2.4 The influence of the treated time

The treated time wherein used to flowing the steam over the zeolite samples in
the range of 1 to 4 hours was studied.

Table 4-9 Physicochemical of steamed Y zeolite samples on various the treated times.

The treated Time (h)	Framework[1] SiO_2/Al_2O_3 ratio	N_{Al}[1]	N_{Si}[1]	% Al removed
1	14.87	22.70	169.3	57.99
2	16.77	20.39	171.61	62.26
3	17.31	19.82	172.18	63.32
4	17.65	19.47	172.53	63.96

1 According to the Breck – Flanigan relationship (Dai,1996).

From Table 4-9, N_{Al}, N_{Si} and framework silica to alumina ratio were calculated from Breck – Flanigan relationship (Dai,1996). The treat time play important role in the dealumination, namely the aluminum was removed over 50 percent from the framework when the zeolite sample subjected to steam in a long period of time.

The results of the correlation between the treated times to crystallinity stability and unit cell size of steamed Y zeolite is shown in Figure 4-16.
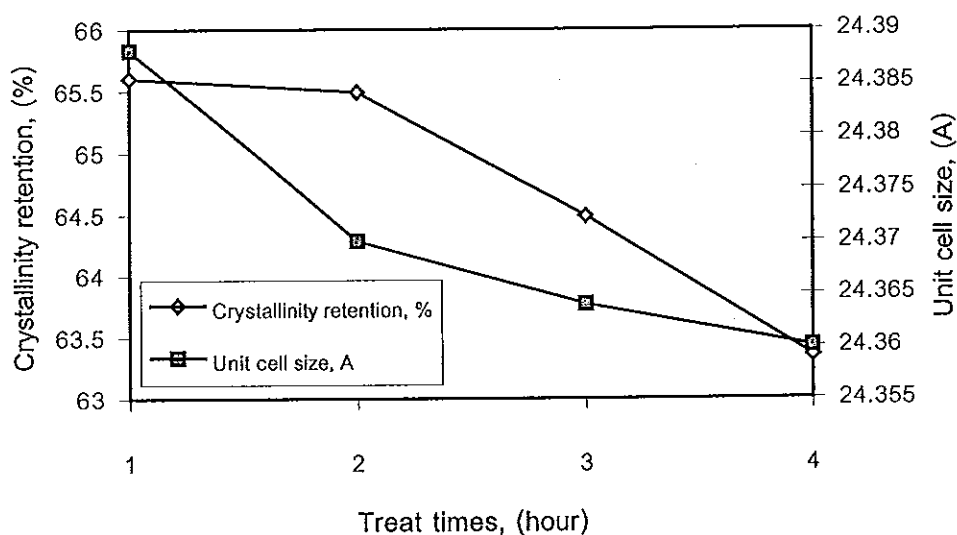

Figure 4-16 Representations between treat times to crystallinity retention and unit cell size of steamed Y zeolite samples.

From Figure 4-16, the degree of crystallinity is constant in the range of the treated time 1-2 hours but the degree of crystallinity largely decreased when the zeolite sample further contacted to the steam in the longer period of the treated time. A part of dealumination depends on the treated time; zeolite unit cell size largely decreased when zeolite samples contacted to steam for 2 hours, however, in the longer periods, the zeolite unit cell size slightly decreased contrasting with crystallinity of which largely decreased.

The treated time that the zeolite sample contacted to steam strongly effected the preparation of USY zeolite. The suitable time is 2 hours, because a USY zeolite could maintain the crystallinity in high degree and low zeolite unit cell size.
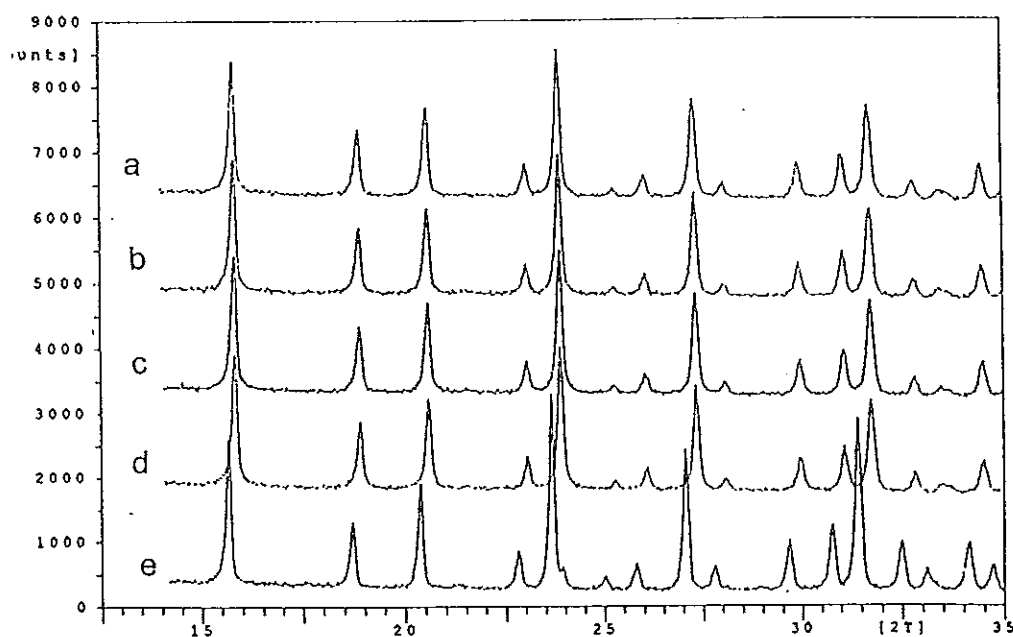
Figure 4-17 Representations of the XRD patterns of steamed USY zeolites, which contacted to steam in several hours as a) 1 hour b) 2 hours c) 3 hours and d) 4 hours compared to e) NaY zeolites standard.

The progress of framework dealumination can be observed from the X-Ray Diffraction scan, since the diffraction peaks are shifted to higher 2θ values (lower-d

spacing) with progressive dealumination. It was shown that the defect sites left by dealumination are filled to a large extent by silica, which leads to a very stable, highly siliceous framework (Figure 4-14 (b)).

Thermal and hydrothermal stability of a ultrastable Y zeolite

While the stability of high–silica Y zeolites is generally higher than that of the parent Y zeolite, there are significant differences in stability, depending upon the preparation method used. For this experiment, USY zeolite in which most of the framework vacancies are filled by silicon insertion, show high thermal and hydrothermal stability as shown in Figure 4-18.
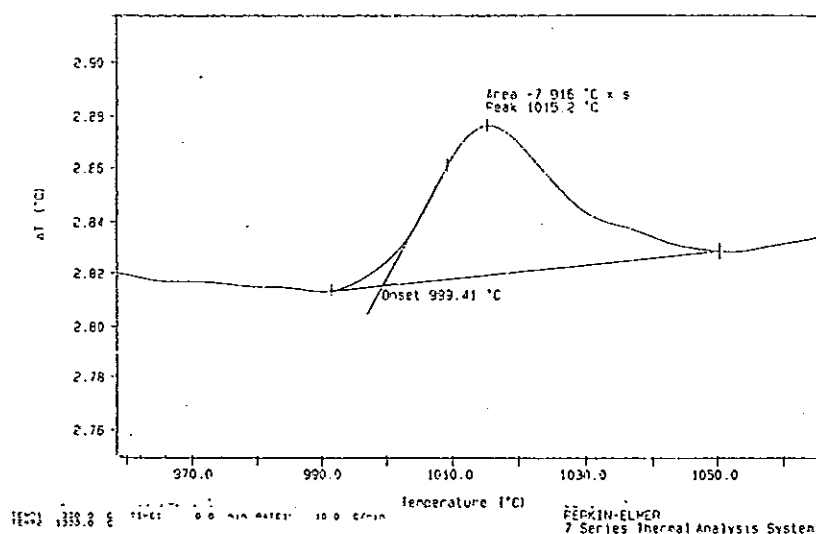
Figure 4-18 Representations the differential thermal analyses of USY zeolite

USY zeolite samples prepared by the procedures described retain the major portion of their crystalline structure after heating to temperature in excess of $1000^{\circ}C$. USY zeolite, the inserted silicon originates from an internal source (i.e., the zeolite itself), resulting in partial damage to the zeolite framework as shown in the form of loss in crystallinity.

4.3 Hydrothermal and chemical treatment (Acid leaching)

The influence of mineral acid to the dealumination of USY zeolite was studied in this topic. The hydrochloric acid (HCl) was used in the concentration of 1 to 4 Normal.

The acid dealuminated Y (USY) zeolite is derived from an ammonium exchanged Y zeolite with relatively low sodium content which is calcined under hydrothermal conditions (steam calcination) prior to dealumination by the HCl.

Physicochemical characteristics of the acid leached USY zeolite are shown in the Table 4-10.

Table 4-10 Physicochemical characteristics of the acid leached USY zeolite samples.

Samples	HCl Conc (Normal)	Crys. (%)	UCS (Å)	FAL/uc.[1]	Framework[1] SiO_2/Al_2O_3	(%) Al removed
1	0	62.67	24.38	21.77	15.58	59.71
2	1	58.90	24.24	5.65	64.82	89.54
3	2	31.60	24.12	< 5.65	> 64.82	> 89.54
4	3	23.15	24.076	< 5.65	> 64.82	> 89.54
5	4	19.78	24.067	< 5.65	> 64.82	> 89.54

1 According to the Breck – Flanigan relationship (Dai,1996).

A part of correlation between HCl concentrations to crystallinity retention and unit cell size of acid leached USY zeolite samples are presented in Figure 4- 19.
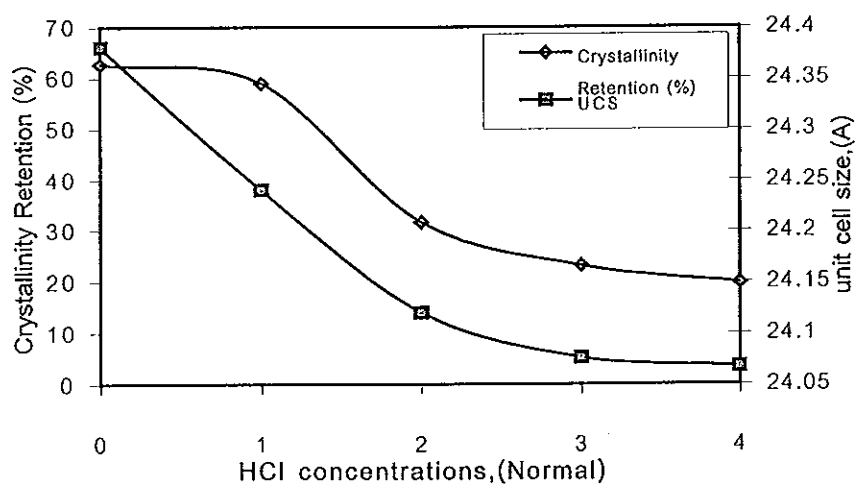
Figure 4-19 Correlation between HCl concentrations to crystallinity retention and unit cell size of acid leached USY zeolite samples.

From Table 4-10, the Breck-Flanigan relationship was used to calculate framework aluminum and per unit cell and framework silica to alumina ratio. It can be seen that the dealumination of acid leached USY zeolite samples are dependent markedly on the concentration of HCl. The amounts of aluminum ion was removed up to 89.54 percent when the USY zeolite sample contacted to 1 Normal of HCl. Thus the acid leached USY zeolite had low aluminum in the framework. Unit cell size and crystallinity retention that shown in Table 4-10 and Figure 4-19 indicated that they were strongly affected by HCl concentrations, since the large loss in crystallinity at high concentration, namely the zeolite structure can not integrity when contacted to high concentration of mineral acid. The large decrease in zeolite unit cell size was caused from the dealumination in which lead to unit cell shrinkage. The HCl concentration 1 Normal markedly effected to unit cell shrinkage from 24.38 to 24.24 Å.

A part of crystallinity stability of acid leached USY zeolite is shown in Figure 4-20 and Table 4-10
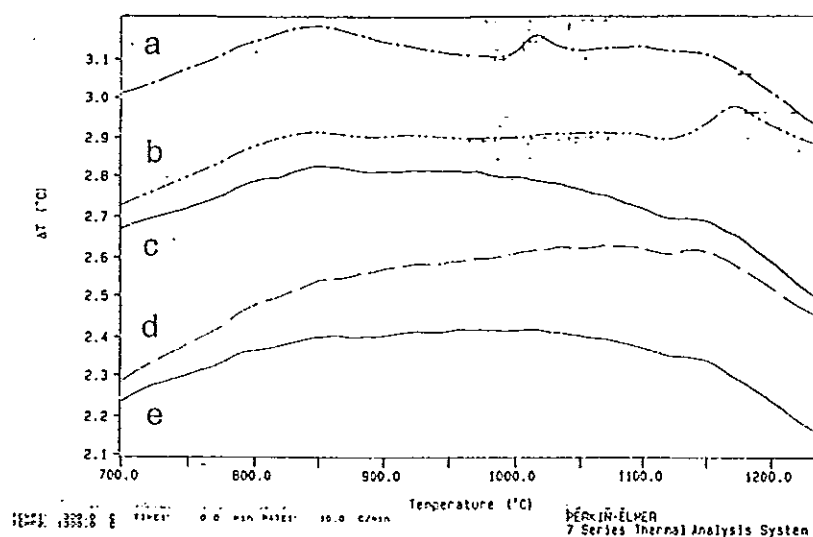
Figure 4-20 Representations the differential thermal analyses of acid leached USY zeolites which contacted to several concentration of HCl as b) 1 N c) 2 N d) 3 N and e) 4 N compared to a) USY zeolite.

Table 4-11 Illustrate data of the crystallinity stability of acid leached USY zeolite samples on various HCl concentrations.

HCl conc' (Normal)	Crystallinity Stability, °C ,(DTA)
0	1015.2
1	1172.04
2	1174.62
3	1155.95
4	1155.82

The data of differential thermal analysis in the Figure 4-20 shows that, the acid leached USY zeolites whereby, prepared by the procedure described retain a major portion of their crystalline structure after heating to temperatures in excess of 1150 °C in which, can be observed from the exotherm that occurred between 1100 to 1200 °C. The exotherm of starting USY zeolite appeared at 1015.2 °C which was lower than the acid leached USY zeolites, since it has high amount of aluminum in the framework and sodium ions, so its structure easily changed to another phase while contact to high temperature.

A part of XRD patterns of acid leached USY zeolite is presented in Figure 4-21

The XRD patterns from Figure 4-21 show that, the peak high was decreased while increasing the HCl concentrations, because of the loss of crystalline structure of these zeolite. The spectrum shifted to higher 2θ values when these samples contacted to high concentration of HCl due to the dealumination.
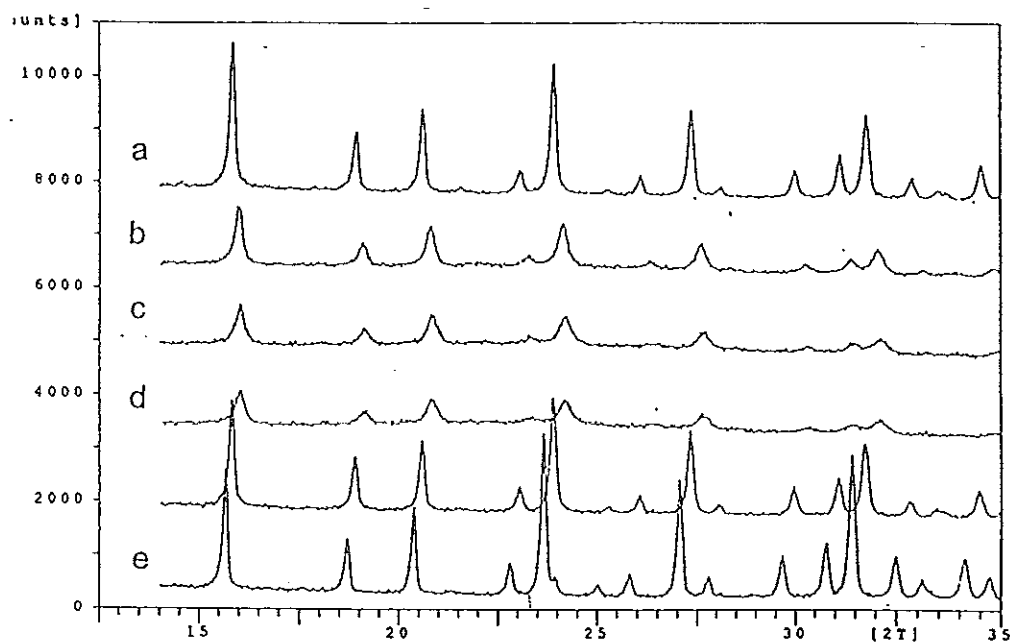
Figure 4-21 Representations of the XRD patterns of acid leached USY zeolites which contacted to several concentrations of HCl as a) 1 N b) 2 N c) 3 N and d) 4 N compared to e) NaY zeolite standard.

A part of surface morphology of acid leached USY zeolite is shown in Figure 4- 22.
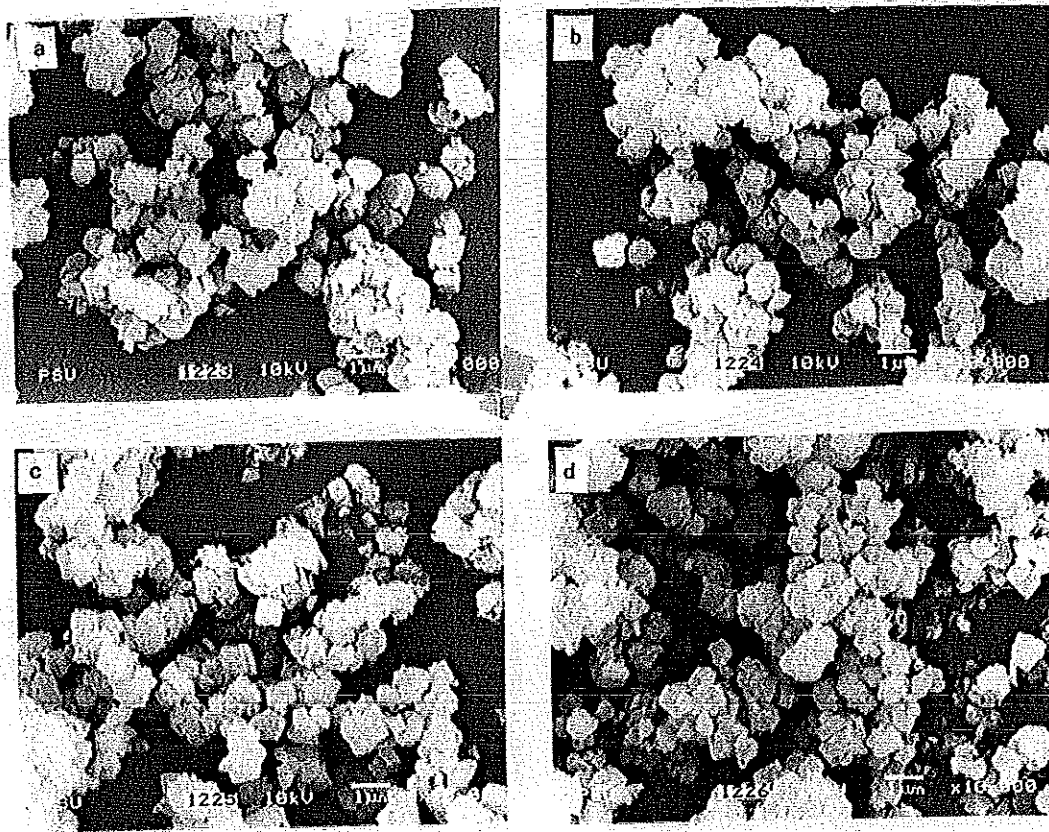
Figure 4-22 Representations of the surface morphology of acid leached USY zeolites which contacted to several concentrations of HCl as a) 1 N b) 2 N c) 3 N and d) 4 N.

Figure 4-22 shows the crystal characteristic of acid leached USY zeolites in which they were subjected to steam and followed by acid leaching in different concentrations, then analyzed the surface morphology of crystal shape and size by scanning electron microscope (SEM). These zeolite crystals were different in shape and size compared with NaY zeolite (See Figure 4-10). The change of these zeolites shape and size was caused by the steam and concentration of HCl, namely framework dealumination occurred in the steam treatment process followed by framework and nonframework dealumination in the acid leaching process that caused to the damage in crystal of these zeolites.

4.4 Microactivity Testing

Catalytic hydrocarbon cracking is an important step in the conversion of crude oil to transportation fuels. Industrial cracking catalysts contain a significant component resembling a USY zeolite, in addition to an amorphous matrix and binder. It is generally accepted that the cracking activity can be attributed to the BrØnsted acidity of the zeolite, and the reaction can be described well with carbenium ion chemistry (Gates, 1992)

The Thai gas oil that was produced by true boiling point distillation unit at chemical engineering department, PSU was used as the gas oil feedstock in the catalytic cracking test. The several zeolite catalysts that were prepared at the chemical engineering department, PSU (shown in Table 4-12) were used in this experiment. A part of microactivity testing (MAT) unit and test method can see in appendix D.

Table 4-12 Physicochemical of raw materials used for prepared catalysts and surface area of steamed catalysts

Catalysts	Crystallinity[1] (%)	Unit cell size[2],a_0, (Å)	Surface area[3], (m^2/g)	Surface area[4], (m^2/g)
USY zeolite	65.5	24.37	462	199
SRY zeolite	69.40	24.52	-	185
HY zeolite	85.16	24.66	558	178
USY-1N zeolite	58.90	24.24	577	233
USY-2N zeolite	32.60	24.12	601	146
USY-3N zeolite	23.15	24.076	436	127
USY-4N zeolite	19.78	24.067	525	123
Kaolin Clay	-	-	43	-
Pheudoboemite, (PBA)	-	-	343	-

1,2,3 based on fresh zeolite

4 based on steamed catalysts

Figure 4-23 Dependence of catalyst activity on zeolite unit cell size for catalyst containing 30% zeolite

Figure 4-23 Shows the correlation between unit cell size to catalytic activity of SRY, USY and USY-1N zeolite catalyst respectively. The catalytic activity of these catalysts is related to the unit cell size, namely it decreased when zeolite unit cells size decreased, because zeolite crystals have a regular network of very small diameter pores. The acid sites that catalyze cracking reactions are distributed on the internal and external surface area of the zeolite. The building blocks for zeolites are silicon or aluminum atom, tetrahedrals, surrounded by four oxygen atoms. Each of the four oxygen atoms is shared by two tetrahedrals, so it contributes one negative charge to each tetrahedron. Silicon is in a +4 oxidation state, so tetrahedron contain silicon is neutral in charge. In contrast, aluminum has one less electron and is a +3 oxidation state. This means each tetrahedron containing aluminum has a net charge of -1 which, must be balanced by a positive ion such as sodium or proton. Protons that balance the negative charge of aluminum tetrahedral have strong acidity which, is know in catalyze cracking reactions. Unit cell size directly relate to aluminum atoms in the framework, so when lower aluminum in the framework leads to catalytic site and total acidity of the zeolite decreased. Therefore, low in catalytic activity..

Figure 4-24 Correlation between unit cell size to gasoline yield and gasoline selectivity of HSY zeolite catalysts

Figure 4-24 is presenting the correlation between unit cell size to gasoline yield and gasoline selectivity of SRY, USY and USY-1N zeolite catalysts. Indicated that gasoline yield decreased along decreasing unit cell size, which corresponding to catalytic activity as described previously, namely when the catalytic site decreased leads to low in conversion of gas oil to gasoline.

Compared the gasoline selectivity between USY and SRY zeolite catalyst, it can be observed that USY zeolite catalyst had higher gasoline selectivity than SRY zeolite catalyst in which according to SRY zeolite catalyst has higher unit cell size thus allows larger gas oil molecules into the structure. So, it can crack the gas oil to other fractions beyond gasoline in the higher yield than USY zeolite catalyst.

The result of coke formation in the cracking of HSY zeolite catalysts is shown it the Figure 4-25
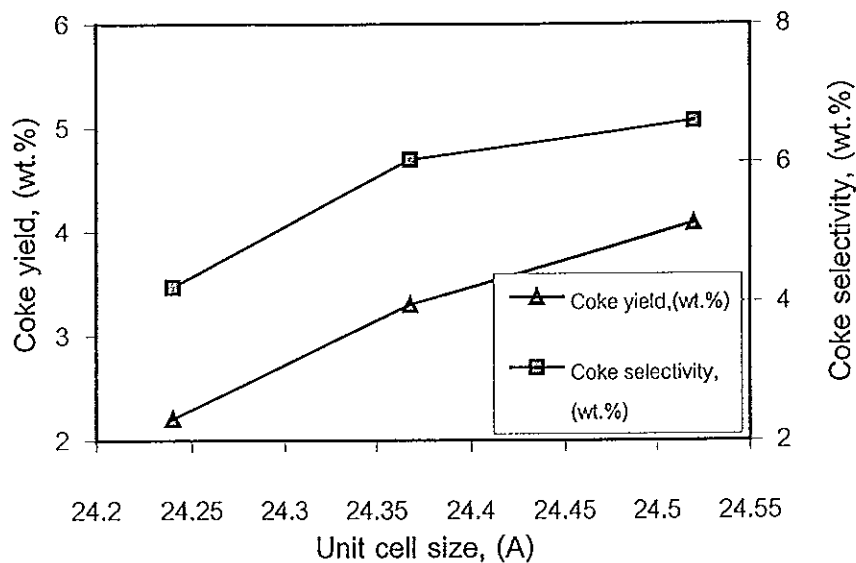
Figure 4-25 Correlation between unit cell size to coke yields and coke selectivity of HSY

zeolites catalysts.

Figure 4-25 shows the relationship between unit cell size to coke yields and coke selectivity of SRY, USY and USY-1N catalysts. Both coke yield and coke selectivity decreased in zeolite unit cell size. Because these catalysts decreased in catalytic site density it lead to increase the isolation of the aluminum acid sites, which enhances their activity and reduces their ability to catalyze reactions involving two or more molecules. These isolated sites give USY zeolite its characteristic ability to increase olefin yield by reducing the effects of a bimolecular reaction called hydrogen transfer. Hydrogen transfer plays a key role in the gas oil cracking process. It reduces the amount of olefin in the product, contributes to coke formation.

The result of catalytic activity of HY and HSY zeolite catalysts is presented in Figure 4-26.
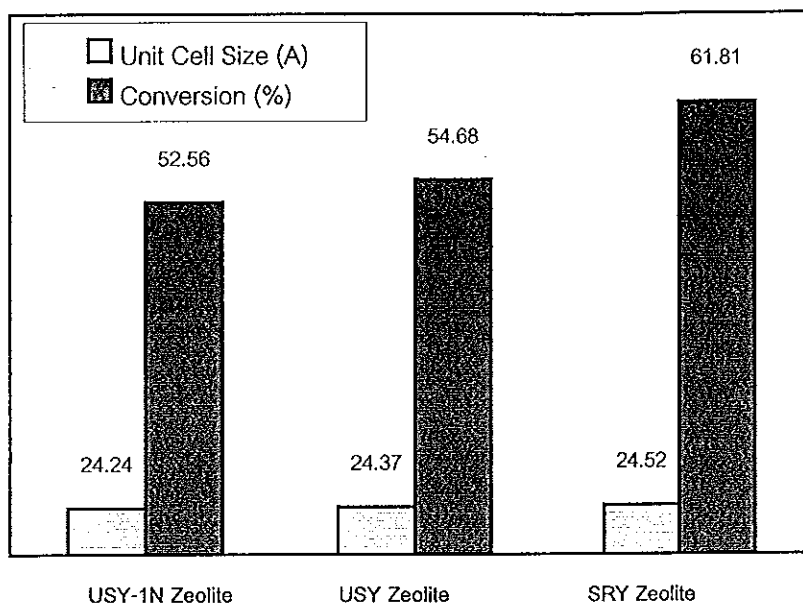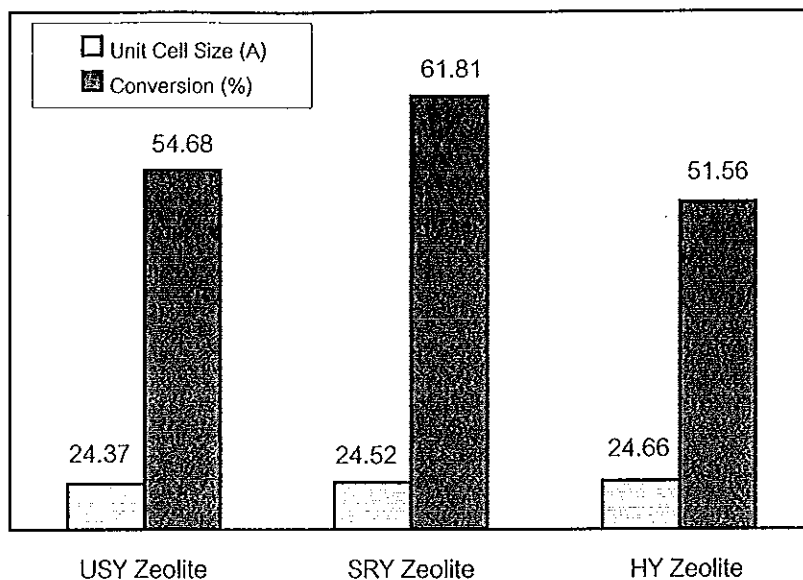
Figure 4-26 Dependence of catalyst activity on zeolite unit cell size for catalyst containing 30% zeolite

Figure 4-26 shows the relationships between zeolite unit cell size to catalytic activity of HY, SRY and USY zeolite catalyst. These indicate that HY zeolite catalyst (a_0 = 24.66 Å) had the lowest catalytic activity according to this catalyst containing only framework aluminum (F_{Al}) are much less active than samples that contain the same amount of F_{Al} together with extraframework (EF_{Al}) (Beyerlein, 1967). There seems to be an optimal relationship between the two. For example, the amount of EF_{Al} for optimal catalytic activity depends on the initial F_{Al} content. It has also been suggested that faujasites steamed to a level of about one EF_{Al} ion per sodalite cage would have the maximum activity (Lungford,1992). Hydrothermal framework dealumination results in the formation of nonframework aluminum species in the zeolite pore and filling of framework vacancies by silicon atoms. This is shown by the ^{29}Si- and ^{27}Al-MASNMR spectra of these materials (Scherzer,1989). The method involving calcination of ammonium 9or hydrogen) form of the zeolite at relatively high temperatures (usually over 500 °C) in the presence of steam. The results in the expulsion of tetrahedral aluminum from the framework into nonframework position, but does not remove the aluminum from the zeolite. The process consists essentially in a high temperature hydrolysis of Si-O-Al

bonds and leads to the formation of neutral and cationic aluminum species (Figure 4-14 and Table 4-8) (Scherzer,1984).The catalytic activity of SRY and USY zeolite catalysts are higher than HY zeolite catalyst, which corresponds to the description above.

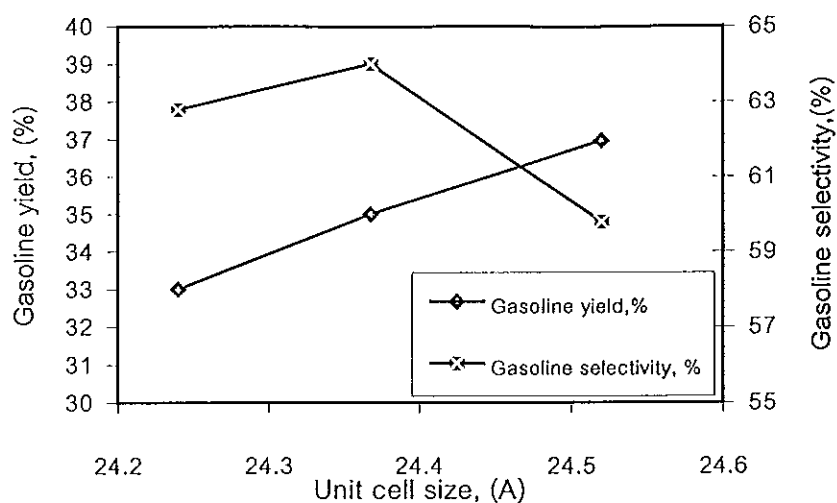The results of the gasoline yield and gasoline selectivity of HY and HSY zeolite catalysts are shown in Figure 4-27.
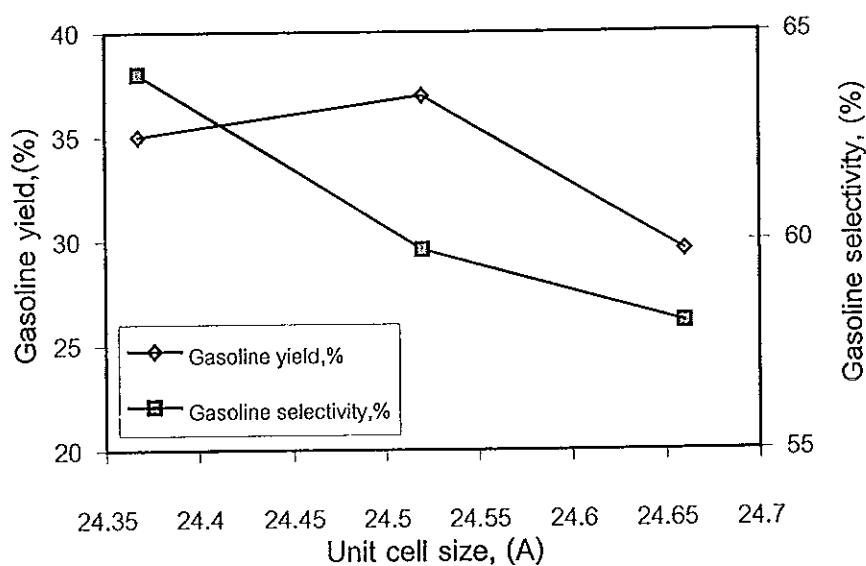
Figure 4-27 Correlation between unit cells size to gasoline yield and gasoline selectivity of HY, SRY and USY zeolite catalysts

Figure 4-27, it can be observed that, both gasoline yield and gasoline selectivity of HY zeolite catalyst had lowest values. Because of this catalyst has a high amount of F_{Al} in which leads to a lower level of acid strength than SRY and USY zeolite catalysts. Therefore, it could be conversion gas oil into other fractions beyond gasoline in high level. A part of USY zeolite catalyst (a_0 = 24.37 Å) had highest gasoline selectivity, since F_{Al} more isolated, so it increased in acid strength wherein well in the conversion of gas oil to gasoline.

The result of coke formation of HY and HSY zeolite catalysts is shown in the Figure 4-28.
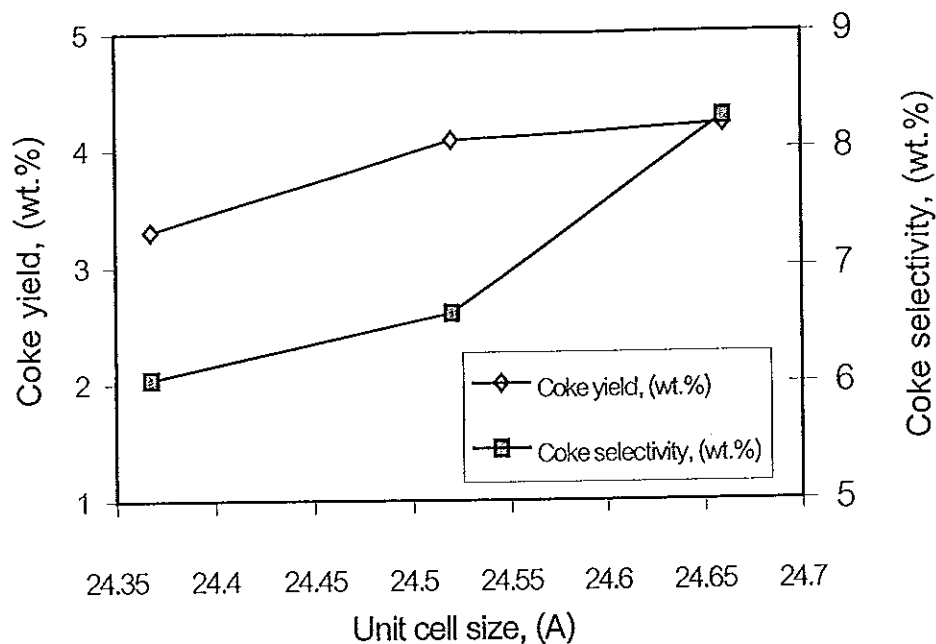
Figure 4-28 Correlation between unit cell size to coke yields and cokes selectivity of HY, SRY and USY zeolite catalysts.

Figure 4-28 shows that both coke yields and cokes selectivity decreased along decreasing zeolite unit cell size in which stated that bimolecular reactions or hydrogen transfer occurred in a low degree. USY zeolite catalyst had lowest coke yield and coke selectivity.

The results of catalytic activity of acid leached USY zeolite catalysts are presented in Figure 4-29.
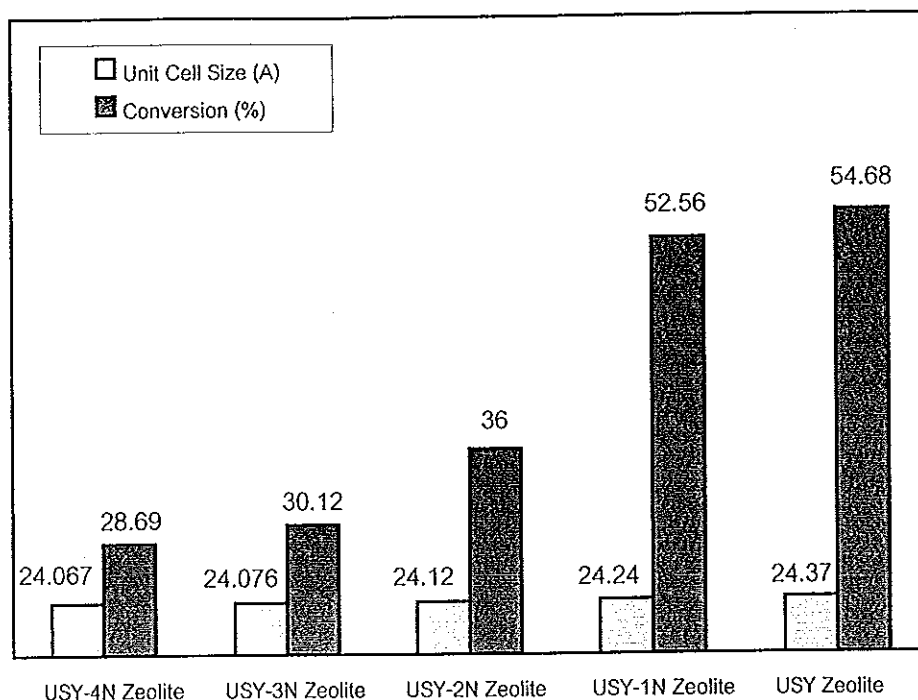
Figure 4-29 Dependence of catalyst activity on zeolite unit cell size for catalyst containing 30%zeolite

Figure 4-29 shows the relation between zeolite unit cell size to catalytic activity of USY and acid leached USY zeolite catalysts. It can be seen that catalytic activity decreased along decreasing zeolite unit cell size. The catalytic activity strongly affected from the HCl concentrations in which can be observed that they largely decreased when the zeolite unit cell size below 24.20 Å, namely USY zeolite contacted with high concentration of HCl caused loss in crystalline structure. The cracking reactions mainly occurred in crystalline phase. Lower in it caused to reduce in cracking reaction. These catalysts also have low framework aluminum, which caused a low in the catalytic site density wherein lead to a reduction in catalytic activity.

A part of gasoline yield and gasoline selectivity of acid leached USY zeolite catalysts are shown in Figure 4-30
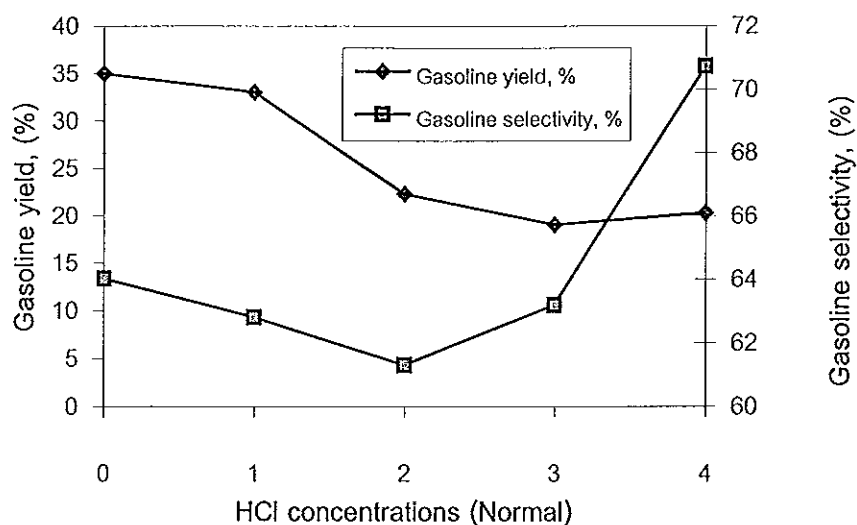
Figure 4-30 Correlation between HCl concentrations to gasoline yield and gasoline selectivity of acid leached USY zeolite catalysts.

This Figure shows that the gasoline yield decreased along increasing HCl concentrations, because of these catalysts have low zeolite unit cell size and crystallinity it leads to lower levels in gas oil conversion. A part of gasoline selectivity increased along increasing HCl concentrations.

The results of coke formation in acid leached USY zeolite catalysts are shown in Figure 4-31.
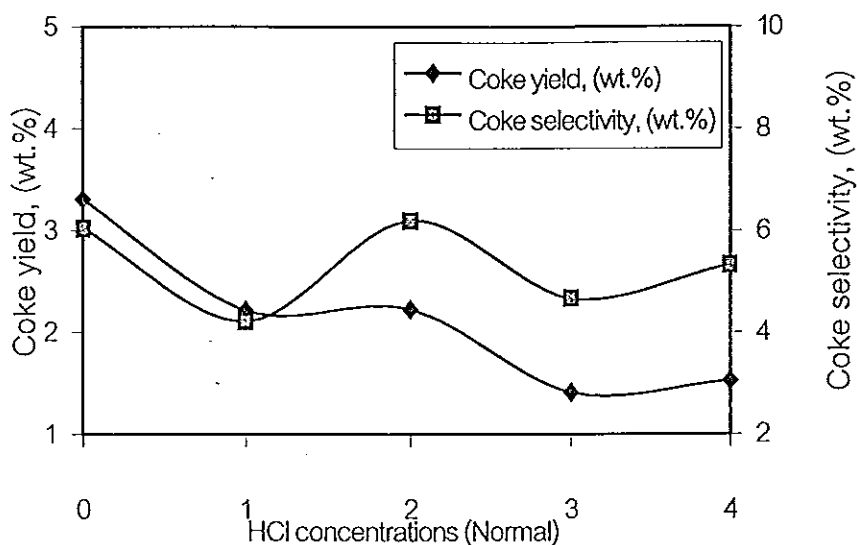
Figure 4-31 Correlation between HCl concentrations to coke yields and coke selectivity

of acid leached USY zeolite catalysts.

Figure 4-31 shown that acid leached USY zeolite made low coke yield and coke selectivity, because of they have low aluminum in the structure, high acid strength, so low hydrogen transfer occurred.

The TGA was used to determine the amounts of coke formation in the zeolite catalysts as shown in Figure 4-32.
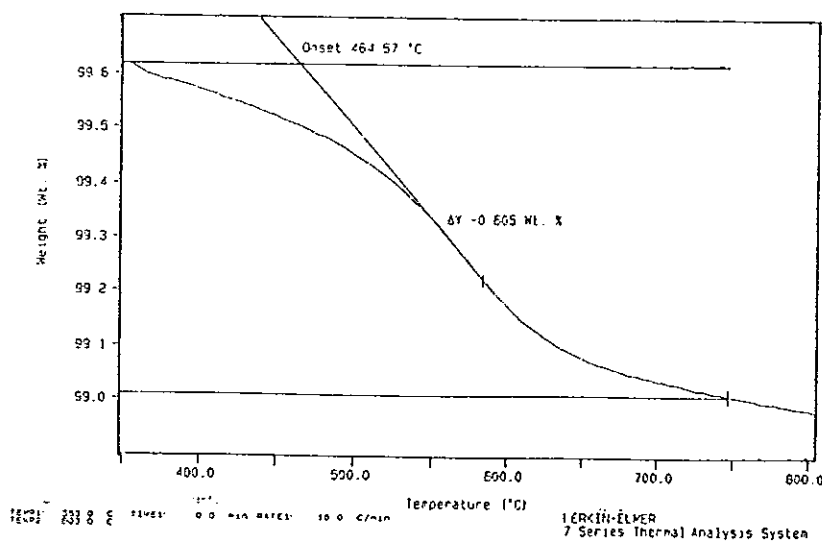
Figure 4-32 Representations of the TGA peak of USY zeolite for determined the amount

of coke formation.

CHAPTER 5

CONCLUSION

This research was studied the influence of various factors in each process that effected on the preparation of a USY zeolite including evaluation the performance of Y zeolite catalysts in the cracking of gas oil by microactivity test (MAT) unit.

Firstly, the ion exchange process for prepared NH_4Y zeolite in which it markedly effected by ion exchange temperature, time and raw material weight ratio. It was found that, desirable condition of these factors is $90^{\circ}C$, 1 hour and 1:1:20 respectively. NH_4Y zeolite has low amounts of sodium ion of 0.90 percent and retained high crystalline structure at 85.16 percent. A steam calcination process was used to prepare a USY zeolite wherein temperature, water (steam) to zeolite ratio and time play an important roles on the crystallinity stability and the reduction of zeolite unit cell size. The suitable condition for preparing a USY zeolite by this process is $600^{\circ}C$, 3 and 2 hours respectively. Prepared USY zeolite at this condition has low unit cell size and retained high crystallinity retention about 24.37 Å and 65.5 percent respectively, and having high thermal stability of 1015.2 $^{\circ}C$. The influence of mineral acid (HCl) concentrations on treating USY zeolites indicated strong affect to their properties. The treatment at higher concentrations more than 1 Normal, destroyed the crystalline and resulted in low catalytic activity. Although, they have low zeolite unit cell size due to the dealumination and have high thermal stability more than $1150^{\circ}C$. Hence, this process should be used mild HCl concentration not over than 1 Normal in preparing a desirable acid leached USY zeolite. Finally, a part of evaluation the performance of the Y zeolite catalysts in cracking of Thai gas oils by microactivity test unit was performed. It was found that a USY zeolite catalyst has good performance as high catalytic activity of 54.68 percent, high gasoline yield and gasoline selectivity of 35 and 64.01 percent respectively. The coke yield and coke selectivity are low of 3.302 and 6.038 weight percent.

129

BIBLIOGRAPHY

American society for testing and material 1991. Standard Test Method for Relative Zeolite Diffraction Intensities:D-3906-80,1146, Easton:The ASTM Committee of standard.

Alafandi,H. and Stamires,D.1980. "Exchanged Faujasite Zeolite Catalyst Containing Same and Process for Producing Same". U.S. Patent, No. 4,477,366,October 16.

Beyerlein, R.A.,et al.1988.J.Phys.Chem.92,1967.

Breck, D.W.1974.Zeolite Molecular Sieves: Structure, Chemistry and use: Structure of Zeolites. New York: John Wiley & Sons.

Breck, D.W.1974.Zeolite Molecular Sieves: Structure, Chemistry and use.New York: John Wiley & Sons.

Breck, D.W., et al.,1985. "Silicon Substituted Zeolite Compositions and Process for Preparing Same". U.S. Patent, No.4,503,023, March 5.

Calsavara,V., et al.,1996. "Reactivity of USY Extraframework Alumina in Alkaline Medium", Zeolites. 17, 340-345.

Chang, C.D.1981. "De-aluminization of Aluminosilicate". U.S. Patent, No.4,273,753, June 16.

Dai, 1996. "FCC Process Employing Low Unit Cell Size Y-Zeolites". U.S. Patent, No. 5,549,813, August 27.

Dyer, A.1988. An Introduction to Zeolite Molecular Sieves: What is a Zeolite?. Great Britain: John Wiley & Sons.

Dyer, A.1988. An Introduction to Zeolite Molecular Sieves: Natural Zeolites and Their Occurrence. Great Britain: John Wiley & Sons.

Dyer, A.1988. An Introduction to Zeolite Molecular Sieves: The Structure of Zeolites. Great Britain: John Wiley & Sons.

Eberly,P.E. et al.1971. "High Silica Crystalline Zeolites and Processes for Their Preparation". U.S. Patent, No.3,591,488, July 6.

Fejes,P.,et al.1985. "Dealumination of Zeolites by Volatile Reagents Mechanism of and Structural Changes Caused by Dealumination", In Zeolites,pp.263-270. Drzaj,B. et al., eds. Amsterdam: Elsevir Science.

Gates, B.C.1992. Catalytic Chemistry. New York: Wiley & Sons.

Garbed, W.E., et al.1976. "Alumina removal from Crystalline Alumino-Silicates with Cr (III) Solutions". U.S. Patent, No.3,937,791, February 10.

Gomes,A.C.L.,et al.,1997. "Influence of Combined Acid Treatment on Physico-chemical Characteristics of Ultrastable Zeolite Y and on Its Catalytic Properties in the Disproportionation of Ethylbenzene", Applied Catalysis A:General. 148,373-385.

Kerr,G.T.1968. J.Phys.Chem. 72,2594.

Kerr,G.T. et al.1969. "Method for Preparing Highly Siliceous Zeolite-Type Materials and Materials Resulting Therefrom". U.S. Patent, No.3,442,795, May 6.

Kerr,G.T. et al.1970. "Hydrothermally Stable Catalysts of High Activity and Methods for Their Preparation". U.S. Patent, No.3,493,519, February 3.

Kokotailo, G.T.1984. "Zeolite Crystallography", In Zeolite: Science and Technology,pp.87-89. Ribeiro, F.R.,et al., eds.,Natherlands: Martinus Nijhoff.

Kuehne, M.A., et al.,1998. "Effect of Framework Al Content on HY Acidity and Cracking Activity", Applied Catalysis A: General. 166, 293-299.

Kung, H.H., et al.1999. "Towards Understanding the Enhanced Cracking Activity of Steamed Y Zeolites", Catalysis Today. 52,91-98.

LaPierre,R.B., et al.,1989. "Method for Preparing Acid Stable Zeolites and High Silica Zeolites Prepared by It". U.S. Patent, No.4,840,930, June 20.

Lechert, H.1984. "The Physical Characterization of Zeolites" In Zeolite: Science and Technology,pp.151-189.Ribeiro, F.R.,et al., eds. Natherlands: Martinus Nijhoff.

Linsten, O.M., and Frestad, A.O.1991. "Process for the Preparation of a Modified Zeolite". U.S. Patent, No. 5,059,567, October 22.

Liu,D.S.; Bao,S.L. and Xu,Q.H.1997. "Structural Evolution of Dealuminated Y Zeolites during KOH Solution Treatment", Zeolites. 18,162-170.

Lok,B.M. and Ized,T.P.J.1982. Zeolites. 2,66.

Lunsford, J.H.,and Lonyi, F. 1992. J.Catal.136, 566.

Lynch, J.; Raatz, F. and Dufresne, P. 1987. "Characterization of the Textural Properties of Dealuminated HY Forms", Zeolites. 7,333.

Maher, P.K. et al.1966. "Zeolite Z-14US and Method of Preparation Thereof". U.S. Patent, No. 3,293,192, December 20.

Maher, P.K. et al.1968. "Ion Exchange of Crystalline Zeolites". U.S. Patent, No. 3,402,996, September 24.

McDaniel, C.V., and Maher, P.K. 1968. "New Ultra-Stable Form of Faujasite", Conf. Molec. Sieves, 1967,Soc.Chem.Ind.,London.

McDaniel, C.V.; Laurel and Maher, P.K. 1969. "Stabilized Zeolites". U.S. Patents, No. 3,449,070, June 10.

McDaniel, C.V.; Laurel and Maher, P.K. 1974. "Zeolite Stability and Ultrastable Zeolites", In Zeolite Chemistry and Catalysis,pp.314-320. Rabo, J.A. ACS, Washington D.C.

Niu, G. et al. 1999. "Thermal and Hydrothermal Stability of Siliceous Y zeolite and Its Application to High-temperature Catalytic Combustion", Applied Catalysis B: Environmental. 21, 63-70.

Paul, O.F., and Lunsford, J.H. 1989. "The Effect of Sodium Poisoning on Dealuminated Y-Type Zeolites", J.of Catalysis.118, 85-98.

Pawelec, B., and Fierro, J.L.G. 1997. "The Effect of Sulfidation on the Ni Distribution in Ni/ USY Zeolites", Zeolites. 18, 250-259.

Peters, A.W. 1993. "Instrumental Methods of FCC Catalyst Characterization" In Fluid Catalytic Cracking: Science and Technology,pp.185-189. Magee, J.S.,et al.,eds. New York: Elsevier Science.

Plank, C.J., et al., 1964. Ind.Eng.Chem.Prod.Res.Dev.,3, 165; Moscoul. "The Zeolite Scene", In Introduction to Zeolite Science and Practice, Studies in Surface Science and Catalysis, 58(1991). Van Bekkum, H., et al.,eds. Amsterdam: Elsevier Science.

Satterfield, C.N.1991. Heterogeneous Catalysis in Industrial Practice: Physical Characterization and Examination. New York: McGrew-Hill.

Scherzer,J. 1984. ACS Symposium Series, 248,157.

Scherzer,J. Anaheim, and Calif, 1984. "Acid Dealuminated Y Zeolite and Cracking Process Employing the Same". U.S. Patent, No. 4,477,336, October 16.

Scherzer,J., and Humphries, A.P. 1985. "Dealumination of Faujasite-Type Zeolites using Ion Exchange Resins". U.S. Patent, No. 4,512,961, April 23.

Scherzer,J. 1989. "Octane-Enhancing, Zeolitic FCC Catalysts: Scientific and Technical Aspects", In Catal.,Rev.-Sci.Eng.,pp. 215-354, 31(3) .

Scherzer,J. 1993. "Correlation between Catalyst Formulation and Catalytic Properties" In Fluid Catalytic Cracking: Science and Teachnology,Studies in Surface Science and Catalysis,pp.166-167. Magee, J.S. and Mitchell, M.M. 76. New York: Elsevier Science.

Skeels, et al. 1986. "Silicon Substituted Zeolite Compositions and Process for Preparing Same". U.S. Patent, No. 4,610,856, September 9.

Tao, L.X., et al., 1995. "The Study of Nickel-Deposited USY Zeolites by f.m.r", Zeolites, 15, 176-180.

Uytterhoeven, J.B.; Christner, L.B. and Hall, W.K. 1965. J. Phys.Chem. 69,2117.

Vaughan, D.E.W., et al., 2000. "Method for Preparing High Silica Faujasitic Zeolites". U.S. Patent, No. 6,054,113, April 25.

Ward, J.W. 1977. "Catalytic Cracking Process using Ammonia-Stable Zeolite Catalyst". U.S. Patent, No. 4,036,739, July 19.

Williams, B.A. et al. 1999. "The Role of of Acid Strength and Pore Diffusion in the Enhanced Cracking Activity of Steamed Y zeolites", Applied Catalysis A: General. 177, 161-175.

Woltermann, G.M.,et al.,1993. "Commercial Preparation and Characterization of FCC Catalysts" In Fluid Catalytic Cracking: Science and Technology, Studies in Surface Science and Catalysis,pp.110-120. Magee,J.S., and Mitchell,M.M.,76. New York: Elsevier Science.

Yang, S.J., and Chen, Y.W. 1995. "The Interaction of Vanadium and Nickel in USY Zeolite", Zeolites. 15, 77-82.

Yoshida, A.; Inoue, K. and Adachi, Y. 1991. "Hydrothermal Stability of US-Ex", Zeolites. 11,233.

Zukal, A., and Patzelova, V. 1986. "Secondary Porous Structure of Dealuminated Y Zeolites", Zeolites. 6, 133.

Appendix A

Characterization Procedure

1. X-Ray Diffraction (XRD) Spectroscopy

   A. Crystallinity analysis

   1) Grind the zeolite sample into very fine particles.

   2) Place about 1.5 g of the zeolite sample and reference in the drying oven at 110 °C for 1 hour.

   3) Cool the zeolite sample in the hydrator (desiccator) at room temperature and 35% relative humidity for at least 16 hours.

   4) Pack the zeolite sample into XRD sample holder then put it into the goniometer.

   5) Close the XRD window.

   6) Start up the power source and adjust the detector speed.

   7) Obtain a XRD pattern by scanning over the angle range from 14 to 35 deg 2θ at 1 deg / min with the chart drive at 10 mm / min.

   8) Turn on the goniometer and the recorder.

   9) The graph of 2θ eight peaks shown in Table A-1 was used to calculate the area under each peak.

   10) Calculate percent of crystallinity by using a formular:

   % crystallinity = $(S_X / S_R) \times 90$

   Where S_X = Sum of peak areas for the zeolite sample

   S_R = Sum of peak areas for the reference (90%) NaY zeolite

   B. Unit cell size analysis

   1) Carry out the following step 1) to 6), which same as the crystallinity analysis.

   2) Obtain a XRD pattern by scanning over the angle range from 20 to 35 deg 2θ at 1 deg / min with the chart drive at 10 mm / min.

3) Turn on the goniometer and the recorder.

4) Calculate zeolite unit cell size by using formular:

$$\text{Unit cell size}, a_0 \text{ (Å)} = 5.0509 / (\sin (2\theta / 2))$$

Where 2θ chose from 22.5 to 25 deg 2θ, normally 23 to 24 deg 2θ

Table A-1 Diffraction Angles 2θ hkl Miller Indices (ASTM D3906-80)

Peak	2θ	hkl
1	15.7 ± 0.2	331
2	18.7 ± 0.2	511,333
3	20.4 ± 0.3	440
4	23.7 ± 0.4	533
5	27.1 ± 0.5	642
6	30.8 ± 0.5	822,660
7	31.5 ± 0.5	555,751
8	34.2 ± 0.6	664

2. Atomic Absorption Spectrometry (AAS)

Acid digestion

1) Drying zeolites 120 $^\circ$ C for 1-2 h.

2) Weigh 0.2000 grams of zeolites and take to teflon beaker.

3) Fill HF 5 ml (by plastic pipette), $HClO_4$ 4 ml and HCl (1:1) 10 ml.

4) Heating solution for a few minutes and observe the $HClO_4$ vapors.

5) Take off the beaker solution from the heater and cool down to room temperature.

6) Fill H_2O_2 2 ml and leave to 3-5 minutes.

7) Heating solution again and observe the $HClO_4$ vapors.

8) Take off the beaker solution from the heater and cool down to room temperature.

9) Fill HCl for make volume to 25 ml in volumetric flask.

Then take the digested samples to analyses the amounts of sodium in which report in the form of Na_2O (wt%) by Atomic Absorption Spectrometry.

3. Scanning Electron Microscope (SEM) (Morphological analysis)

1) Dry zeolite samples at 110 °C for 1 hour.

2) Put one side of the two-face tape on the copper stub and press the other side on the dry zeolite sample.

3) Coat the zeolite sample as well as stub with gold and then put it into the chamber of SEM.

4) Switch on the system of SEM, chose the picture of crystal at optimum multiplication and take the SEM photograph.

4. Differential Thermal Analysis (DTA) (Thermal analysis)

1) Tare the DTA alumina sample lid and pan.

2) Weigh the zeolite sample in the pan and put the lid on the pan.

3) Crimp the zeolite sample.

4) Record weight of zeolite sample.

5) Place the zeolite sample in the left DTA cup and place an empty DTA alumina sample pan and lid in the right DTA cup.

6) Make a run using the following criteria:

- Run a baseline, under analyzer parameter

- Scan rate = 10.0 °C / min

- Temperature range = 300 – 1300 °C

- Use the hard key "GO TO LOAD"

- End condition; use the hard key " GO TO LOAD"

5. TGA

- Weigh the zeolite sample.

- Place the zeolite sample in the pan and observe the starting weight.

- Heating the furnace to the desired temperature, normally 350-800 $^\circ$C and scan rate = 10.0 $^\circ$C/ min.

- Purge O_2 for burn the carbon.

- Record the weight change.

X-Ray Diffraction Data

1. The data from XRD analyser of NaY zeolite standard

A. Crystallinity Analysis
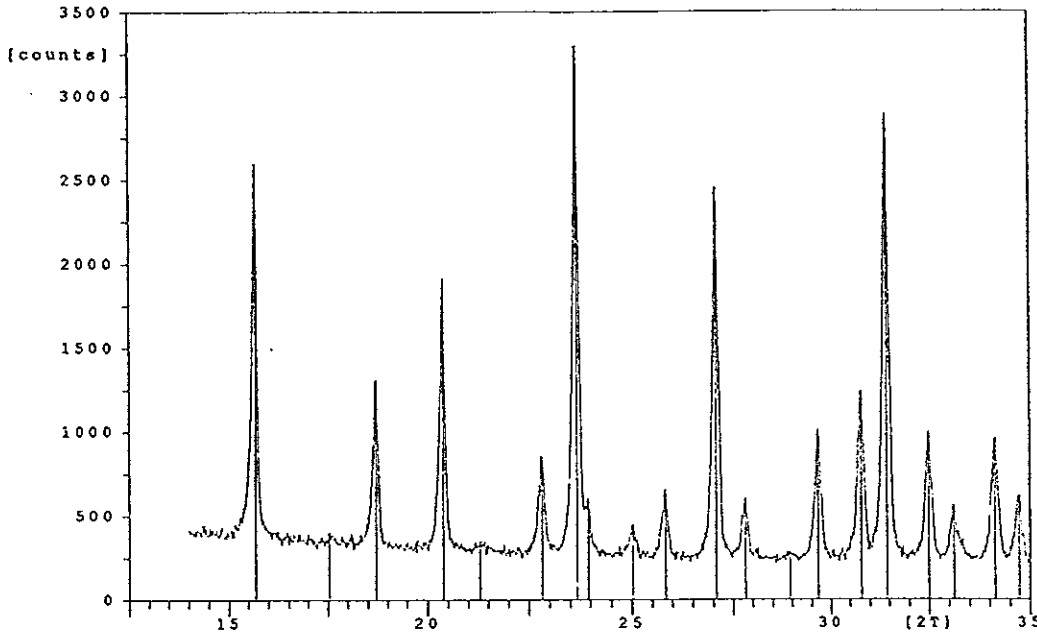
DIFFRACTION LINES :

Angle [°2q]	d-value a1 [Å]	d-value a2 [Å]	T.width [°2q]	Height [counts]	Backgr. [counts]	Rel.int. [%]	Signific
15.685	5.64527	5.65916	`0.100	2144	376	70.9	11.03
17.545	5.05077	5.06319	0.240	30	346	1.0	0.89
18.710	4.73882	4.75048	0.120	986	328	32.6	9.72
20.390	4.35201	4.36271	0.100	1608	306	53.2	8.55
21.305	4.16712	4.17737	0.240	40	296	1.3	1.20
22.825	3.89294	3.90251	0.140	529	282	17.5	7.91
23.675	3.75506	3.76430	0.120	3025	276	100.0	16.67
23.960	3.71103	3.72016	0.060	313	276	10.4	2.19
25.025	3.55546	3.56421	0.140	182	266	6.0	3.58
25.830	3.44645	3.45493	0.080	388	262	12.8	1.56
27.075	3.29073	3.29883	·0.180	2200	253	72.7	33.16
27.810	3.20541	3.21329	0.180	357	246	11.8	8.34

File: C:\APDW\DATA\R_NAYSTD.DI   9-oct-1999 14:44

Philips Analytical   PC-APD, Diffraction software

Angle [°2q]	d-value a1 [Å]	d-value a2 [Å]	T.width [°2q]	Height [counts]	Backgr. [counts]	Rel.int. [%]	Signific
28.940	3.08277	3.09035	0.200	34	243	1.1	0.75
29.670	3.00856	3.01596	0.120	767	243	25.4	6.70
30.785	2.90208	2.90922	0.140	986	243	32.6	10.39
31.445	2.84266	2.84965	0.160	2642	243	87.3	25.71
·32.495	2.75316	2.75994	0.160	756	243	25.0	11.29
33.120	2.70262	2.70927	0.120	296	243	9.8	2.18
34.125	2.62529	2.63175	·0.180	713	243	23.6	12.81
34.730	2.58093	2.58728	0.120	372	243	12.3	4.15

X-Ray Diffraction Data (Continuation)

B. Unit cell size Analysis

DIFFRACTION LINES:

Angle [°2q]	d-value a1 [Å]	d-value a2 [Å]	T.width [°2q]	Height [counts]	Backgr. [counts]	Rel.int. [%]	Signific
20.375	4.35518	4.36589	0.120	1246	202	57.6	11.42
21.295	4.16905	4.17931	0.160	76	202	3.5	0.83
22.805	3.89631	3.90589	0.100	384	202	17.8	3.19
23.660	3.75740	3.76665	0.100	2162	202	100.0	10.63
24.995	3.55966	3.56842	0.080	180	202	8.3	0.96
25.795	3.45105	3.45954	0.100	299	202	13.8	2.86
27.055	3.29312	3.30122	0.120	1490	202	68.9	11.41
27.785	3.20823	3.21613	0.120	396	202	18.3	5.00
28.460	3.13366	3.14137	0.200	497	202	23.0	12.77
29.640	3.01153	3.01894	0.120	630	202	29.1	6.08
30.760	2.90439	2.91153	0.100	841	202	38.9	5.40
31.410	2.84575	2.85275	0.140	2125	202	98.3	18.36

File: C:\APDW\DATA\UL_NAYST.DI

25-mar-1999 18:44

Philips Analytical

PC-APD, Diffraction software

Angle [°2q]	d-value a1 [Å]	d-value a2 [Å]	T.width [°2q]	Height [counts]	Backgr. [counts]	Rel.int. [%]	Signific
32.470	2.75523	2.76201	0.140	630	202	29.1	9.68
33.090	2.70501	2.71166	0.080	196	202	9.1	1.28
34.090	2.62791	2.63437	0.120	562	202	26.0	5.52
34.690	2.58382	2.59017	0.100	299	202	13.8	2.52

X-Ray Diffraction Data (Continuation)

2. The data from XRD analyser of USY zeolite

A. Crystallinity Analysis
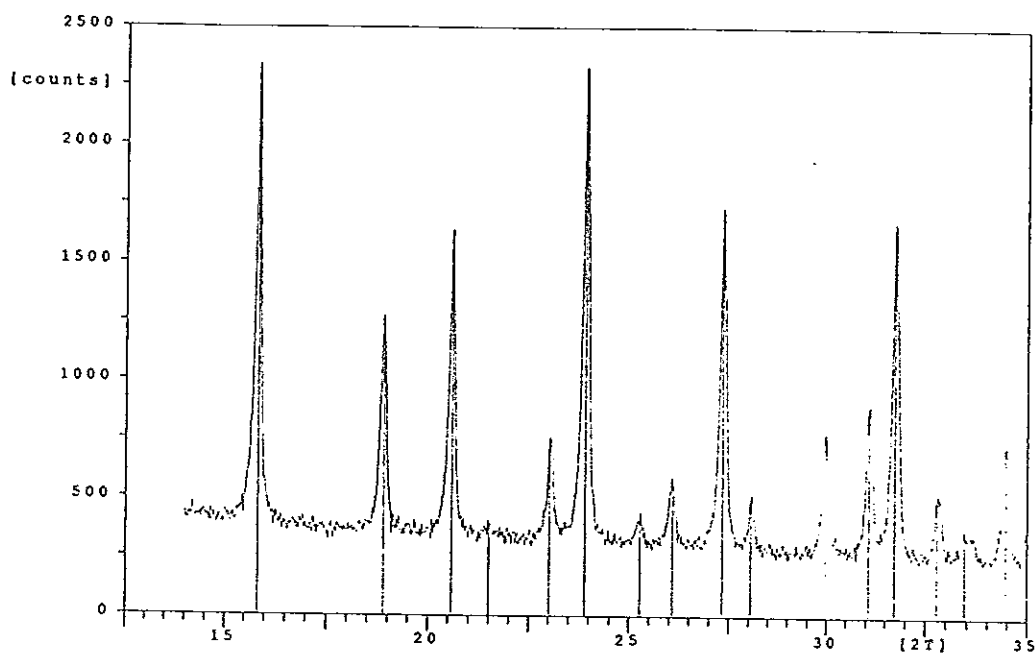
DIFFRACTION LINES :

Angle [°2q]	d-value a1 [Å]	d-value a2 [Å]	T.width [°2q]	Height [counts]	Backgr. [counts]	Rel.int. [%]	Signific
15.835	5.59213	5.60589	0.080	1936	400	96.0	4.85
18.895	4.69284	4.70438	0.120	918	357	45.5	7.78
20.585	4.31122	4.32182	0.100	1296	346	64.3	6.45
21.500	4.12976	4.13992	0.240	46	339	2.3	0.86
23.015	3.86123	3.87073	0.100	420	324	20.8	2.58
23.895	3.72098	3.73013	0.140	2016	317	100.0	17.26
25.265	3.52223	3.53089	0.160	104	306	5.2	1.21
26.080	3.41398	3.42238	0.140	276	299	13.7	4.01
27.325	3.26119	3.26921	0.160	1436	289	71.3	17.06
28.050	3.17852	3.18634	0.060	151	286	7.5	1.40
29.970	2.97912	2.98645	0.160	506	272	25.1	8.51
31.075	2.87566	2.88273	0.160	595	269	29.5	9.44

File: C:\APDW\DATA\R1450-1.DI   26-jan-1999 10:43
==
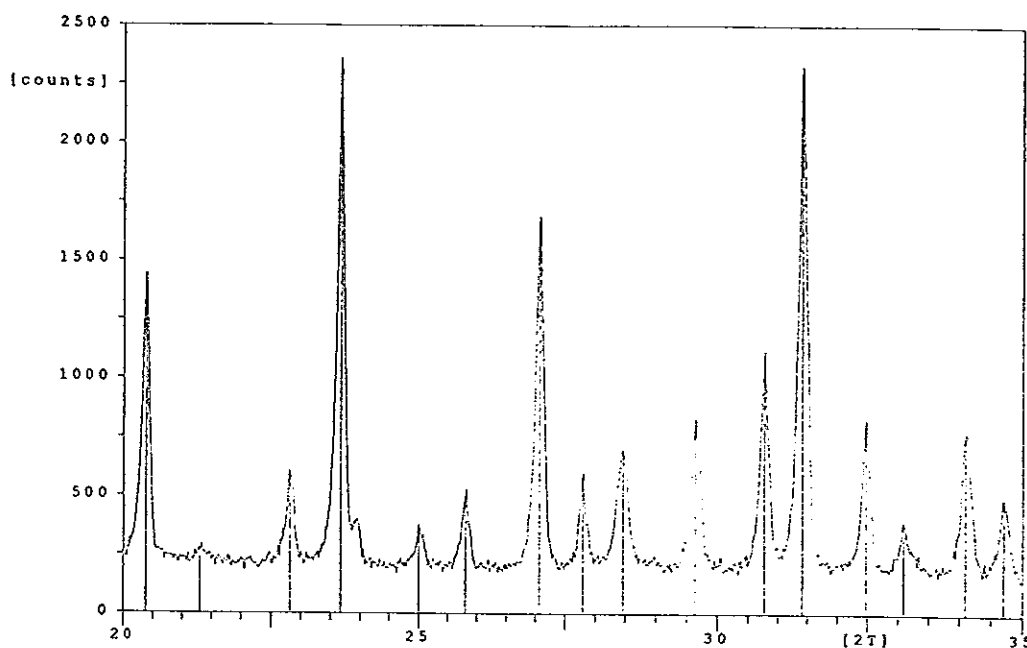Philips Analytical   PC-APD, Diffraction software

Angle [°2q]	d-value a1 [Å]	d-value a2 [Å]	T.width [°2q]	Height [counts]	Backgr. [counts]	Rel.int. [%]	Signific
31.725	2.81821	2.82514	0.140	1399	266	69.4	12.65
32.775	2.73028	2.73700	0.160	213	259	10.6	5.50
33.435	2.67788	2.68447	0.120	100	256	5.0	0.87
34.455	2.60090	2.60730	0.160	462	256	22.9	7.87

X-Ray Diffraction Data (Continuation)
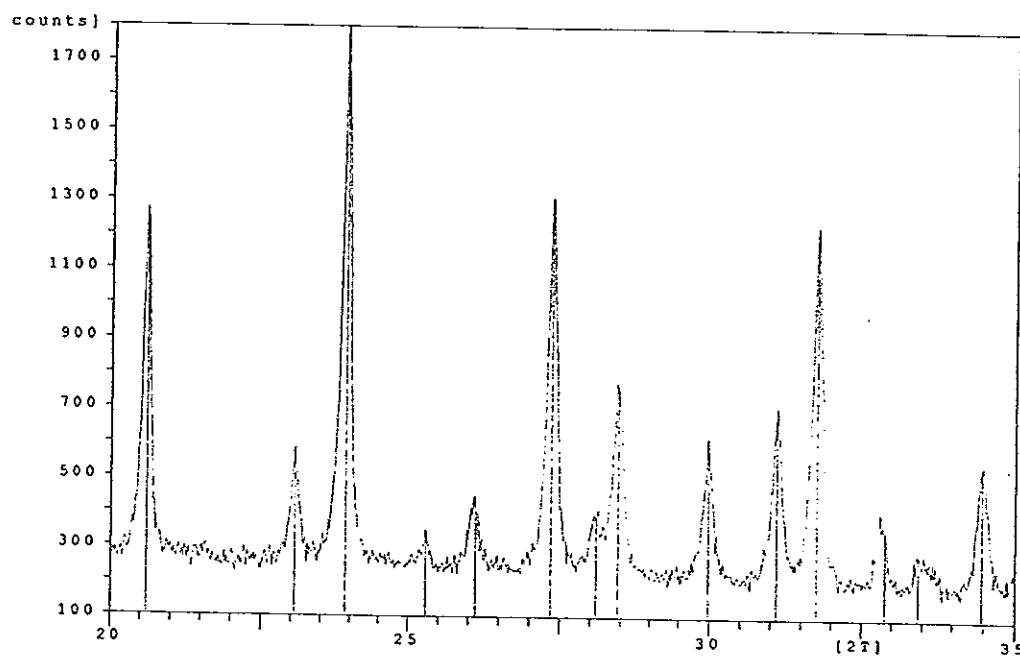
B. Unit cell size Analysis

D - F F R A C T I O N   L I N E S :

Angle [°2q]	d-value a1 [Å]	d-value a2 [Å]	T.width [°2q]	Height [counts]	Backgr. [counts]	Rel.int. [%]	Signific
20.605	4.30708	4.31767	0.120	1050	193	69.7	9.06
23.055	3.85462	3.86410	0.120	392	193	26.0	3.59
23.925	3.71638	3.72553	0.140	1505	193	100.0	15.14
25.290	3.51880	3.52746	0.060	156	193	10.4	0.85
26.110	3.41012	3.41851	0.080	202	193	13.4	2.04
27.345	3.25885	3.26687	0.140	1116	193	74.1	11.01
28.095	3.17353	3.18134	0.140	188	193	12.5	1.98
28.455	3.13420	3.14191	0.140	571	193	37.9	6.15
29.980	2.97815	2.98548	0.100	392	193	26.0	2.59
31.100	2.87340	2.88047	0.120	484	193	32.2	4.44
31.750	2.81605	2.82297	0.120	1037	193	68.9	6.70
32.890	2.72100	2.72769	0.160	161	193	10.7	4.06

File: C:\APDW\DATA\UL1249-4.DI

9-oct-1999 12:54

Philips Analytical

PC-APD, Diffraction software

Angle [°2q]	d-value a1 [Å]	d-value a2 [Å]	T.width [°2q]	Height [counts]	Backgr. [counts]	Rel.int. [%]	Signific
33.440	2.67749	2.68408	0.160	92	193	6.1	1.33
34.470	2.59980	2.60620	0.160	350	193	23.2	6.69

Appendix B

Steam Calcination (by CLY-1 Hydrothermal Aging Unit)

B.1 Installation and Preparation

B.1.1 Power Supply

It is better to have a three-phase electrical power. Each L-N voltage is 220V, AC, 20 A. If the lab isn't equipped with three-phase power supply, so the three lines should be shorted in the power switch. The water pump and the recorder are lined to AC 220 V.

B.1.2 Air Supply

There has to be an air supply, its pressure is about 0.4 MPa. It can be from a pipeline or a small air compressor. On the aging unit, the air pressure is adjusted to 0.3 MPa. Regulator pressure is adjusted to 0.1 MPa and the airflow is adjusted to 30 ml/min.

B.1.3 Water

The water used for aging should be deionized water. Before starting aging, the water is to be filled in the water tank to the full scale.

B.1.4 Temperature Adjustment

The furnace must have a long enough isothermal length ($\sim$ 10 cm). If the isothermal length is not long enough, you can adjust the furnace temperature as follows:

Fulfill the aging tube with porcelain rings or sand. Set the three temperatures controller of the furnace at nearly a desired temperature (normally 600 $^{\circ}$C), start heating and air stripping. When the temperature are stable, start water pump at a rate of 45 ml/hour. After 30 min, gradually adjust the three temperature controllers for the furnace until the isothermal length reaching its maximum at a desired temperature.

B.2 Aging Procedure

B.2.1 Load Catalyst

The catalyst is to be loaded in the middle of the isothermal section of the micro reactor as follows:

1. Fill porcelain rings to the bottom of the micro reactor up to the isothermal section (about 22 cm. from the bottom) then, added some of broken rings, the thickness of 1 cm.

2. Put a quartz cotton layer of about 0.5 cm. before added the catalyst to micro reactor.

3. Better to fill 15 grams (dry basis) catalyst inside the tube.

4. Put a quartz cotton layer of about 0.5 cm. on the top of the catalyst bed.

5. Fill some broken porcelain chips in and follows by porcelain rings.

6. Take the micro reactor into the furnace and line up.

B.2.2 Pre-Air Stripping and Start Heating

1. Open the air-in valve on the unit panel, adjust the air pressures to 0.3 MPa, regulated pressure be 0.1 MPa, and adjust the airflow to 30 ml/min.

2. Turn the 'power' switch on.

3. Set the heating time for 2 hours.

4. Set the aging time for a desired time (normally 2 hours).

5. Set the alarm time at aging time minus 1 min.

6. Push the button ' heat' to start heating.

7. Turn on pump power and set pump rate at 0.81 ml/min.

B.2.3 Start Hydrothermal Aging

When the aging temperature reached a desired temperature and stable, push the ' start ' button to start aging (use water-pump to start pump water, water valve and the air valve close, and aging time start going on automatically)

B.2.4 Post Air Stripping

When the aging time has passed, the water-pump stops, water valve closed and the air valve opened automatically by LOGO, the post air stripping begins.

B.2.5 Finish

After about 15 minutes post air stripping, you can turn off the power and close the air supplies, took out the micro reactor and cools it down in the ambient air. Finally, took out the catalyst and separate it from porcelain rings.

Figure B-1 Hydrothermal aging unit

Appendix C

Hydrothermal Deactivation (by CLY-1 Hydrothermal Aging Unit)

C.1 Installation and Preparation

C.1.1 Power Supply

It is better to have a three-phase electrical power. Each L-N voltage is 220V, AC, 20 A. If the lab isn't equipped with three-phase power supply, so the three lines should be shorted in the power switch. The water pump and the recorder are lined to AC 220 V.

C.1.2 Air Supply

There has to be an air supply, its pressure is about 0.4 MPa. It can be from a pipeline or a small air compressor. On the aging unit, the air pressure is adjusted to 0.3 MPa. Regulator pressure is adjusted to 0.1 MPa and the airflow is adjusted to 30 ml/min.

C.1.3 Water

The water used for aging should be deionized water. Before starting aging, the water is to be filled in the water tank to the full scale.

C.1.4 Temperature Adjustment

The furnace must have a long enough isothermal length ($\sim$ 10 cm). If the isothermal length is not long enough, you can adjust the furnace temperature as follows:

Fulfill the aging tube with porcelain rings or sand. Set the three temperatures controller of the furnace at nearly 800 $^\circ$C, start heating and air stripping. When the temperature are stable, start water pump at a rate of 45 ml/hour. After 40 min, gradually adjust the three temperature controllers for the furnace until the isothermal length reaching its maximum at 800 $^\circ$C.

C.2 Aging Procedure

C.2.1 Load Catalyst

The catalyst is to be loaded in the middle of the isothermal section of the aging tube as follows:

1. Fill porcelain rings to the bottom of the micro reactor up to the isothermal section (about 23 cm. from the bottom) then, added some of broken rings, the thickness of 1 cm.

3. Put a quartz cotton layer of about 0.5 cm. before added the catalyst to micro reactor.

4. Better to fill 15 grams catalyst inside the tube.

5. Put a quartz cotton layer of about 0.5 cm. on the top of the catalyst bed.

6. Fill some broken porcelain chips in and follows by porcelain rings.

7. Take the micro reactor into the furnace and line up.

C.2.2 Pre-Air Stripping and Start Heating

1. Open the air-in valve on the unit panel, adjust the air pressures to 0.3 MPa, regulated pressure be 0.1 MPa, and adjust the airflow to 30 ml/min.

2. Turn the 'power' switch on.

3. Set the heating time for 2 hours.

4. Set the aging time for 4 hours.

5. Set the alarm time at aging time minus 1 min.

6. Push the button ' heat' to start heating.

7. Turn on pump power and set pump rate at 0.75 ml/min.

C.2.3 Start Hydrothermal Aging

When the aging temperature reached 800 $^{\circ}$C and stable, push the' start ' button to start aging (use water-pump to start pump water, water valve and the air valve close, and aging time start going on automatically)

C.2.4 Post Air Stripping

When the aging time has passed, the water-pump stops, water valve closed and the air valve opened automatically by LOGO, the post air stripping begins.

C.2.5 Finish

After about 15 minutes post air stripping, you can turn off the power and close the air supplies, took out the micro reactor and cools it down in the ambient air. Finally, took out the catalyst and separate it from porcelain rings.
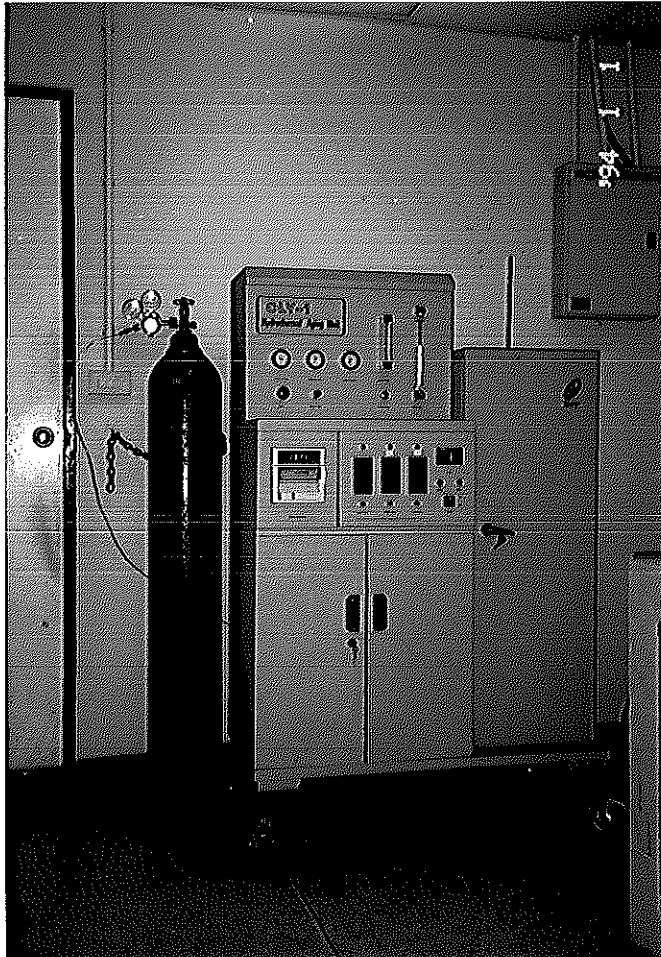
Appendix D

Microactivity Test (by WFS-1D Microactivity Test Unit)

There are two parts in the test system: test unit (MAT unit) and gas chromatography set.

D.1 MAT Unit

In this work, use MAT unit model WFS-1D in which produced by Research Institute of Petroleum Processing, SINOPEC. WFS-1D is designed according to the standard method developed by RIPP and mainly used to test the activity index of cracking catalyst. The standard test method of cracking catalyst microactivity index in China is RIPP 92-90, the conditions are:

Standard feed gas oil (applied by use Thai gas oil):

Reaction temperature:	$460 \pm 1\ ^{\circ}C$
Feed oil weight:	1.56 ± 0.01 g
Feeding time:	70 sec.
Post stripping time:	10 min.
Stripping nitrogen flow-rate:	20-30 ml/min.

D.1.1 Reaction and Collection System

The system includes the reactor, the heating furnace, the condenser well and the collecting bottle. The reactor is the heart of the reaction system where the reaction takes place. The screw bar is at the reactor's upper section, around which the feed oil is vaporized. Under the bar there is an isothermal section, the length is about 7 cm. where the catalyst is to be loaded. At the bottom, liquid product is collected in receiver bottle by pass through a long needle that is joined with the receiver bottle by rubber tube. The bottle is immersed in the condense well filled with ice and water. A medical syringe needle sticks into the rubber tube, through it the cracking gas exits.

D.1.2 Feed Oil Injection System

This includes the injection pump, the six-ways valve and the feed oil bottle. It is used to smoothly inject $1.56 \pm 0.01g$ feed oil into the reactor within 70 sec.

D.1.3 Stripping System

It includes the pressure regulator, the gas-flow regulator, pressure gauge and rotary flow meter. The functions of this system are:

1. Pre-stripping: The nitrogen stripping before oil injection can ensure the catalyst is in the nitrogen atmosphere and water-free.

2. Post-stripping: After oil injection, the nitrogen stripping can get residual oil in the tuber into reactor and strip out all reaction production from reactor.

D.1.4 Measurement and Control System

The system includes the temperature controllers, the solenoid valves and the programmable logic controller (PLC). The two temperature controllers are the same; one indicates the catalyst bed temperature, the other one a control temperature of the furnace. They are intelligent controllers produced by Shimandan (Shimadzu), Japan, with PID self-tuning, automatic cold conjunction temperature compensation, thermocouple linearisation and deviant correction. Due to unique of the furnace manufacture technology, the reactor has more than 7-cm. long isothermal catalyst bed with only one heater.

The PLC controls the injection pump and the six-port valve. The operating procedures are as follows (refer to Figure D-1):

1. Preparation step: If the nitrogen source is supplied, when the power switch turns on, the PLC will draw the six-port valve to the position shown by the dotted lines. That is the pre-stripping.

2. Oil injection step: After the reactor bed temperature has stabled, push the ' start ' button, then the six-ways valve will turn to the position shown by the solid lines, the syringe plug goes forward, the feed oil is injected into the reactor through the six-ways valve.

3. Oil suction step: After 70 seconds of oil injection, the six-ways valve turns back to the dotted lines position. Then post-stripping begins and syringe

plug goes backward, the feed oil is sucked into the syringe from the feed oil bottle.

4. Squeezing step: When the oil-suction has lasted for 70 seconds, the syringe plug goes forward again for 20 seconds to squeezing out gas bubbles.

5. Post-stripping: When post-stripping lasts about 10 min. the speaker song music, the system goes back to the preparation step again. In order to keep the syringe plug always stay at a certain position, only in this period the reset button is enable.

D.2 PC Work Station (Option)

D.2.1 Functions

PC workstation is designed to work with WFS-1D to change and save test parameters, remote control, print report, display the history or real time trace of process variables. It is linked to the test unit through a serial communication card, but the test unit can work independently.

D.2.2 Operations

D2.2.1 Start up

1. Enter Windows 3.11

2. Double click Group WFS-1D

3. Double click the icon WFS-1D of the group

4. Input the operator's name and click 'OK' then go into the working window

D.2.2.2 Operations in the main working window:

1. To change the temperature controller's parameter: There are two temperature controllers. The upper one is used to indicate the reaction temperature. The lower one is used to control the furnace's temperature. The set value can be changed on its window, click ' SV' to send data to the controller. The PID parameters can be changed by click the 'PID', clock the PID diagram blank place can close the PID window.

2. To change the operation time parameters: There is operation time table on the right of the main working window. The feeding time (T1), sucking time (T2), preparing time (T3) and purging time (T4) all can be changed. The ranges are:

$$0 \leq T1 \leq 150 \text{ s}$$

$$T1 \leq T2 \leq T1 + 30 \text{ s}$$

$$T3 = T2 - T1 \text{ (s)}$$

$$T4 \leq 991 - T1 \text{ (s)}$$

After they are set or changed, click 'OK' then click 'SEND', these parameters can be sending to PLC of the test unit.

D.2.3 Comments

There are several command blocks at the main working window button:

1. 'RUN'   : begin to run.

2. 'RESET'   : to reset the system.

3. ' EXIT'   : to quit from the main working window.

4. 'SAVE'   : to save the parameters onto the system's hard disk.

5. 'LOAD'   : to load the parameters from the system's hard disk.

6. 'QUIT'   : to quit from the WINDOWS.

7. 'CALCULATOR'   : to use system's calculator.

8. ' REPORT'   : to print test report. Each report can contain two test reports. According to the prompt input parameters, and then click 'OK', the computer can calculate out the needed parameters, and then click 'PRINT' and the report can be print out. Click 'EXIT' to quit from the window.

9. 'TRACE'   : to display the temperature's trace. In this window there are several command blocks.

- 'HISTORY'   : to display history traces, the test number can be selected by click 'SELECT' and 'TIME'.

- 'SET SCALE'   : to set the temperature's scale by input the minimum / maximum temperature.

- 'EXIT'   : to quit from this window.

D.3.3 Gas Chromatography set and Integrator

The G.C. is Shimadzu G.C.-14B, the integrator is Shanghai HP 3295. For the use of detecting cracking catalyst microactivity index, the conditions in analysis are:

Carrier gas   : nitrogen (OFN), flow rate: 35-40 ml/min

Combustion gas   : hydrogen, flow rate: 40 ml /min

Auxiliary gas   : air, flow rate: 40 ml /min

Temperature of vaporization chamber (injector)   : 280 $^\circ$C

Temperature of detector chamber   : 280 $^\circ$C

Temperature of column chamber   : rises from 35 $^\circ$C to 80 $^\circ$C by rate of 15°C/min., then rises from 80 $^\circ$C to 235 $^\circ$C by rate of 8 $^\circ$C/min, hold at 235 $^\circ$C for 10 min.

Sample injection volume   : 0.4 μl

D.4 Preparation before Operation

D.4.1 Reactor's Temperature

In order to have the reactor's catalyst bed temperature correctly indicated, its thermocouple should be calibrated regularly (half or one year) with standard or recently calibrated thermocouple and standard differential potential meter. The deviation value should be input into the temperature controller.

The catalyst bed temperature of the reactor should be controlled at 460$\pm$1°C. It can be obtain by adjusting the furnace temperature controller's set value.

D.4.2 Tested Catalyst

In order to have the test catalyst correctly weighted, before load it into reactor it should be dried in oven for an hour at 110-120 $^\circ$C.

D.4.3 Feed Oil

Heavy oil isn't suitable for this apparatus.

D.4.4 Feed Oil Weight Calibration

In order to have a correct injected oil weight, it is suggested to calibrate the weight every day before do experiment. The method is to insert the joint to a small bottle,
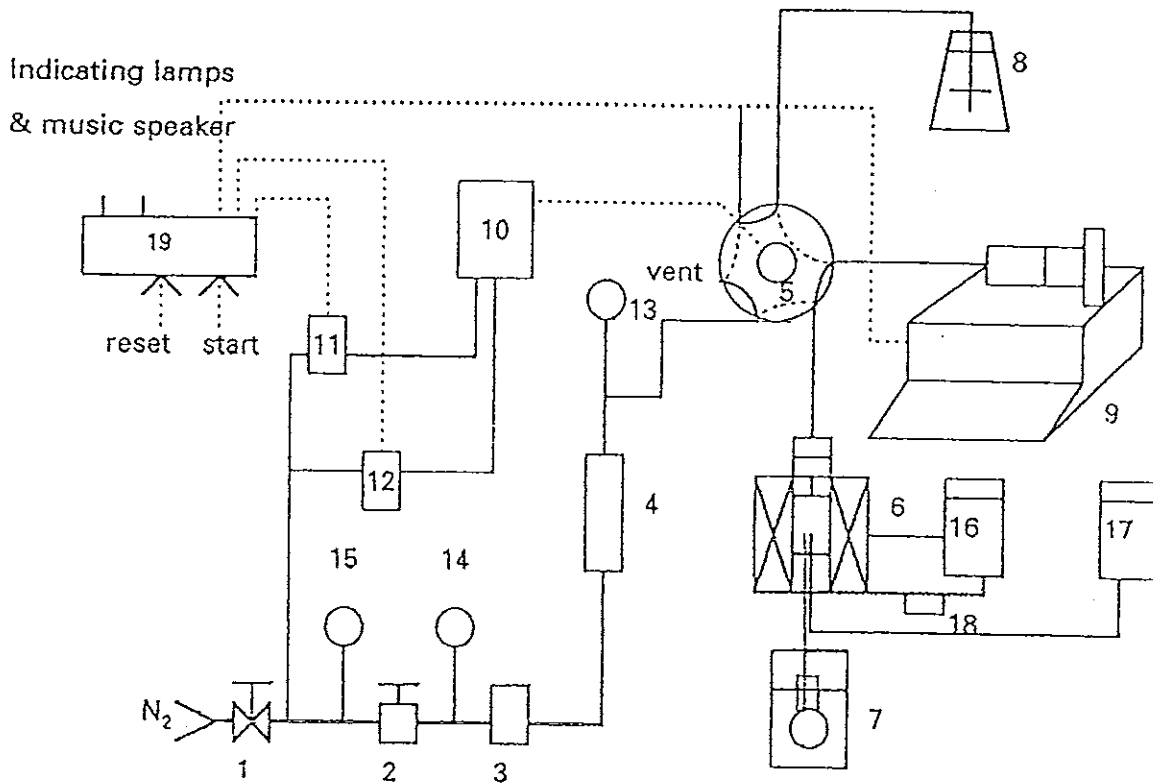
1: valve   2: pressure regulator   3: flow regulator   4: rotary flow meter

5: six-port valve   6: reactor & heater   7: ice bath & collect bottle   8: feed oil bottle

9: injection pump   10: six-port valve driver   11: solenoid valve   12: solenoid valve

13: reaction pressure gauge 0-0.16 MPa 14: regulated pressure gauge 0-0.4 MPa

15: inlet pressure gauge 0-0.16 MPa   16: temperature controller (furnace)

17: temperature monitor (reactor)   18: solid relay

19: programmable logic controller

Figure D-1 The process diagram of MAT unit

then push the 'start' botton. When the squeezing step has finished, push the 'reset' button and weigh the bottle. If the oil weight is not 1.56 $\pm$ 0.01 g, adjust the pump's speed and calibrate again.

Example: Calibration of the feed pump

Feed oil: Thai gas oil

Flow rate ml / min	1.54	1.54	1.54
Measured Value (g)	1.558	1.562	1.56

D.5 Operation Steps

1. Adjust the gas tank pressure to 0.30-0.35 MPa and then, turn on the power switch, WFS-1D goes stripping status automatically.

2. Put some quartz fiber into the reactor's bottom, weigh 5 g. of catalyst and load it into the reactor. Put the reactor into the furnace and link it to the six-port valve.

3. Link the collect bottle to the reactor with rubber tube and then put the bottle into the ice water well.

4. When the reactor's temperature has stabled for 5 min., push the 'start' button then, the unit work in automatic for injection, suction, squeezing and post-stripping. After 10 minutes stripping, the speaker sings music indicated that the test has finished.

5. Take off the collect bottle and wipe out the water on the bottle, weigh the bottle and note down the collected oil weight, put it in a refrigerator for G.C. analysis.

6. Take out the reactor from the furnace and take out the catalyst.

D.6 Analyses of Reacted Product and Data Disposal.

The liquid product is analyzed with G.C.

D.6.1 Calculation the microactivity index:

Conversion (MAT) = 100 - $\left[\dfrac{(100 \text{- } A) \times B}{C} \right]$

Where: A = Gasoline yield, analyzed by GC, % wt.

B = Liquid product from MAT, g.

C = Feed oil, g.

D.6.2 Calculation the percent of gasoline:

Gasoline percent $= \dfrac{A \times B}{C}$

D.6.3 Calculation the gasoline selectivity:

Gasoline selectivity $= \dfrac{\text{gasoline (\%)}}{\text{Conversion (\%)}} \times 100$
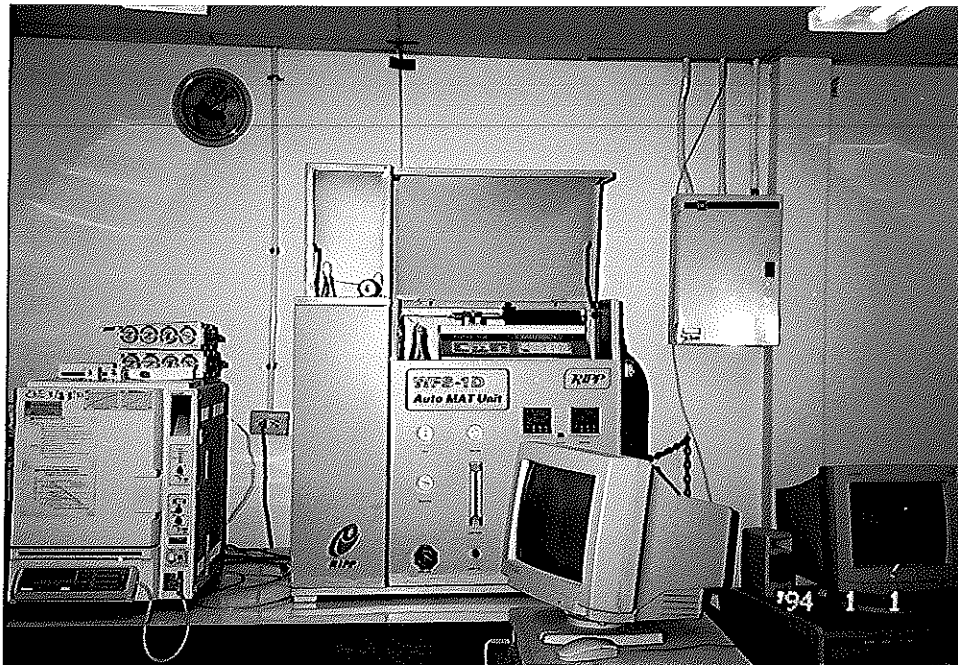

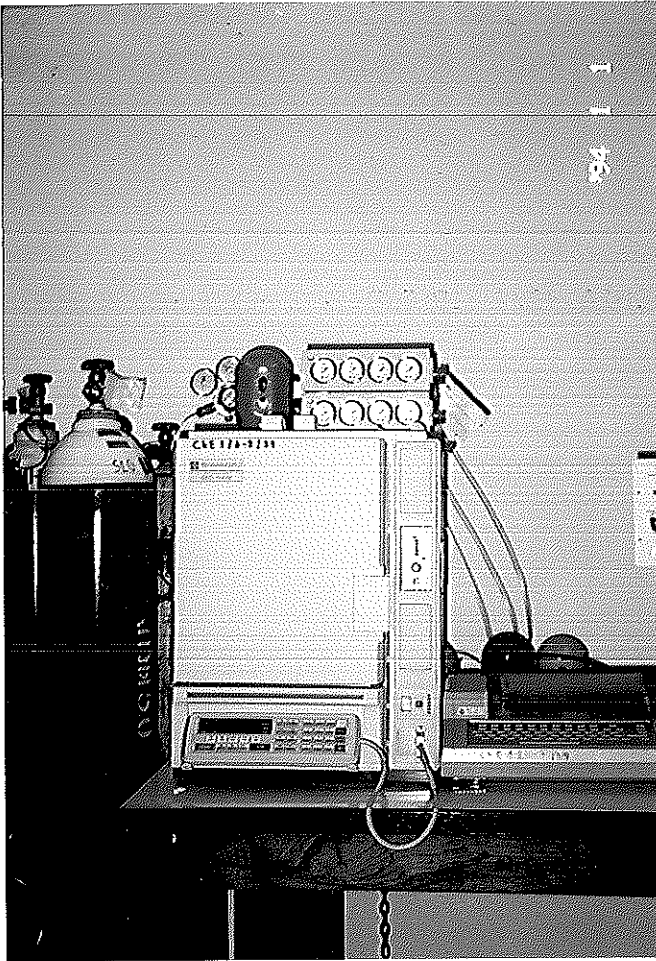Figure D-2 Microactivity test unit

Figure D-3 Gas chromatograph unit

Example:

1. Gasoline yield (gasoline area, % by weight): Analyze liquid product from MAT unit with Gas Chromatograph
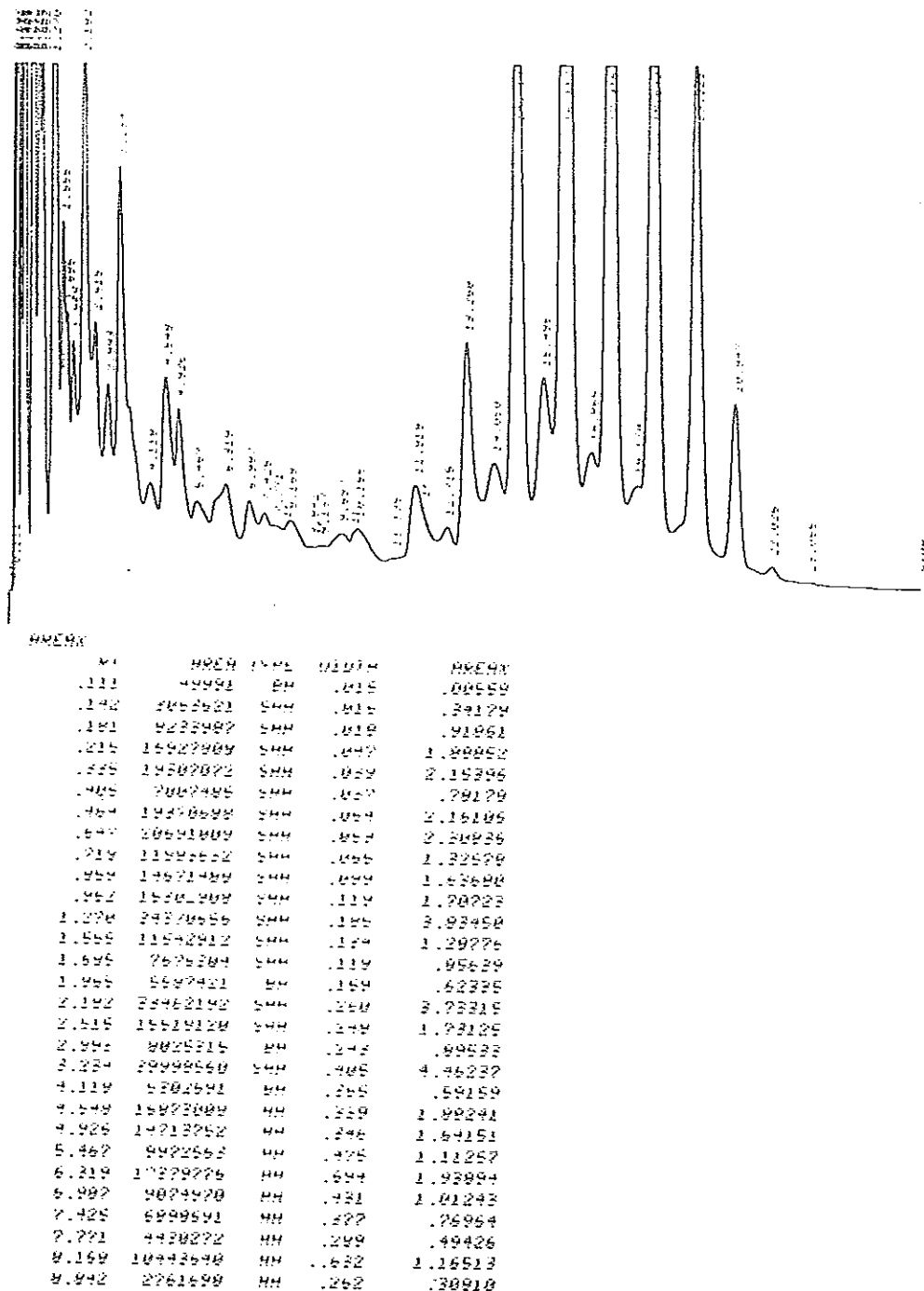

Figure D-4 Chromatogram of USY zeolite catalyst

Calculate the gasoline area and then calculate the conversion (%), gasoline yield (%) and gasoline selectivity (%) by above formulas.

Appendix E

Experimental Data

Table E-1 Data of the influence of temperatures to Na_2O exchange in each exchange
order

Temperature (^oC)	30	60	90
Exchange Order	Na_2O Exchange	Degree (%)	
NaY zeolite	0	0	0
1	51.17	56.42	84.83
2	60.33	64.33	87.5
3	75.58	86.42	92.5

Table E-2 Data of the dependence of crystallinity retention to ion exchange
temperatures in each exchange order

Temperature (^oC)	30	60	90
Exchange Order	Crystallinity	Retention (%)	
NaY zeolite	89.32	89.32	89.32
1	91.45	95.78	90.88
2	77.36	80.36	85.99
3	67.47	70.06	85.16

Table E-3 Data of the influence of times to Na$_2$O exchange in each exchange order

Time (hour)	1	2	3
Exchange Order	Na$_2$O Exchange	Degree (%)	
NaY zeolite	0	0	0
1	84.83	79.08	81.33
2	87.5	85.75	86.58
3	92.5	93.75	94.75

Table E-4 Data of the dependence of crystallinity retention to ion exchange times in
each exchange order

Time (hour)	1	2	3
Exchange Order	Crystallinity	Retention (%)	
NaY zeolite	89.32	89.32	89.32
1	90.88	92.59	94.88
2	85.99	89.97	89.52
3	85.16	81.59	80.27

Table E-5 Data of the influence of the weight ratios to the Na$_2$O exchange degree in
each exchange order

Weight ratio	1:0.5:20	1:1:20	1:1.5:20
Exchange Order	Na$_2$O Exchange	Degree (%)	
NaY zeolite	0	0	0
1	81.83	84.83	86.33
2	86.25	87.5	89.83
3	91.83	92.5	92.62

Table E-6 Data of the dependence of crystallinity retention to raw material weight ratio in each exchange order

Weight ratio	1:0.5:20	1:1:20	1:1.5:20
Exchange Order	Crystallinity	Retention (%)	
NaY zeolite	89.32	89.32	89.32
1	88.32	90.88	90.37
2	87.59	85.99	89.06
3	71.12	85.16	86

Table E-7 Data of the exchange order to Na_2O exchange degree

Exchange Order	Na_2O Exchange Degree (%)
NaY zeolite	0
1	87.5
2	91.08
3	97.42

Table E-8 Data of the correlation of the treated temperatures to crystallinity retention and unit cell size of steamed Y zeolite samples

The treated temperatures ($^\circ$C)	Crystallinity Retention (%)	Unit Cell Size (Å)
400	67.37	24.50
500	66.86	24.41
600	65.50	24.37
700	61.15	24.36

Table E-9 Data of the correlation of water to zeolite ratios to crystallinity retention and

unit cell size of steamed Y zeolite samples

The water to zeolite ratios	Crystallinity Retention (%)	Unit Cell Size (Å)
2.25	66.26	24.39
3	65.50	24.37
4.5	61.55	24.38
9	59.37	24.38

Table E-10 Data of the correlations of the treated times to crystallinity retention and unit

cell size of steamed Y zeolite samples

The treated times	Crystallinity Retention (%)	Unit Cell Size (Å)
1	65.55	24.39
2	65.50	24.37
3	64.49	24.364
4	63.35	24.36

Table E-11 Data of the correlation between HCl concentrations to crystallinity retention

and unit cell size of acid leached USY zeolite samples

HCl Concentrations (Normal)	Crystallinity Retention (%)	Unit Cell Size (Å)
0	62.67	24.38
1	58.90	24.24
2	31.60	24.12
3	23.15	24.076
4	19.78	24.067

Table E-12 Data of the results from Microactivity Testing (MAT)

Catalysts	Conversion (%)	Gasoline Yield (%)	Gasoline Selectivity(%)	Coke Yiled (% by wt.)	Coke Selectivity (% by wt.)
HY zeolite	51.56	29.55	58.05	4.21	8.27
SRY zeolite	61.81	36.96	59.80	4.08	6.60
USY zeolite	54.68	35	64.01	3.30	6.04
USY-1N	52.56	33	62.79	2.21	4.21
USY-2N	36	22.3	61.3	2.23	6.18
USY-3N	30.12	19.03	63.18	1.41	4.66
USY-4N	28.69	20.29	70.73	1.53	5.32

Appendix F

Equipment Figures

Figure F-1 Representations the Stainless steel vessel, volume 1, 10 and 15 liters.
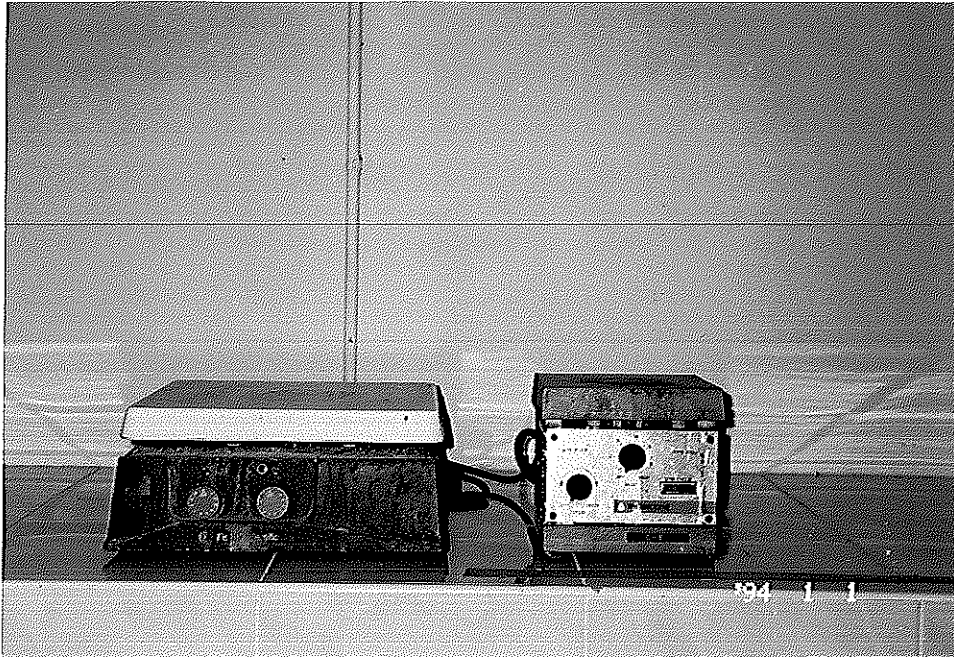
Figure F-2 Representations the Heater.

Figure F-3 Representations the Electric mixer with stirring rod.
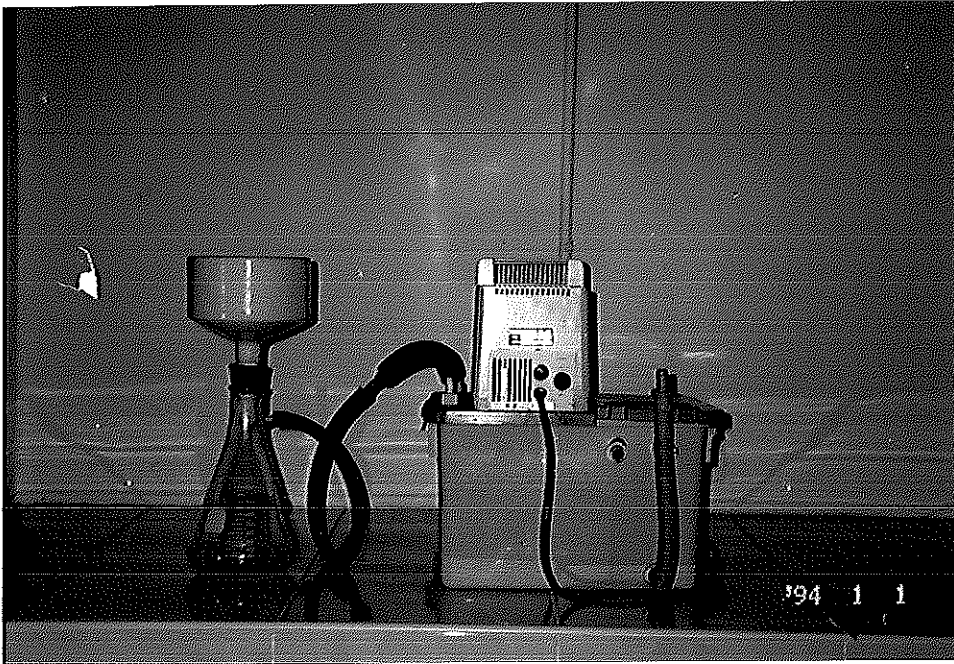
Figure F-4 Representations the Vacuum pump.

Figure F-5 Representations the Hot air oven.

Figure F-6 Representations the Furnace.

Figure F-7 Representation the Mortar.

VITAE

Name Mr. Wachira Ritthichai

Birth Date November 6, 1975

Nationality Thai

Educational Attainment

Degree	Name of Institution	Year of Graduate
B.Sc.(Chemistry)	Prince of Songkla University	1998